



**NTNU – Trondheim**  
Norwegian University of  
Science and Technology

# Dynamic Response of Ship Hull due to Slamming

**Md Emdadul Hoque**

Marine Technology

Submission date: June 2014

Supervisor: Bernt Johan Leira, IMT

Norwegian University of Science and Technology  
Department of Marine Technology



## **Preface**

This thesis has been written as the conclusion of my Master of Science degree in Marine Technology at Norwegian University of Science & Technology. The ISSC 2015 committee II.2 Dynamic Response has identified the need of validation of dynamic response prediction method against measured response data and the endeavor for this thesis was part of this process.

The work has been done in this thesis was challenging as well as interesting for me because I have had to cover from theoretical slam induced load on ship hull to the documentation and interpretation of the results due to slamming load on ship hull on computer tool analysis.

I have had the courses like Sea loads, Hydrodynamics and Finite Element Methods etc in the earlier semesters which has provided me with solid background knowledge. Apart from this I have also studied earlier ISSC committee II.2 publications and number of research papers relevant to my job which has helped me to get a grip in the entire thesis work. The whole process has given me the opportunity to become precise and collective in terms of three-dimensional Finite Element model development, Advanced Finite Element Analysis, Ship hull dynamic Responses and the interpretation of the Analysis results.

I am thankful to my supervisor Professor Bernt Johan Leira, not only for giving me the opportunity to work with ISSC 2015 Committee II.2 but also having insightful discussions with me which has helped me a lot to finish my Master's thesis successfully.

Finally, endless support from my family has been crucial in the completion of this thesis. Last but not least I want to thank all of friends for your patience, support, tips as well as big picture discussions.

Trondheim, June 10, 2014

*Md Emdadul Hoque*

.....

Md Emdadul Hoque



## Summary

In this thesis full-fledged Finite Element Analysis is done for Free vibration analysis and Dynamic Forced Response Analysis of ship hull due to the slam induced load in sea way. This topic is of concern for ships and offshore structures in terms of safety, serviceability assessment including habitability. The aim is to investigate the validation available of dynamic response prediction methods.

Three-dimensional Finite Element model is developed according to the ship (135m dry cargo vessel) particulars provided by the ISSC committee II.2 Dynamic Response. Preliminary model was developed in SESAM/GeniE and later this model is used for Hydrodynamic Analysis in SESAM/HydroD and Finite Element Analysis in ABAQUS/CAE. Mass data and Bottom pressure time traces were also provided by the committee which was used for further model development and input for slamming load respectively. Committee was also provided the estimated characteristics sea state. Added mass matrices and Total damping matrices has been calculated in HydroD which was introduced in ABAQUS for Wet mode models.

Low frequency natural hull girder frequencies with associated vibration modes for Dry-mode and Wet-mode models (Lightship condition, Ballast condition, Fully Loaded condition) were determined. The validity of the frequency analysis results were verified through the further investigations involving study of Classification society and ISO rules and regulations. Implicit dynamic analysis was done for the Acceleration and Strain time traces in the specified location of the ship due to the impulse load. Calculated response data will be compared to the measured data on the actual ship while at sea.

The result from free vibration analysis and forced dynamic response analysis were in agreement with the accepted knowledge. A number of approximations made in the phase of model development and calculations of hydrodynamic parameter were done assuming zero forward speed which has influence on the results. In order to realize the true potential value of this work it would be necessary to compare actual ship response data to calculated data and sorting out the possible disagreements. This work is a possible source to demonstrate the adequacy of hull structural analysis tool which can potentially leading to future design improvements.



## Table of Contents

1	Introduction.....	8
1.1	Approach.....	9
1.2	Literature Review .....	10
2	Definition of terms and parameters.....	12
2.1	Abbreviations.....	12
2.2	Terminology .....	14
3	Theory and Background.....	16
3.1	Linear wave induced motion.....	16
3.1.1	Added mass and damping terms .....	18
3.1.2	Restoring forces and moments.....	19
3.1.3	Heave in irregular waves .....	19
3.1.4	Linear time-domain response.....	20
3.1.5	Wave Loads .....	22
3.2	Second order Non-linear problems .....	23
3.3	Wave Impact Loads .....	23
3.3.1	Consequence of Slamming .....	24
3.3.2	Effect of slamming.....	26
3.3.3	Local hydro-elastic slamming effects .....	26
3.3.4	Slamming on rigid bodies .....	27
3.3.5	Wagner's slamming model .....	32
3.3.6	Design pressure on rigid bodies.....	36
3.3.7	Effect of air cushions on slamming .....	38
3.3.8	Impact of a fluid wedge and green water.....	38
3.3.9	Global wet deck slamming effects .....	39
3.3.10	Water entry and exit loads .....	42
3.3.11	Three-body model.....	44
3.3.12	Global Hydro-elastic effects on mono-hulls .....	47
4	Wave induced responses.....	50
4.1	Hull Structural response.....	50
4.2	Whipping vibration analysis .....	51
4.3	Hull Frequency determination .....	52
4.3.1	Empirical Analysis.....	52
4.3.2	20-Station Beam Model .....	52
4.3.3	Finite Element Model .....	52



4.4	Dynamic Analysis.....	53
4.4.1	Overview.....	53
4.4.2	Implicit Versus Explicit.....	54
4.4.3	Time integration methods.....	55
4.4.4	Damping in dynamic analysis.....	56
4.4.5	Frequency Extraction procedure.....	57
4.4.6	Eigen Extraction methods.....	57
5	Input Data.....	58
5.1	Ship data.....	58
5.2	FE Model.....	59
5.3	Panel Model.....	60
5.4	ABAQUS model.....	61
6	Analysis and Results.....	66
6.1	Natural frequency and vibration modes.....	66
6.1.1	Wet mode frequencies and mode shapes.....	67
6.2	Response time traces.....	78
6.2.1	Acceleration time traces.....	79
6.2.2	Strain time traces.....	82
7	Discussion and Conclusions.....	87
8	Recommendation for future work.....	90
9	References.....	91
	Appendices.....	95
9.1	Appendix A.....	95
9.2	Appendix B.....	100
9.3	Appendix C.....	105



## List of Figures

Figure 1: Co-ordinate system.....	16
Figure 2: Super position wave excitation, added mass, damping and restoring loads.....	18
Figure 3: Heave response in irregular long-crested head waves.....	20
Figure 4: Global forces and moments on hull girder [1] .....	22
Figure 5: Wet deck slamming [1] .....	25
Figure 6: Prediction of pressure distribution during water entry of a rigid wedge.....	29
Figure 7: Slamming pressure parameters during water entry of a blunt 2D rigid body.....	29
Figure 8: The vertical slamming force on symmetric wedge.....	30
Figure 9: Vertical slamming force on a wedge with knuckles. Dead rise angle is 20 deg. ....	31
Figure 10: Water entry of a wedge with constant velocity $V$ . Definition of inner and jet flow domains.....	32
Figure 11: Definition of parameters in analysis of impact forces (Wagner model).....	32
Figure 12: Boundary-value problem for the velocity potential in simplified analysis. ....	33
Figure 13: Definition of polar co-ordinates ( $r_1, 1$ ) and ( $r_2, 2$ ) used in evaluating the complex function.....	34
Figure 14: Water entry of a wedge shaped elastic cross section.....	36
Figure 15: Stiffened panel consisting of plate and longitudinal stiffener. ....	37
Figure 16: Deformation of the free surface and formation of an air pocket during entry of a rigid body.....	38
Figure 17: Impact of fluid wedge and green water .....	39
Figure 18: Measured vertical acceleration at the forward perpendicular (FP) of the ulstein test catamaran.....	40
Figure 19: Position of slamming on the wet deck in regular head sea waves as a function of wave length. ....	41
Figure 20: 2D boundary value problem for velocity potential due to wet deck slamming.....	42
Figure 21: Outline of the experimental hull arrangements (top view) ( Ge 2002) .....	43
Figure 22: Degrees of freedom of segmented model.....	44
Figure 23: Elastic connection between two adjacent rigid body segments.....	44
Figure 24: Illustration of rotational sign for and adjacent bodies .....	45
Figure 25: Calculated shapes of eigen modes for 3-body model.....	46
Figure 26: Comparison between experimental and numerical value. ....	47
Figure 27: Ship vibrating with two-node deformation. ....	47
Figure 28: 2D added mass in heave for Lewis form sections .....	49
Figure 29: Ship preliminary model in GeniE.....	59
Figure 30: Panel model in SESAM/HydroD .....	60
Figure 31: Element properties.....	63
Figure 32: Mesh model in ABAQUS .....	64
Figure 33: Frequency Analysis Steo in ABAQUS .....	65
Figure 34: Global Torsion Mode at 0.42593 Hz.....	68
Figure 35: 2-node Vertical Bending Mode at 0.77186 Hz.....	69
Figure 36: Global Torsion and Horizontal Bending Mode at 0.79031 Hz .....	69
Figure 37: 3- node horizontal bending at 1.3188 Hz .....	70
Figure 38: Global Torsion Mode at 0.41509 Hz.....	71
Figure 39: 2-node Vertical Bending Mode at 0.73877 Hz.....	72
Figure 40: Global Torsion and Horizontal Bending Mode at 0.77515 Hz .....	72
Figure 41: 3- node horizontal bending at 1.3055 Hz .....	73
Figure 42: Global Torsion Mode at 0.38389 Hz.....	75
Figure 43: 2-node Vertical Bending Mode at 0.70975 Hz.....	75
Figure 44: Horizontal bending /torsion mode at 0.71513 Hz .....	76



Figure 45:3- node horizontal bending at 1.2276 Hz .....	76
Figure 46:3- node vertical bending at 1.4119 Hz .....	77
Figure 47: 135 m dry cargo vessel, sensor locations indicated.....	79
Figure 48: Acceleration time traces Frame 35 [Deck, SB] .....	79
Figure 49: Acceleration time traces frame 100.5 [Deck, SB].....	80
Figure 50: Acceleration time traces, Frame 100.5 [Bottom, CL] .....	80
Figure 51: Acceleration time traces, frame 154.5 [Deck, SB].....	80
Figure 52: Acceleration time traces, Frame 161[Bottom, CL] .....	81
Figure 53: Acceleration time traces, Frame 161.5[Deck, SB] .....	81
Figure 54: Acceleration time traces, Frame 164.5 [Deck, SB] .....	81
Figure 55: Acceleration time traces, Frame 170 [Deck, SB] .....	82
Figure 56: Acceleration time traces, frame 170.5 [Deck, SB].....	82
Figure 57: Strain time traces, Frame 35[Deck, SB].....	83
Figure 58: Strain time traces, Frame 100.5 [Deck, SB].....	83
Figure 59: Strain time traces, Frame 100.5 [Bottom, CL] .....	83
Figure 60: Strain time traces, Frame 154.5 [Deck, SB].....	84
Figure 61: Strain time traces, Frame 161 [Bottom, CL] .....	84
Figure 62: Strain time traces, frame 161.5 [Deck, SB].....	84
Figure 63: Strain time traces, Frame 164.5 [Deck, SB] .....	85
Figure 64: Strain time traces, Frame 170 [Deck, SB].....	85
Figure 65: Strain time traces, Frame 170.5 [Deck, SB].....	85
Figure 66: Velocity trace in the bow area , Frame 170, SB .....	88
Figure 67: Displacement trace in amidship., SB.....	88
Figure 68: Stress [mises] plot in bow and stern area, SB .....	89
Figure 69: General Arrangement .....	97
Figure 70: Lines Plan.....	98
Figure 71: Typical pressure trace fr.161 and 161.5 (measure 5) .....	99
Figure 72: Typical strain trace Frame 35 (measure 5).....	100





## List of Tables

Table 1: Hilber- Hughes- Taylor integrator parameters[41] .....	55
Table 2: Wet mode natural frequencies [Lightship] .....	67
Table 3: Wet mode natural frequencies [Ballast condition] .....	70
Table 4: Wet mode natural frequencies [Loaded].....	74
Table 5: Comparison between dry mode and wet mode natural frequencies .....	78
Table 6: Mass data .....	96



# 1 Introduction

Technology is changing day by day. From concept design to the service condition of a ship or an offshore floating structure involved with lot of procedure, estimation and calculation. Well established rules and guidelines for all the aspects (designing, construction, operation) during the Ship shelf life are available of. The main area of this thesis work is about the dynamic response of ship. Dynamic Structural response of ships and floating offshore structures is a concern in terms of safety and serviceability assessment, including habitability. There are different procedure and technique are available to predict the dynamic response of ship. To estimate the response to the highest level of accuracy validation of existing prediction methods is important and it is a continuous process.

The purpose of the work is to investigate the adequacy of various hull structural analysis tools for predicting ship hull dynamic response due to slamming.

In 2002 TNO participated in a joint industry project (JIP), concerning a long term measuring campaign on an ocean going general cargo ship. The owner Wangenborg has kindly granted ISSC community access to the ship particulars, while all JIP partners agreed to share some of measured time traces.

Fluid-structure interaction (FSI) problems have been studied in many diverse research areas for several decades. There are many FSI problems that are relevant in the maritime research area such as sloshing in a tanker ship, propulsion system, green water and wave-induced loads on a ship or offshore structure. Ship hull is vulnerable to unsteady wave, wind, and current loading. Among those external loads mentioned earlier wave induced forces present the most considerable design problem for ship owners, shipbuilders and classification societies. Dynamic wave- induced loads are mostly two types: Global loads and Local Loads. Global loads are induced by the unsteady hydrodynamic pressure because of the fluid oscillatory motions surrounding the hull while the local or secondary loads, such as slamming and whipping are due to wave impacts.

Study of transient dynamic response of ship structure due slamming pressure impulsive load is the main focus of this thesis work. ISSC 2015, Committee II.2, benchmark provided all the information related to vessel and corresponding sea state. Slamming response time traces is predicted at location of sensors [Strain, acceleration, pressure] along the hull girder. At the final stage, comparison will be made with actual measured data from a trip in the Laurentian trough off the coast of Nova Scotia, Canada.



## 1.1 Approach

The work has been progressed in several stages. At the first stage, External loads which acts on the ship hull girder due to waves and transient loads for example due slamming have been studied. A detail study has performed about slam induced loads on the ship hull. Experimental results from other work, theoretical background, corresponding load models, load calculation procedure and computer tools for dynamic analysis, vibration and frequency analysis are also studied. In the second stage finite element theory has been emphasized. Natural frequency extraction procedure and implicit dynamic analysis procedure has considered for computer tool ABAQUS/CAE. In the next stage, Hull girder model is established in SESAM/GeniE from the ship particulars given by the committee. Two different models were exported from GeniE: one was panel model for Hydrodynamic analysis in SESAM/HydroD and other one was for ABAQUS/CAE that was imported later on as part model. The part model is further developed in ABAQUS for respective purposes. Hydrodynamic properties are calculated in HydroD Considering the specified characteristic sea state in which the ship sails, in terms of significant wave height  $H_s$ , wave zero crossing period  $T_p$ , main heading and sailing speed. The dry and wet natural modes and frequencies have been analyzed for the 2 and 3- node mode shapes in ABAQUS. At the last stage, for given time histories of the load impulses that act on the fore part of the hull, dynamic response analysis has been performed. The corresponding time series of acceleration, strain has been established for different Loading conditions.



## 1.2 Literature Review

Full scale measurements and model test have been done in the previous years. Most of the measurements and tests were focused on larger ships i.e. Container ships, bulk carriers, frigates and LNG carriers. Researches were focused on the effect of wave-induced vibration on fatigue performance as well as wet deck slamming for high speed catamarans.

Gaidai Et al.[5] Proposed a formulation for prediction of the extreme stresses measured in the deck amidships of a container vessel during operation in harsh weather using the full scale measurement data. The method opens a new window to predict simply and efficiently both short-term and long-term extreme response statistics.

Lee et al. [6] reported time domain whipping and springing analyses for a 10000 TEU class container ship using computational tools as a part of a joint industry project (JIP). The results from the computational analyses in regular waves have been correlated with those from model tests undertaken by MOERI. It was reported that the wave induced vertical bending moments with whipping vibration were reasonably well predicted by 3D no-linear hydro elasticity method.

Ochi and Motter [7] offered a complete description of the slamming problem. Account of a large number of unknowns required for the determination of the whipping stresses they have suggested some simple formulae for the calculation of the wave-induced slamming loads, for practical purposes. All these formulae were based on experiments with frigate models. They stressed the importance at the design stage of the combined effect of wave-induced and whipping stresses, i.e. the total bending moment induced by the waves.

The work of Kawakami et al, [8] was based on experimental work for a tanker, proposed an expression for the time history of the slamming loads. They found that the Ochi and Motter [7] work slightly under predicts the maximum slamming pressure when compared with the experimental measurements.

Belik et al. [9] understood that the bottom slamming could be divided into two separate components: impact and momentum slamming. Based on this assumption they used the Ochi and Motter [7] method for the determination of the maximum slamming pressure and the Kawakami et al. expression for the determination of the time history of the slamming impact force. After that, they carried out calculations for the vertical bending moments and shear forces in regular head seas.

Belik and Price [10] used the same formulation to made comparisons for two different slamming theories using time simulation of ship responses in irregular seas. They



found that slamming response magnitude depend on the numerical model adopted in the calculation of the slamming loads.

The non-linear ship motions were calculated by Yamamoto et al. [11] based on the equations given by the linear theory but with time-varying coefficients dependent on the instantaneous sectional draft. They included the hydrodynamic impact component given by the rate of change of the sectional added mass, considering that this force only acts on the vessel when the section is penetrating the water. Afterwards they did some experiments and calculations on a bulk carrier model for head seas. They found that the accuracy of the calculation of the hydrodynamic coefficients has a Significant influence on the results of the slamming forces, and the computation with accurate coefficients results in better agreement with experiments.

Tao and Incecik [16] found the large-amplitude motions and bow flare slamming pressures in regular waves. The non-linear restoring, damping and fluid momentum forces were considered in predicting ship motions in the time domain. The momentum slamming theory and Wagner theory were used to predict the bow flare slamming pressures. The bow flare slamming pressures were calculated by separating the pressure into the water immersion impact pressure and the wave striking impact pressure. A satisfactory correlation between the results of predictions and model test measurements was obtained.

Sames et al. [17] applied a finite-volume method to predict impact coefficients around the bow region of a ship during slamming. Ship motions in regular waves were predicted by a linear panel method which takes into account incident, diffracted and radiated waves. The impact pressures were calculated by processing the results of the computed pressure coefficients and the transfer functions of ship motions in the time domain. No comparisons with the measurements were given.

Comparisons between the full-scale measurements and theoretical predictions were carried out by Aksu et al. [18] for a fast patrol boat travelling in rough seas. Due to the uncertainty of the wave measurements in a real sea state, the experimental results of the vertical bending moments were compared with calculations for two different sea states in a histogram form and satisfactory results were found.

It was found by Ramos and Guedes Soares [13] that the several slamming load formulations can produce large differences in the slamming pressures, loads and also in primary stresses. The Ochi and Motter method under predicts the pressures, loads and also bending moments when compared with the other methods.

[19]



## 2 Definition of terms and parameters

This section contains the definition of the technical words and abbreviations have been used in the report.

### 2.1 Abbreviations

$\eta_1$ , translatory displacement in X-direction with respect to origin, surge  
 $\eta_2$ , translatory displacement in Y-direction with respect to origin, sway  
 $\eta_3$ , translatory displacement in Z-direction with respect to origin, heave  
 $\eta_4$ , angular displacement of the rotational motion about the X-axis, roll  
 $\eta_5$ , angular displacement of the rotational motion about the Y-axis, pitch  
 $\eta_6$ , angular displacement of the rotational motion about the Z-axis, yaw  
 $F_k$ , Force component  
 $A_{kj}$ , added mass co-efficient  
 $B_{kj}$ , damping co-efficient  
 $C_{kj}$ , Restoring co-efficient  
 $\rho$ , Density of water  
 $g$ , acceleration due to gravity  
 $A_{wp}$ , water plane area  
 $B$ , maximum wedge breadth  
 $\phi$ , velocity potential  
 $\lambda$ , wavelength  
 $F_n$ , Froude number  
 $A$ , submerged cross sectional area  
 $d$ , sectional draft  
 $a_{33}$ , 2D infinite frequency added mass in heave  
 $b$ , sectional beam  
 $f_{33}^{exe}$ , hydrodynamic excitation load per unit length  
 $U$ , ship speed  
 $C_B$ , block co-efficient  
 $f_{33}^{HD}$ , 2D vertical force on the hull due to dynamic pressure  
 $\phi_3$ , velocity potential due to forced heave with unit velocity  
 $C(x)$ , mean submerged cross-sectional curve of the hull surface  
 $n = (n_1, n_2, n_3)$ , the normal vector to the hull surface with positive direction into the fluid  
 $T$ , wave period  
 $Q_A$ , shear force at point A  
 $M_A$ , bending moment at point A  
 $M_{gen}$ , mass matrix



**B**<sub>gen</sub>, Damping matrix

**K**<sub>gen</sub>, restoring matrix

**r**, displacement matrix

**F**<sub>gen</sub>, the forces due to wet deck slamming and linear wave excitation loads

**w**, elastic deflection of beam

**EI**, bending stiffness

**h(x)**, is the time-independent wetdeck height above calm water

$\eta_B(x,t)$ , vertical ship motion

**S**, motion at any point on the body

**V**, displaced volume of water

**z<sub>b</sub>**, z co-ordinate of the centre of buoyancy

$\beta$ , dead rise angle

**P<sub>a</sub>**, atmospheric pressure

**C<sub>p</sub>**, pressure co-efficient

**t**, time variable

**F<sub>3</sub>**, the vertical slamming force



## 2.2 Terminology

**Ahead:** Forward of the bow

**Amidships (or midships):** In the middle portion of ship, along the line of the keel.

**Beam Sea:** A sea where waves are moving perpendicular to the direction a ship is moving.

**Bow:** The front of a vessel.

**Bulbous bow:** A protruding bulb at the bow of a ship just below the waterline which modifies the way water flows around the hull, reducing drag and thus increasing speed, range, fuel efficiency, and stability.

**Cargo Ship:** Any sort of ship or vessel that carries cargo, goods, and materials from one port to another, including general cargo ships (designed to carry break bulk cargo), bulk carriers, container ships, multipurpose vessels, and tankers. Tankers, however, although technically cargo ships, are routinely thought of as constituting a completely separate category

**Course:** The direction in which a vessel is being steered, usually given in degrees.

**Dead rise:** The design angle between the keel (q.v.) and horizontal.

**Displacement:** The weight of water displaced by the immersed volume of a ship's hull, exactly equivalent to the weight of the whole ship.

**Flare:** A curvature of the topsides outward towards the gunwale.

**Following sea:** Wave or tidal movement going in the same direction as a ship

**Forecastle:** A partial deck, above the upper deck and at the head of the vessel; traditionally the sailors' living quarters. The name is derived from the castle fitted to bear archers in time of war

**Freeboard:** The height of a ship's hull (excluding superstructure) above the waterline. The vertical distance from the current waterline to the lowest point on the highest continuous watertight deck. This usually varies from one part to another.

**FSI:** Fluid Structure Interaction

**Head sea:** A sea where waves are directly opposing the motion of the ship.

**Hull Girder:** The primary hull structure such as the shell plating and continuous strength decks contributing to flexural rigidity of the hull and the static and dynamic behavior of which can be described by a free-free non-uniform beam approximation.





**Hull Girder Vibration:** That component of vibration which exists at any particular transverse plane of the hull so that there is little or no relative motion between elements intersected by the plane.

**JIP:** Joint Industry Project.

**Length Between perpendiculars:** The length of a vessel along the waterline from the forward surface of the stem, or main bow perpendicular member, to the after surface of the sternpost, or main stern perpendicular member. Believed to give a reasonable idea of the vessel's carrying capacity, as it excludes the small, often unusable volume contained in her overhanging ends

**Local Vibration:** The dynamic response of a structural element, deck, bulkhead or piece of equipment which is significantly greater than that of the hull girder at that location.

**Severity of Vibration:** The peak value of vibration (velocity, acceleration or displacement) during periods of steady-state vibration, representative behavior

**Wheelhouse:** Location on a ship where the wheel is located; also called pilothouse or bridge



### 3 Theory and Background

Ship response in a seaway is a complicated phenomenon involving the interactions between the ship dynamics and several distinct hydrodynamic forces. All ship responses are nonlinear at least to some extent, but in some cases when nonlinearities are quite small a linear theory may yield good outcome.

The assumption of linearity for the ship response allows us to use many powerful analysis techniques developed in other fields. The ship's motion can be considered to be made of three translation components and three rotational components. A Strip theory is developed for the ship motion in regular waves at forward speed and with an arbitrary heading.

#### 3.1 Linear wave induced motion

To estimate the ship responses, it is important to understand the complete motions of a ship with all six degrees of freedom and also the coupling between them. Linear equation of motion for ship is given with arbitrary heading in a train of regular sinusoidal waves.

Small motion is the basis of linearization. Exception occurs for resonant situations when damping is small, i.e. roll response in beam seas, heave resonance of semi-submersible oil-drilling ships, near-pitch resonance of SWATH ships.[48]

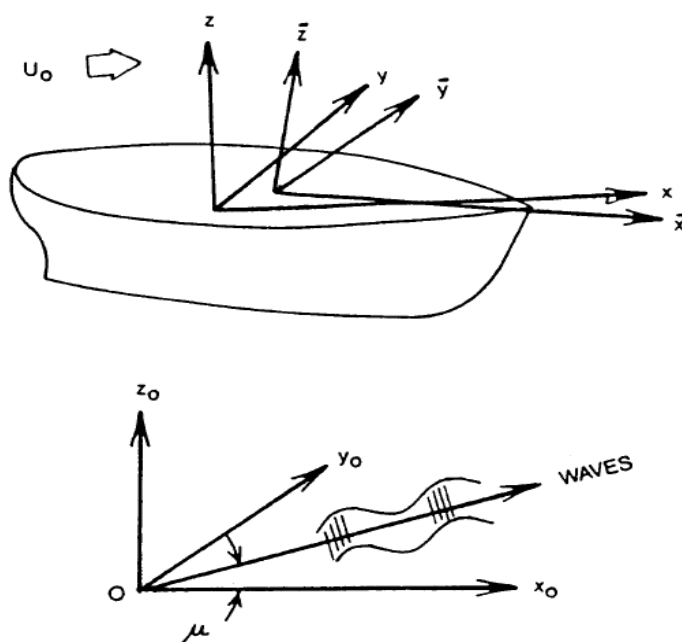


**Figure 1: Co-ordinate system**



Linear equations in six degrees freedom using body axes in general form is given by,

$$\sum_{k=1}^6 \Delta_{jk} \ddot{\eta}_k(t) = \mathbf{F}_j(t) \quad j = 1, 2, \dots, 6 \quad (1)$$

$\Delta_{jk}$ = Generalized inertia matrix component for the ship

$d^2/dt^2 (\eta_k)$ = acceleration in mode k

$F_j$ = Total forces and moments acting on the body.

In the above equation for  $J= 1, 2, 3$  are the force equations and  $j=4,5,6$  are the moment equations.

If equation 1 is written in Euler's equation of motion (with only fluid forces and gravitational forces acting on the ship) results in

$$\sum_{k=1}^6 \Delta_{jk} \ddot{\eta}_k = \mathbf{F}_j(t) = \mathbf{F}_{Gj} + \mathbf{F}_{Hj} \quad j = 1, 2, \dots, 6 \quad (2)$$

$F_{Gj}$ =Component of gravitational force

$F_{Hj}$ =Component of fluid force acting on the ship.

In linear theory ship response is linear (i.e. directly proportional with to) wave amplitude and happens at the frequency as the incident wave.

Gravitational forces simply refer to the weight of the vessel acting at the COG normally cancels by the buoyant forces. Hydrodynamic and hydrostatic forces are obtained by integrating the fluid pressure within the underwater part of the hull. Fluid force equation is given by

$$\mathbf{F}_{Hj} = \iint_{S'} P n_j ds \quad j = 1, 2, \dots, 6 \quad (3)$$

$P$ = Fluid pressure which is calculated by Bernoulli's equation.

$S$ = under water hull surface area.

Pressure includes both the hydrodynamic and hydrostatic part. Net hydrostatic force acting on ship in any direction due to a unit displacement is given by the hydrostatic coefficients. Total velocity potential is needed to find the hydrodynamic force acting on a ship. Hydrodynamic force which is resulted from the incident and diffracted waves is called exciting force. Hydrodynamic force which is resulted from radiated waves are related to added mass and damping. First part of Exciting force may easily calculated by integrating the incident velocity potential over the body surface. For the



second component of exciting force diffraction potential is integrated over the surface of the hull.[48]

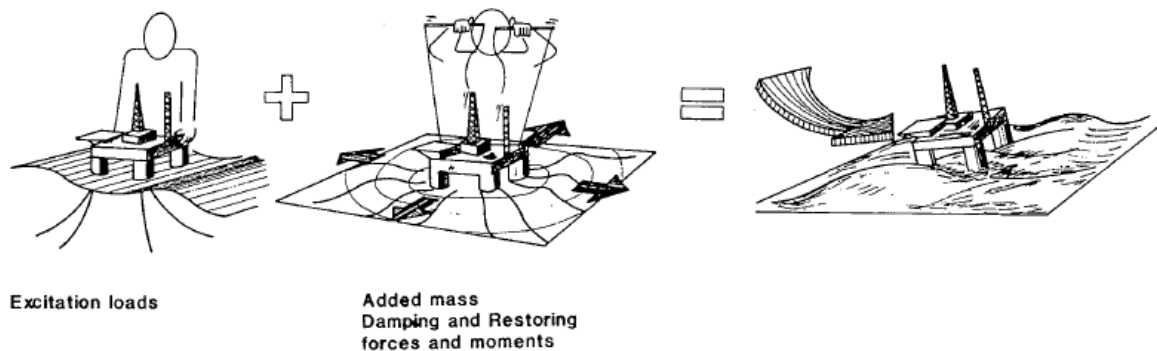


**Figure 2: Super position wave excitation, added mass, damping and restoring loads**

Radiation forces are the unsteady hydrodynamic force component. Radiation force is effectively a transfer function from unit motion. Added mass which is a apparent mass- added to the mass of the ship likewise damping is the hydrodynamic force on the body (in phase with the velocity). [48]

Linearized equation of motion is given by

$$\sum_{k=1}^6 [-\omega_e^2 (\Delta_{jk} + A_{jk}) + i\omega_e B_{jk} + C_{jk}] \bar{\eta}_k = F_j^I + F_j^D \quad j = 1, 2, \dots, 6 \quad (4)$$

### 3.1.1 Added mass and damping terms

Force harmonic rigid body motions result added mass and damping loads which are steady state hydrodynamic forces and moments. There is total 36 damping and 36 added mass coefficient. If the structure has zero forward speed and there is no current it can be shown that coupled added mass and damping coefficient for any two motion of ship is always same(For example  $A_{13}=A_{31}$  and  $B_{15}=B_{51}$ ). A finite amount of water oscillates rigidly connected to the body is not the true concept for understanding added mass. Added mass should better be understood from hydrodynamic pressure induced forces point of view.

Added mass and damping coefficient are dependable on the frequency and also motion mode (for example added mass is not same for sway and heave with same frequency). Added mass moment fairly depend upon the choice of axes of rotation. For a ship added mass and damping co efficient normally calculated based on strip theory. The principle is to divide the underwater part of the ship into several strips.



Two dimensional coefficients are calculated first for each strip and get combined afterwards. In strip theory flow variation in cross –sectional plane is considered much larger than the flow variation in longitudinal direction. Damping coefficient and added mass Co efficient can be fairly dependent on the body shape. Conformal mapping or source technique is used for two dimensional ship sections. When a body comes close to the free-surface, a wall or another body added mass value will be influenced. [49]

There is significant effect on added mass and damping coefficient due to forward speed structure or current. Ship forward speed is related to the frequency of encounter. Complete three dimensional realizations of linear wave-induced motion and loads at forward speed are problematical. For practical purpose strip theory still plays a good role even it does not account all the physical effects. It is better to know the limitations to work with strip theory- this is basically a high frequency theory stands more applicable in head and bow sea than the flowing and quating sea for a ship with forward speed. Strip theory is also limited to the ships with low length to beam ratios.

### 3.1.2 Restoring forces and moments

For a free floating body, restoring forces follow from hydrostatic and mass considerations.

Force and moments components may be written as

$$F_k = -C_k \eta_j \quad (5)$$

Non- zero coefficients for X-Z plane of symmetry for submerged volume in heave is given by

$$C_{33} = \rho g A_{WP} \quad (6)$$

$A_{WP}$ = water plane area

To assess the amplitude of motion of ship- natural or resonance periods, damping level and wave excitation level are important parameter. Large motion is expected if the ship is excited with oscillation periods in the vicinity of a resonance period.

Implication of linear theory for specific vessel response (heave in head sea) illustrated below.

### 3.1.3 Heave in irregular waves

Heave response in irregular waves which non-dimensional response is always unity at zero wave frequency and trends to be zero for high frequency. As frequency



approaches zero wave length become infinite- ship just follows the wave surface, hence the heave and wave amplitude become equal. On the other hand wave length becomes small as the wave frequency increases; that is , become ripples to which ships do not respond. A typical shape of heave response operator at fixed forward speed with varying wave spectra given below. [48]

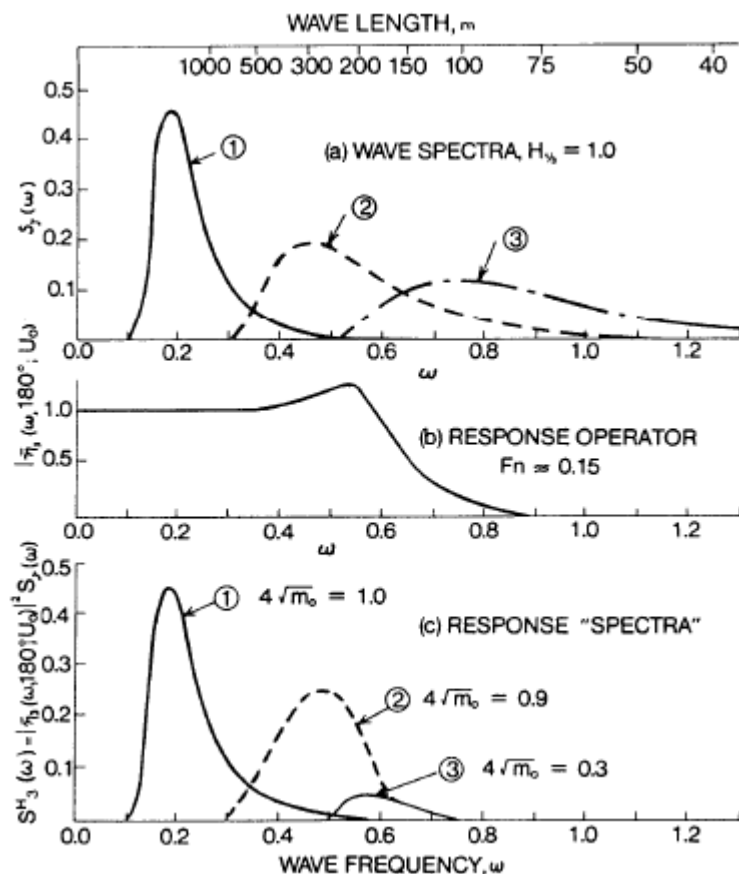


**Figure 3: Heave response in irregular long-crested head waves**

### 3.1.4 Linear time-domain response

There are some scenarios where transient response accounted. Examples of transient responses are waves generated by a passing ship, coupling between nonlinear sloshing in a ship tank and ship motions wet deck slamming on a catamaran in regular incident waves. Transient Vertical force that excites transient response in heave, pitch, and global elastic vibration modes are resulted from wet deck slamming. For example we can consider two-node vertical bending mode that has a natural period on the order of 1 s. Ship response at the wave encounter period which is order of 10 s. There is a conflict of which frequency we should use in calculating added mass and damping. For these two different periods the added mass and damping will be quite different.



Here we limit ourselves to heave and pitch. Linear equation of motion may be written as

$$\begin{aligned}
 & (M + A_{33}(\infty)) \ddot{\eta}_3 + B_{33}(\infty) \dot{\eta}_3 + C_{33} \eta_3 \\
 & + \int_0^t h_{33}(\tau) \dot{\eta}_3(t - \tau) d\tau \\
 & + A_{35}(\infty) \ddot{\eta}_5 + B_{35}(\infty) \dot{\eta}_5 + C_{35} \eta_5 \\
 & + \int_0^t h_{35}(\tau) \dot{\eta}_5(t - \tau) d\tau = F_3(t) \\
 & A_{53}(\infty) \ddot{\eta}_3 + B_{53}(\infty) \dot{\eta}_3 + C_{53} \eta_3 \\
 & + \int_0^t h_{53}(\tau) \dot{\eta}_3(t - \tau) d\tau \\
 & + (I_{55} + A_{55}(\infty)) \ddot{\eta}_5 + B_{55}(\infty) \dot{\eta}_5 + C_{55} \eta_5 \\
 & + \int_0^t h_{55}(\tau) \dot{\eta}_5(t - \tau) d\tau = F_5(t).
 \end{aligned} \tag{7}$$

$A_{JK}(\infty)$  = mean infinite-frequency added mass coefficient

$B_{JK}(\infty)$  = mean infinite-frequency damping coefficient

$$\begin{aligned}
 h_{jk}(t) &= -\frac{2}{\pi} \int_0^{\infty} \omega (A_{jk}(\omega) - A_{jk}(\infty)) \sin \omega t \, d\omega \\
 &= \frac{2}{\pi} \int_0^{\infty} (B_{jk}(\omega) - B_{jk}(\infty)) \cos \omega t \, d\omega.
 \end{aligned} \tag{8}$$

$h_{JK}(t)$  = retardation functions (also referred to as impulse response functions)



$A_{JK}$  and  $B_{JK}$  behave asymptotically for large frequencies which is difficult to estimate. Boundary Element Method (BEM) will be good tool to tackle this situation. Hull surface is approximated by panels. Response calculation is influenced by the high-frequency behavior of  $A_{JK}$  and  $B_{JK}$ . [49]

### 3.1.5 Wave Loads

Wave loads may be needed for structural design purposes from two different aspects:

1. Instantaneous local hydrodynamic pressures on the hull surface due to ship motions and ship-wave interactions. These pressures may be needed over the entire hull surface or only on some portion of it. Slamming (water impact) is the important case.
2. Integrated instantaneous pressures (global wave loads), giving for instance:
  - a. Vertical and torsional bending moments and shear forces at midships or other stations
  - b. Transverse vertical bending moments, vertical shear forces, and pitch connecting moments on half of a part obtained by intersecting along the center plane.[1]

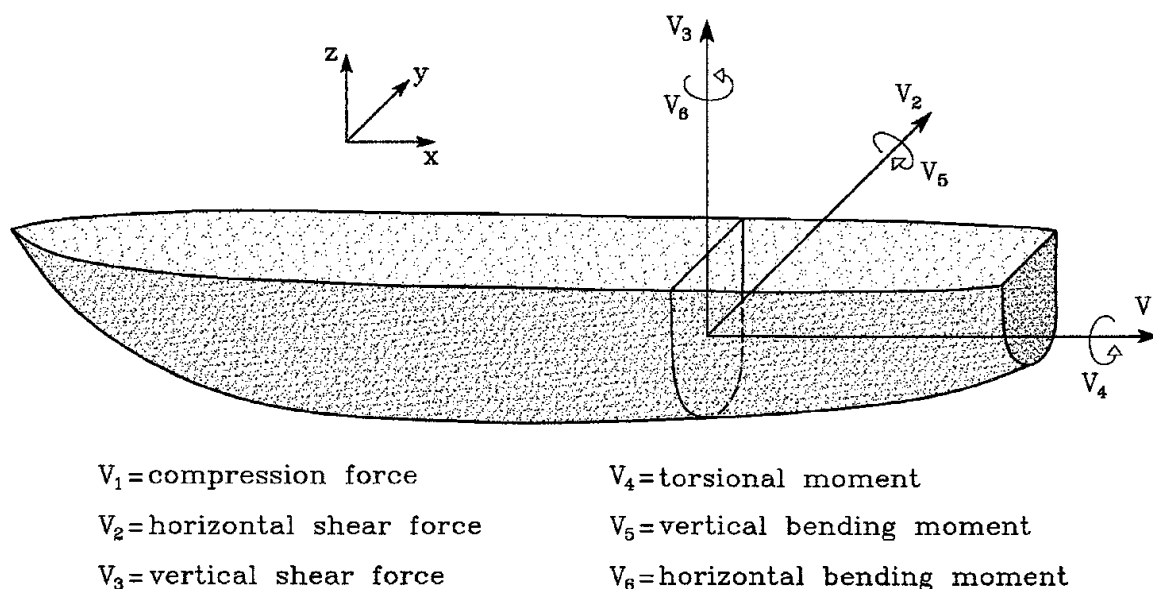


**Figure 4: Global forces and moments on hull girder [1]**

Global wave loads are expected to be significant for ships have length larger than 50m. Minimum strength requirement for hull girder strength is normally satisfied for





scantlings obtained from local strength requirements (of plates and stiffeners due to lateral pressure). [1]

### **3.2 Second order Non-linear problems**

To solve non-linear wave –structure problem in ship hydrodynamics, perturbation analysis is the most common way. In linear analysis, body boundary condition and free-surface condition are satisfied on the submerged surface and mean position of the free surface respectively. In second order theory, the fluid pressure being same to the atmospheric pressure on instantaneous position of the free surface to accounted the non-linearities in the velocity of fluid particle the free surface. We consider all the terms which are linear to the wave amplitude or square to the wave amplitude. For irregular seas, the second order loads are sensitive to the wave frequency range with significant wave energy. To calculate mean wave (drift) forces and moment direct integration method or maruo’s formula may use. Added mass resistance is sensitive to the mean wave period. Added resistance curve has a very distinct peak around heave and pitch resonance for a ship at finite Froude number. Viscous effect has contribution to the wave drift force when they small. Consideration of second order non-linear problems is important for several marine structures like the design of mooring and thruster systems, analysis of offshore loading systems, evaluation of towing of large gravity platforms from the fabrication site to the operation site, added resistance of ships in waves, performance of submarines close to the free surface and analysis of slowly oscillating heave, pitch and roll of large volume structures with low water plane area. [48]

### **3.3 Wave Impact Loads**

Slamming (water impact) load has great importance in structural design .The probability of slamming is found by defining a threshold relative impact velocity of slamming occurrence. This threshold is not related to threshold velocity. There is no threshold for slamming as a physical process. TO come up with good understanding about slamming threshold it is necessary to study theoretical models or perform experiments on water impact against wet deck and hull structures of ship and also necessary in order to develop rational criteria for operational limits due to slamming. The criteria should be related to slamming loads used in the structural design i.e. structural response due to slamming. [1]



### 3.3.1 Consequence of Slamming

1. Compressibility of water, i.e. initial acoustic phase, typically for short time duration
2. Air-cushion/bubbles, i.e. air cavities can be entrapped and oscillate due to air compressibility (the cavity is exaggerated in the sketch). Relevant for  $\beta < 2-3$ deg. [50]
3. Hydro-elasticity, i.e. coupling of the hydrodynamic and structural problems, relevant for  $\beta < 5$  deg. and when the loading time associated with water entry is small or comparable to the natural wet period of the structure (**NB**: the structure does not have only one natural period, typically the highest natural period is relevant but one can not exclude that also other natural periods could be excited and matter). Hydro-elasticity means that the hydrodynamic loads affect the structural elastic vibrations and in return the elastic vibrations affect the fluid flow and related pressure field. At the beginning the pressure is the slamming pressure and then it oscillates as a consequence of the coupling. [50]
4. Cavitation, i.e. when local water pressure equals the vapour pressure  $p_{vap}$  and liquid becomes gas. This can happen for instance if hydro-elastic behaviour is excited because we are close to the free surface so the hydrostatic pressure is small and the pressure can oscillate greatly due to hydro-elasticity and become lower than  $p_{vap}$ . [50]
5. Ventilation, i.e. when local water pressure goes below the atmospheric pressure  $p_a$  and air is attracted between the structure and the water. It can occur in connection with hydro-elasticity. Another example of occurrence is in connection with asymmetric impacts with vortex shedding leading to high local velocities and so low static pressures [50]

In terms of physical effects connected with slamming, we can say

1. Gravity effects are not relevant because the involved fluid accelerations are typically much larger than gravity acceleration  $g$ , e.g. even  $200g$ .
2. Froude number is very important because fixes the impact velocity, i.e. Froude scaling must be respected when doing in model tests. [50]
3. Viscous effects, i.e. Reynolds number, are of secondary importance because the time scales involved in the slamming are too short for them to matter.



4. Some effects are relevant in specific cases, e.g. for tanks: boiling for LNG tanks, mixtures of liquid and gas, ambient (ullage) pressure in case of air cavities entrapment, ambient (ullage) density [50]
5. The relevance of some effects has not been fully clarified yet, like: surface-tension effects, though they are expected to be of minor importance; sound speed, i.e. acoustic effects, though it is expected to be of secondary importance. [50]

### Wetdeck Slamming

Wet deck is defined as the lowest part of the cross-structure connecting two adjacent side hulls of a multihull vessel. In head sea conditions wetdeck slamming is likely to occur for a vessel with forward speed. An example of wedge shaped wet deck with cross section with dead rise angle  $\beta_w$ . In some cases it might be zero. If the side hulls come out of the water as a consequence of the relative vertical motions between the vessel and the water surface, subsequent slamming on the side hulls expected to occur.[1]

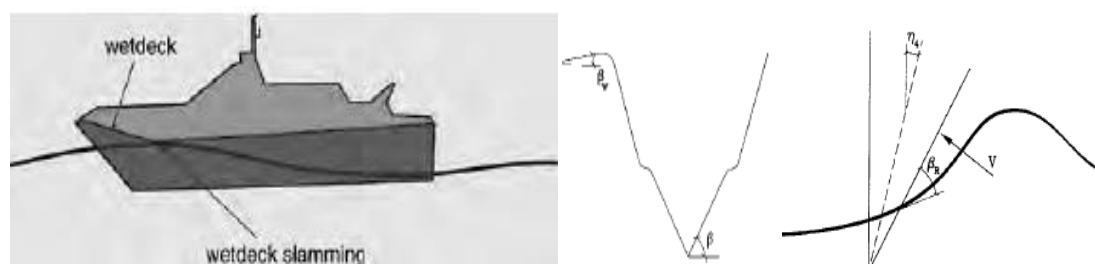


**Figure 5: Wet deck slamming [1]**

Local slamming loads depend upon the impact velocity  $V_R$ . When  $\beta$  is larger than about  $5^\circ$ , the maximum slamming pressure is proportional to  $V_R^2$  for constant  $V_R$ . In righthand side of figure 5 – it shows a steep wave impacts on the hull and the relative small angle  $\beta_R$  between the impacting free surface and the hull surface. The presence of roll can decrease  $\beta_R$  and thereby cause increased slamming loads. The slamming loads are sensitive to  $\beta_R$ , when the angle  $\beta_R$  is small.[1]

### Green Water on deck.

Green water on deck happens as a consequence of “dive-in” in following seas, especially at reduced speed in large waves and when the frequency of encounter becomes small. It can also happen as a consequence of large relative vertical motions



between the vessel and the water. The water can enter the deck as a plunging breaker, causing slamming loads on the deck.

### 3.3.2 Effect of slamming

Slamming causes with both local and global effect. Whipping is referred as the global effect of slamming. Hydro elasticity may be important for global loads and also have some local effects in the case of very high slamming pressures of very short duration. When the angle between the impacting free surface and hull surface is small, very high pressures may occur. *Hydro-elasticity* means that the fluid flow and the structural elastic reaction are considered simultaneously and that we have mutual interaction, that is,[1]

- The elastic vibrations cause a fluid flow with a pressure field
- The hydrodynamic loading affects the structural elastic vibrations

In conventional Structural analysis (without hydro-elasticity or dynamic effects), hydrodynamic loading is considered as rigid structure. The loading is applied in a quasi-steady manner when the resulting static structural elastic and plastic deformations and stresses are calculated. Many physical features, such as compressibility and air cushions affect the fluid flow. Solution of complete hydrodynamic problem is quite complex and approximation must be made. For simplification we can neglect the compressibility of the water. It seems very high slamming pressures are not important for steel and aluminum structures. As the high pressure peaks are localized in time and space. The force impulse that is important for the structural response.[1]

### 3.3.3 Local hydro-elastic slamming effects

Different physical effects occur during slamming generally effects of viscosity and surface tension are negligible. Air cushion may be formed between the body and the water if the local angle between the water surface and the body surface is small at the impact position. Compressibility influences the flow of the air in the cushion. The airflow interacts with the water flow. When the air cushion collapses, air bubbles are formed. Local dynamic hydro-elastic effects may occur when the angle between the water surface and body surface is small. Vibrations lead to subsequent cavitations and ventilations. The effect of compressibility on maximum local stress is likely to become small. [1]



### Free vibration phase of hydro-elastic slamming

Theoretical study has been done assuming 2D beam theory for strips of the plates. The whole plate is assumed as wetted and the structure is represented as euler beam model and it is considered that load levels do not cause plastic deformation. [1] Beam equation of motion is given by

$$M_B \frac{\partial^2 w}{\partial t^2} + EI \frac{\partial^4 w}{\partial x^4} = p(x, w, t) \quad (9)$$

P= Hydrodynamic pressure that is a function of the beam deflection

In free vibration phase slamming pressure is zero. But the pressure comes as a consequence of vibration i.e. added mass effect is considered. The solution is given by

$$w(x, t) = \sum_{n=1}^{\infty} a_n(t) \Psi_n(x). \quad (10)$$

The dry normal modes are a good approximation of the wet normal modes when the added mass distribution is similar to the mass distribution.[1]

#### 3.3.4 Slamming on rigid bodies

When the local angle at impact position between the water surface and the body surface is not very small, slamming pressures can be used in a static structural response analysis to find local slamming-induced stresses. [1] In hydrodynamic calculations body can be assumed as rigid body. Irrotational and compressible water can be assumed. Air flow is negligible. Local flow acceleration is large relative to gravitational acceleration when slamming pressure is considered. Theoretical studies are done assuming 2D vertical water entry of a symmetric body. An indicator of the importance of 3D flow effects is the ratio  $64/\pi^4 \approx 0.66$  between maximum pressures during water entry of a cone and a wedge with constant velocity and small dead rise angles [51]

There are two methods for study of slamming impact.

- Wagner method
- Von Karman Method



Von Karman method neglects the local up rise of the water, whereas a Wagner method accounts for that. Wagner method assumes impact of a blunt body. Beukelman (1991) showed on basis of experimental results for three-dimensional models that forward speed has a strong influence on the pressure level when the deadrise angle was lower than  $\approx 2^\circ$ . It is difficult numerically to handle the intersection between the body and the free surface for small local deadrise angles considering exact nonlinear free-surface conditions are used. The numerical solution is very much influenced by small intersection angle between the free surface and the body and may cause large errors in the predictions of the intersection points and destroy numerical solution. The 2D boundary element method (BEM) by Zhao and Faltinsen (1993) tackled this by introducing a control surface normal to the body surface at the spray root which may apply to a broad class of body shapes as well as time-varying water entry velocity. When it comes to 3D geometry, forward speed with incident waves, and ship-generated steady and unsteady waves make it complicated (impact analysis) to a situation that does not seem feasible to solve numerically.[1]

### **Pressure distribution**

Numerical result for water entry of rigid wedges with constant entry velocity was presented by Zhao and Faltinsen (1993) for  $4^\circ < \beta < 81^\circ$ . Figure 6 shows the predicted pressures for  $20^\circ \leq \beta \leq 81^\circ$ . In the distribution curve, for  $\beta \leq 20^\circ$  it become pronouncedly peaked and concentrated close to the spray root. As the angle goes smaller, sensitivity to pressure increases. [1]

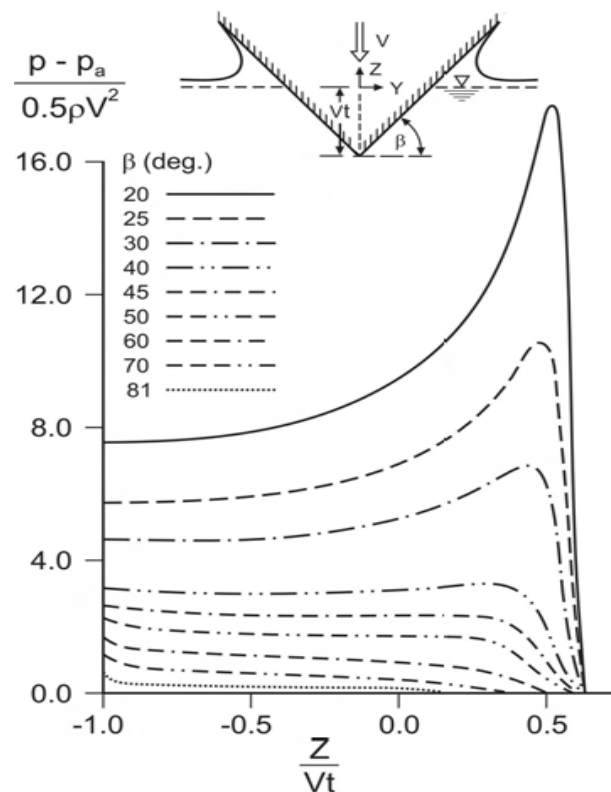


**Figure 6: Prediction of pressure distribution during water entry of a rigid wedge**

Maximum pressure occurs at the apex (or keel) when  $\beta > 45$  deg. For larger angles and low impact velocities, other pressure contributions may be as important as the slamming part. The position and value of the maximum pressure, the time duration, and the spatial extent of high slamming pressures are the parameters that characterized the slamming load on rigid body with small dead rise angle. [1]

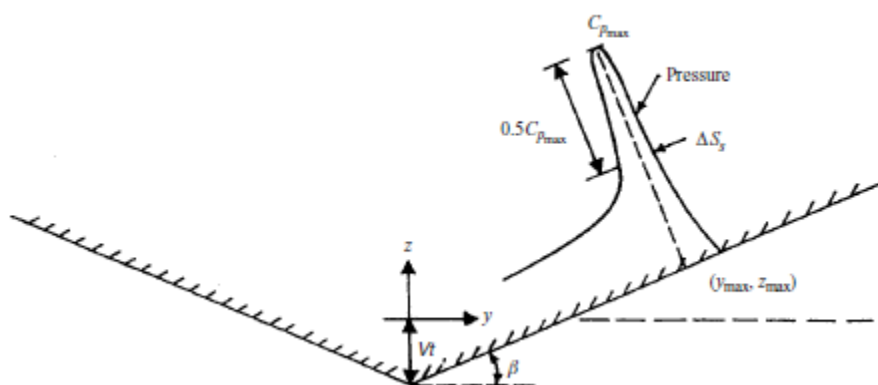


**Figure 7: Slamming pressure parameters during water entry of a blunt 2D rigid body.**



The free-surface conditions are approximated as Wagner (1932) did in the outer flow domain, that is, not for the details at the spray roots. The wetted body surface is found by integrating in time the vertical velocity of the fluid particles on the free surface and determining when the particles intersect with the body surface. This is done by predetermining the intersection points on the body and then determining the time to reach these points in a time-stepping procedure. Because the velocity in the generalized Wagner method is singular at the body-water surface intersection, special care is shown by using a local singular solution. Direct pressure integration is used to predict the water entry force. [1]

### Water entry force

Theoretical slamming force due constant water entry velocity for wedge is given below.

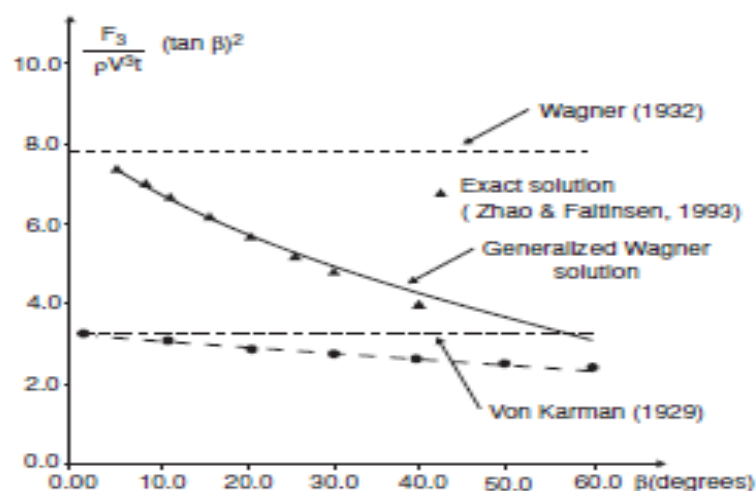


**Figure 8: The vertical slamming force on symmetric wedge**

Different methods are used and related to an exact solution of the potential flow incompressible water entry problem without gravity. For small dead rise angle Wagner's flat plate approximation stands quite well. A von Karman type of solution clearly under predicts the force for  $\beta < \approx 30^\circ$  to  $40^\circ$  [1]





## Asymmetric impact

A hull structure may have asymmetric transverse sections, hence the hull may be tilted, the water surface may be sloping, and/or the structure may have both a horizontal and vertical velocity during an impact. If asymmetric water entry of a wedge is considered, the occurrence of cross-flow at the apex is always expected initially to cause a ventilated area near the apex of the wedge. One side of the wedge could be fully ventilated, depending on heel and dead rise angle, and the velocity direction of the body. Flow separation from the apex associated with viscosity may occur if partial ventilation occurs only initially. de Divitiis et al. [52] studied the unsymmetrical impact of wedges with constant velocity by means of a similarity solution. Flow is assumed as irrotational and incompressible.[1]

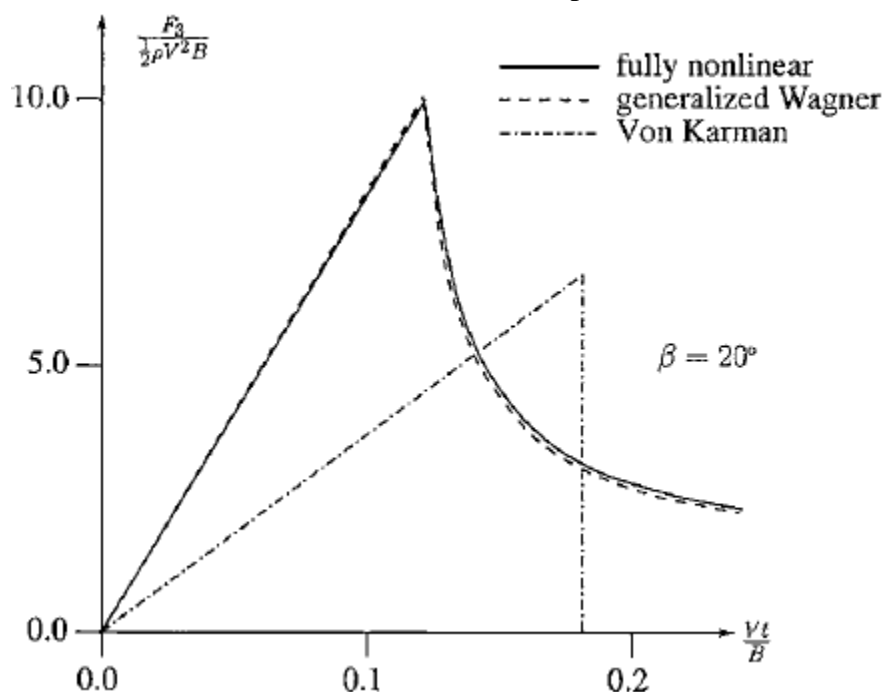


**Figure 9: Vertical slamming force on a wedge with knuckles. Dead rise angle is 20 deg.**

Figure 9 shows non dimensional time between the predicted peaks by the different methods is an effect of the up rise of water.

The symmetry axis of the wedge is vertical, and the water entry velocity has a horizontal component  $U$  and a vertical component  $V$ . Depending on the deadrise angle  $\beta$  and the direction of the velocity,  $\alpha = \tan^{-1} V/U$ , the flow can separate from the wedge apex and be fully ventilated on the leeward side of the wedge. If  $\beta > 45^\circ$ , the critical value  $\alpha^*$  of  $\alpha$  for separation to occur is very small, whereas  $\alpha^* = 60^\circ$  for  $\beta = 7.5^\circ$ . When the flow separates from the wedge, it is similar to water entry of a flat plate.



### 3.3.5 Wagner's slamming model

Wagner's [53] slamming model discussed in-depth in this section. Wagner's model assumes a local small dead rise angle but it provides simple analytical results. This model provides good understanding how slamming pressures depend on structural form and time-dependent water entry velocity. This model also shows it is the space-averaged pressure that matters for structural stresses.[1]

Flow at the intersections between the free surface and the body surface does not discussed in detail in this model. Local flow which is normally a flow –ends up as spray. Outer flow domain is located below (outside) the inner and jet domains shown in figure 10.

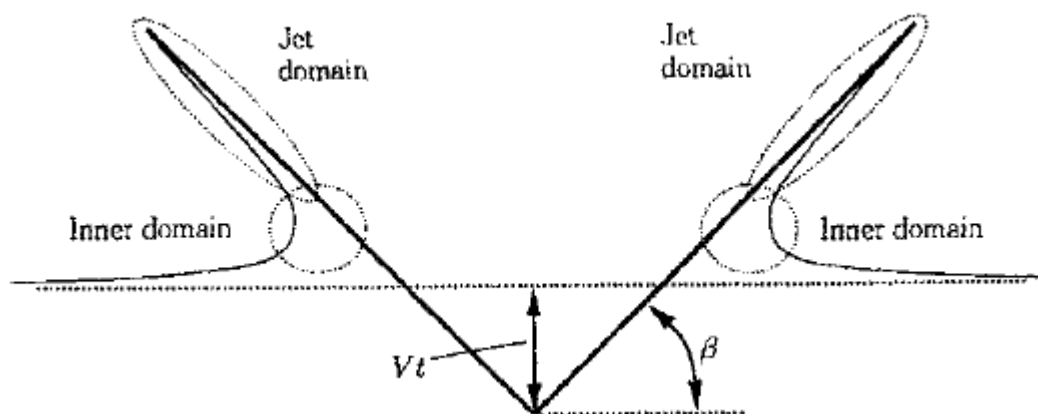


**Figure 10: Water entry of a wedge with constant velocity  $V$ . Definition of inner and jet flow domains.**

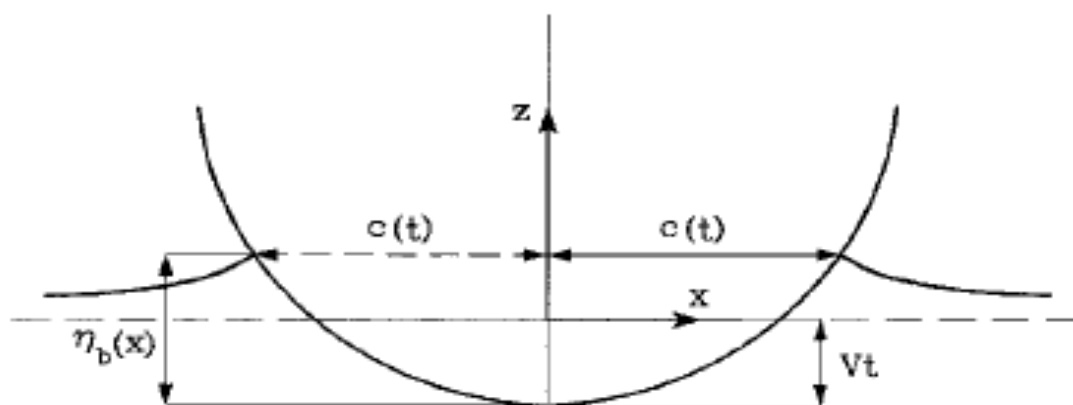


**Figure 11: Definition of parameters in analysis of impact forces (Wagner model)**



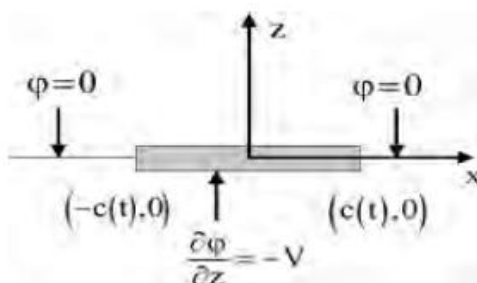
Parameters are defined for impact forces and pressures on a body by means of wagner's outer flow domain solution.

$V$  = Constant water entry velocity.

$V_t$  = Instantaneous draft relative to the undisturbed free surface.

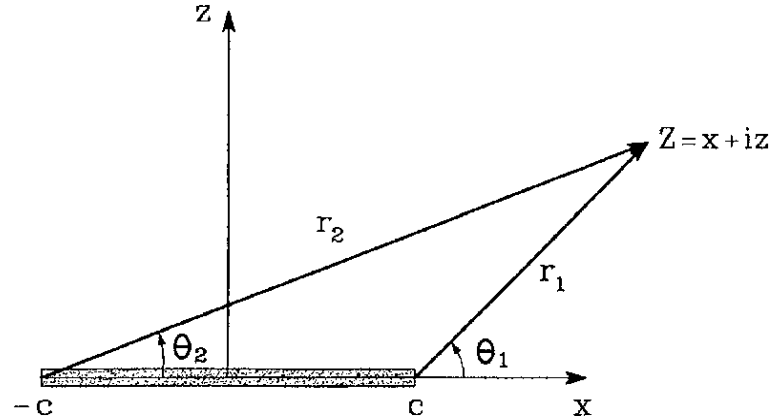
The predicted intersections in the outer flow domain model between the free surface and the body surface are in a very close vicinity of the spray roots. Figure 11 shows the impacting symmetric body and the free surface in the outer flow domain. It also shows there is an up rise of the water caused by the impact. The volume of the water above  $z = 0$  is equal to the volume of water that the body displaces for  $z \leq 0$ . The difference between the von Karman and Wagner methods is that a von Karman method neglects the local up rise of the water which means the wetted surface length is smaller. [1]

Figure 12 presents the boundary-value problem that must be solved at each time instant. The body boundary condition requiring no flow through the body surface is transferred to a straight line between  $x = -c(t)$  and  $c(t)$  using Taylor expansion. As the body is blunt local dead rise angle which is the angle between the  $x$ -axis and the tangent to the body surface is small. The end points  $x = \pm c$  correspond to the instantaneous intersections between the outer flow free surface and the body surface shown in figure 11.



**Figure 12: Boundary-value problem for the velocity potential in simplified analysis.**

Free-surface condition  $\phi = 0$  on  $z = 0$  has been used as a consequence of fluid accelerations in the vicinity of the body dominating over gravitational acceleration during impact of a blunt body. [1]



**Figure 13: Definition of polar co-ordinates  $(r_1, 1)$  and  $(r_2, 2)$  used in evaluating the complex function.**

In an earth-fixed co-ordinate system with positive  $Z$ -axis upward, Euler equation states that

$$\frac{\partial \mathbf{u}}{\partial t} + \mathbf{u} \cdot \nabla \mathbf{u} = -\frac{\nabla p}{\rho} - g\mathbf{k} \quad (11)$$

$\mathbf{u}$  is the fluid velocity,  $p$  is the pressure, and  $\mathbf{k}$  is the unit vector along the  $z$ -axis. Both  $\mathbf{u} \cdot \nabla \mathbf{u}$  and  $g\mathbf{k}$  are small relative to  $\partial \mathbf{u} / \partial t$ .

$$\rho \frac{\delta \mathbf{u}}{\delta t} = -\nabla p \quad (12)$$

Substituting  $\mathbf{u} = \nabla \phi$  gives that (Approximation)

$$\nabla \left( \rho \frac{\partial \phi}{\partial t} + p \right) = 0. \quad (13)$$

If we assume no surface tension and atmospheric pressure  $p_a$  on the free surface

$$p - p_a = -\rho \frac{\partial \phi}{\partial t}$$

Because  $p = p_a$  on the free surface, we get that  $\partial \phi / \partial t = 0$  on the free surface. Finally it then is to assume small deviations between  $\phi$  on  $z = 0$  and the free surface and transfer this condition to  $z = 0$ , by Taylor expansion.

The complex velocity potential can be expressed as

$$\Phi = \phi + i\psi = iVZ - iV(Z^2 - c^2)^{1/2}. \quad (14)$$

$\phi$  is the velocity potential and  $\psi$  is the stream function.



Complex velocity is given by

$$\frac{d\Phi}{dZ} = u - iw = iV - iV \frac{Z}{(Z^2 - c^2)^{1/2}} \quad (15)$$

Introducing  $Z - c = r_1 e^{i\theta_1}$  and  $Z + c = r_2 e^{i\theta_2}$ , where  $\theta_1$  and  $\theta_2$  vary from  $-\pi$  to  $\pi$

$$(Z^2 - c^2)^{1/2} = \sqrt{r_1 r_2} e^{i\frac{1}{2}(\theta_1 + \theta_2)}.$$

We can write  $\theta_1 = -\pi$  and  $\theta_2 = 0$  when  $|x| < c$  and  $z = 0^-$

$$(Z^2 - c^2)^{1/2} = -i(c^2 - x^2)^{1/2} \quad \text{for } |x| < c, z = 0^-.$$

When  $x > c$  and  $z = 0$ , both  $\theta_1$  and  $\theta_2$  are zero

$$(Z^2 - c^2)^{1/2} = (x^2 - c^2)^{1/2} \quad \text{for } x > c, z = 0$$

For  $x < -c$  and  $z = 0$  means that  $\theta_1 = \theta_2 = \pi$

$$(Z^2 - c^2)^{1/2} = -(x^2 - c^2)^{1/2} \quad \text{for } x < -c, z = 0.$$

For,  $\phi = 0$  for  $|x| > c$  on  $z = 0$

$$\frac{d\Phi}{dZ} = u - iw = iV + V \frac{x}{(c^2 - x^2)^{1/2}}$$

Velocity potential can be written as

$$\phi = -V(c^2 - x^2)^{1/2}, \quad |x| < c(t)$$

Pressure equation can be written as

$$p - p_a = \rho V \frac{c}{(c^2 - x^2)^{1/2}} \frac{dc}{dt} + \rho \frac{dV}{dt} (c^2 - x^2)^{1/2} \quad (16)$$

The first term is denoted as the slamming pressure.

It is associated with the rate of change of the wetted surface which is approximately  $2dc/dt$ .

The two-dimensional vertical force acting on the impacting body can be expressed as



$$\begin{aligned}
 F_3 &= \int_{-c}^c p dx = \rho V c \frac{dc}{dt} \int_{-c}^c \frac{dx}{\sqrt{c^2 - x^2}} + \rho \frac{dV}{dt} \int_{-c}^c \sqrt{c^2 - x^2} dx \\
 &= \rho \pi V c \frac{dc}{dt} + \rho \frac{\pi c^2}{2} \frac{dV}{dt}
 \end{aligned}
 \tag{17}$$

The term  $\rho \pi c^2/2$  appearing in the last term is the two-dimensional added mass in heave  $a_{33}$

$$F_3 = \frac{d}{dt}(a_{33}V) = a_{33} \frac{dV}{dt} + V \frac{da_{33}}{dt}
 \tag{18}$$

Second term in the above equation is the slamming force. This is a common way to express the slamming force in connection with the von Karman method.[1]

### 3.3.6 Design pressure on rigid bodies

If the dead rise angle is small, one should not put too much emphasis on the peak pressures. It is the pressure integrated over a given area that is of interest in structural design as long as hydro elasticity does not matter. When hydro-elasticity matters, maximum pressures cannot be used to estimate structural response. [1]

For better illustration of average pressures appropriate for the design of a local rigid structure, we can consider a structural part shown on the following figures.

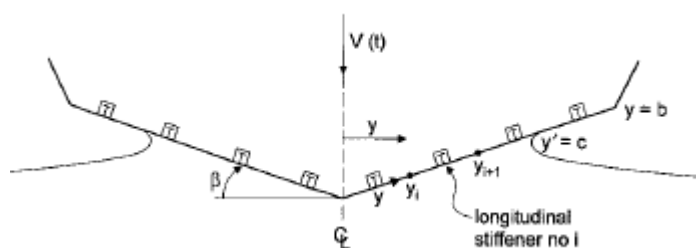


**Figure 14: Water entry of a wedge shaped elastic cross section**

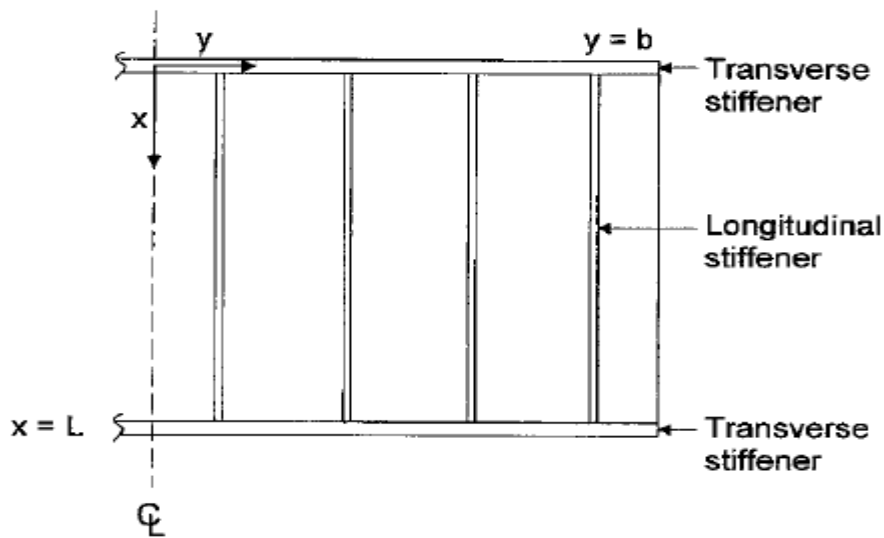


**Figure 15: Stiffened panel consisting of plate and longitudinal stiffener.**

By assuming the transverse frame to be much stiffer than the longitudinal stiffener, the resulting stresses in the longitudinal stiffener are normally more important than those in the transverse frame. If the  $x$ -direction means the longitudinal direction of the ship, the instantaneous slamming pressure does not vary much with the position  $x$  between two transverse frames. The instantaneous loads of importance for the stresses in the longitudinal stiffener number  $i$  is then the space averaged slamming pressure is the first approximation  $y_i$  and  $y_{i+1}$  (Figure 14). This space averaged pressure varies with time, and it is the largest value that is the prime importance. Wagner's [53] solution is used for water entry of a wedge to find the space-averaged pressure assuming the dead rise angle to be small. The space-averaged pressure from  $y_i$  to  $y_{i+1}$  has a maximum when  $c = y_{i+1}$ . The maximum value is given by,

$$\begin{aligned}
 p_{av}^{\max} - p_a &= 0.5\rho V^2 \frac{\pi}{\tan \beta} \left( \frac{y_{i+1}}{y_{i+1} - y_i} \right) \\
 &\quad \times \left( \frac{\pi}{2} - \sin^{-1} \left( \frac{y_i}{y_{i+1}} \right) \right). \tag{19}
 \end{aligned}$$



### 3.3.7 Effect of air cushions on slamming

When a body with a horizontal flat bottom or a small deadrise angle hits a horizontal free surface, a compressible air pocket is created between the body and the free surface in an initial phase (Figure 16)



**Figure 16: Deformation of the free surface and formation of an air pocket during entry of a rigid body**

$\phi$  = velocity potential for the water motion,  
 $U_n^T$  = normal velocity of air pocket.

The pressure in the air cushion will in reality deform both the structure and the free surface. The scenario in Fig 1.13 for an air cushion may have too short a duration for the detailed behavior to influence the maximum slamming induced structural stresses. However, air pockets may be created as a consequence of the shape of the impacting free surface. One scenario could be plunging breaking waves against the ship side. This causes an air cushion in a 2D flow situation. However, the air has the possibility to escape in a 3D flow situation. Another scenario is in connection with wet deck slamming (Figure 16) [1]

### 3.3.8 Impact of a fluid wedge and green water

Theoretical results for slamming pressures on a rigid vertical wall due to an impacting fluid wedge with interior angle  $\beta$  and velocity  $V$ . Results are based on neglecting gravity- it does not need to be a vertical wall but can be any flat surface perpendicular to the impacting fluid wedge. If the interior angle  $\beta$  is close to  $90^\circ$ , we could obtain similar results by using a Wagner-type analysis.[1]



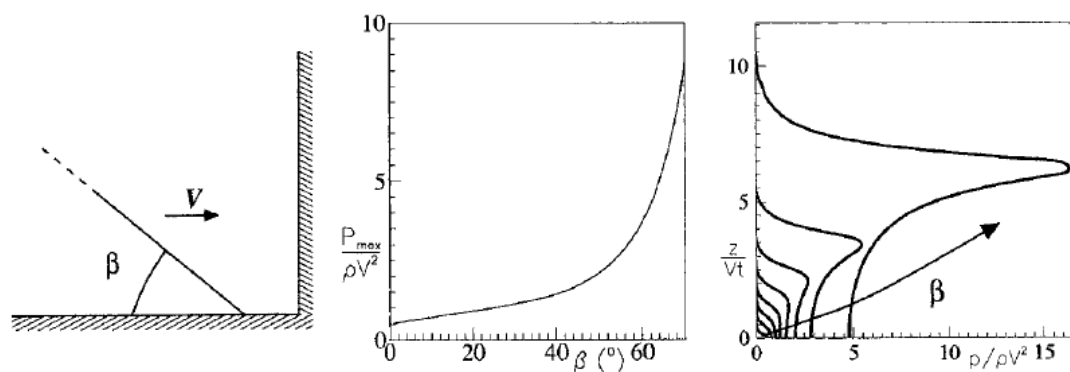


**Figure 17: Impact of fluid wedge and green water**

First from Left: sketch of the equivalent problem of a fluid (half) wedge impacting a flat wall at  $90^\circ$ .

Center: maximum pressure on a wall due to the water impact.

Right: pressure distribution along the vertical wall for  $5^\circ \leq \beta \leq 75^\circ$  with increment  $\beta = 10^\circ$ .

The results are numerically obtained by neglecting gravity and using the similarity solution by Zhang et al. [54]

### 3.3.9 Global wet deck slamming effects

Global structural strength of ship is influenced by the slamming effect. For mono hull vessels, these effects are associated with bow flare slamming effects. Transient heave, pitch and global vertical elastic vibrations are excited because of the wet deck slamming. The dominant elastic vibrations in head sea are in terms of two node longitudinal vertical bending. The phenomenon is called whipping and also induces global shear forces, bending moments and stresses.[1]

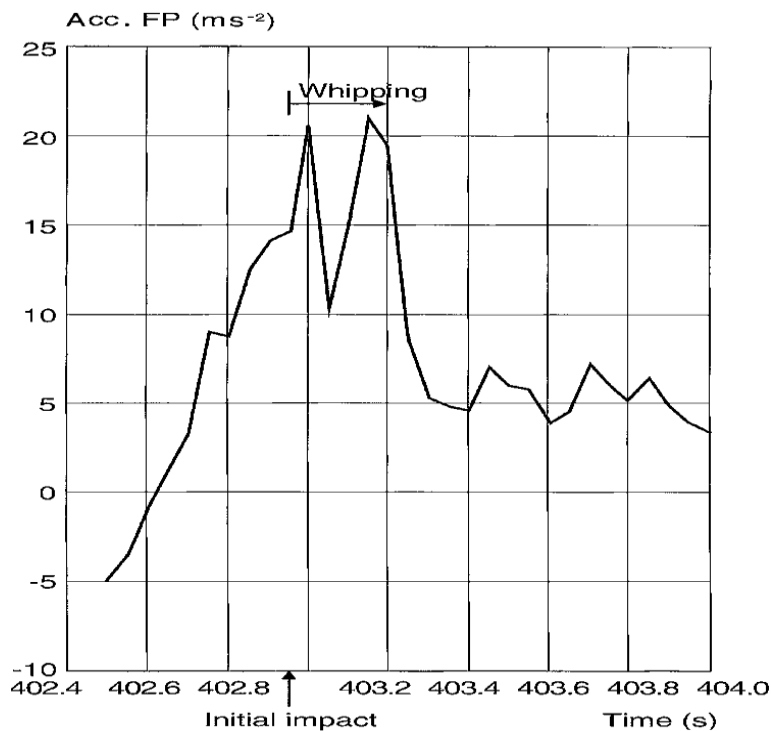


**Figure 18: Measured vertical acceleration at the forward perpendicular (FP) of the ulstein test catamaran.**

Figure 18 shows a full scale measurement of vertical accelerations at the bow of the 30-m long Ulstein test catamaran in head sea conditions with significant wave height  $H_{1/3} = 1.5$  m. The forward speed was 18 knots and the vessel was allowed to operate up to  $H_{1/3} = 3.5$  m.[1]

The natural period of the global two-node bending is of the order of 1 s when whipping matters because local hydro-elastic slamming has typically a time scale of the order of 10–2s. It is considered that the structure locally rigid in the global structural analysis. Slamming effect on the structural strength of a ship is considered in case of head sea and longitudinal vertical bending about a transverse axis.[1]

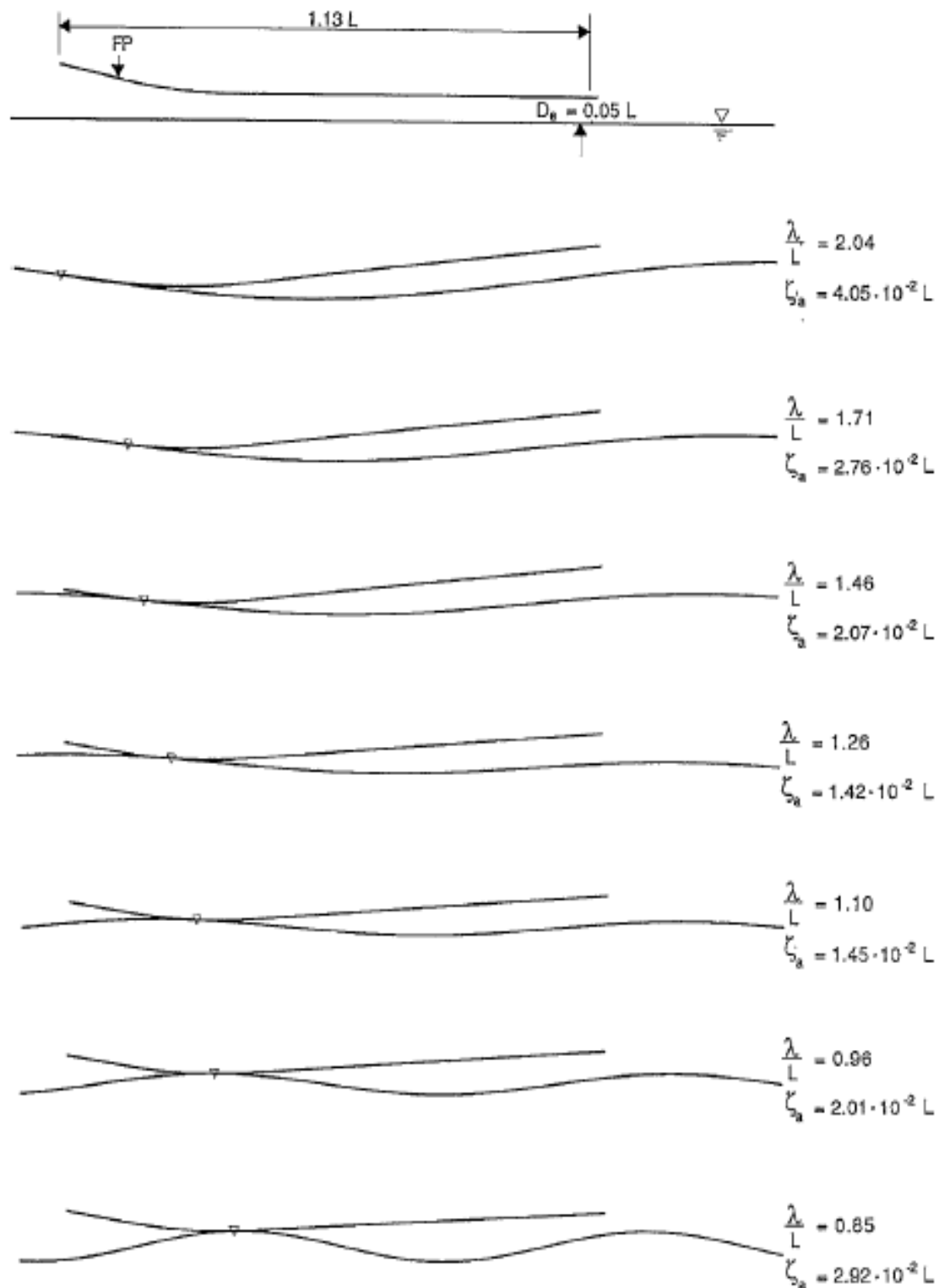


**Figure 19: Position of slamming on the wet deck in regular head sea waves as a function of wave length.**



The figure shows a longitudinal cross section at the centerplane of the catamaran. The bow ramp is seen in the fore part.  $Fn = 0.5$ ,  $\zeta a = \zeta_{slam}$  = lowest incident wave amplitude when slamming occurs,  $L = LPP$  = length between perpendiculars. Figure 19 show that the longer the wavelengths are, the closer to the bow the initial impact occurs. The figure also presents the minimum wave amplitude  $\zeta a$  for slamming to occur for a given incident wavelength. This minimum wave amplitude is smallest for  $\lambda/L=1.26$  for the current cases. The smaller the minimum wave amplitude, the larger the amplitude of the relative vertical motion divided by  $\zeta a$ . When the water does not initially hit at the end of the forward deck, the water surface has to be initially tangential to the wet deck surface at the impact position.[1]

### 3.3.10 Water entry and exit loads

Both the water entry and water exit phases is the concern in The global slamming analysis. This is the combination of both wagner and Von karman method.

Assumptions:

- Incident regular head sea waves act on a catamaran at forward speed
- The wet deck has a plane horizontal transverse cross section

In Von Karman method wetted area can be found by examining the relative vertical displacement

$$\eta_R = \eta_B(x, t) - \zeta_a \sin(\omega_e t - kx) + h(x). \quad (20)$$

$h(x)$ = time-independent wet deck height above calm water

$\eta_B(x,t)$ = vertical ship motion, which includes global elastic vibrations in addition to rigid body heave and pitch motions. For  $\eta_x$  is less than zero slamming occurs.

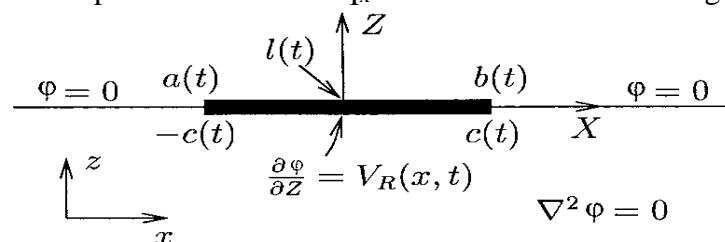


**Figure 20:2D boundary value problem for velocity potential due to wet deck slamming**

$a(t)$ ,  $b(t)$  and  $l(t)$  are ship fixed  $x$ -coordinates.  $X$ - $Z$  is the local 2D coordinate system on the wetted part of the deck.



Figure 20 shows the boundary value problem that we have to solve at each time instant to find the velocity potential  $\phi$  due to slamming

$$V_R = \frac{\partial \eta_B}{\partial t} - U \left( \tau - \frac{\partial \eta_B}{\partial x} \right) - \omega_0 \zeta_a \cos(\omega_e t - kx)$$

Here  $\eta_B = \eta_3 - x\eta_5$  and  $\partial \eta_B / \partial x = -\eta_5$  in the case of no global elastic vibrations. The second term is the velocity component of  $U$  normal to the wet deck. The angle  $\tau$  expresses the local geometry, for example, due to the bow ramp and also includes the trim due to hydro-elastic and steady forward speed dependent hydrodynamic forces on the vessel in calm water. There is also a contribution from the time averaged non-linear hydrodynamic loads due to unsteady wave body interaction. The former effect is normally neglected.[1]

As the wetted length is small relative to the incident wavelength, so we can do the approximation,

$$V_R = V_1 + V_2 X.$$

This follows by keeping the constant and linearly varying terms of a Taylor expansion of  $V_R$  about  $X = 0$  as the flow associated with  $V_2 X$  in is anti-symmetric about  $X = 0$ ,  $V_2$  does not contribute to the vertical force.

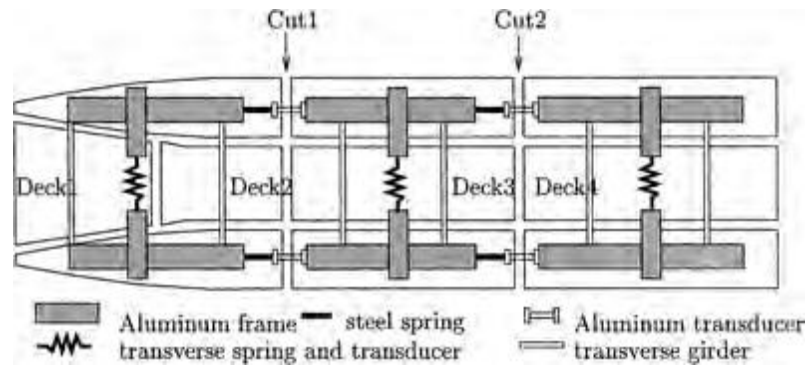


**Figure 21: Outline of the experimental hull arrangements (top view) ( Ge 2002)**

Froude-kriloff and hydrostatic forces on the wet deck will also contribute, which are generally smaller than the slamming and added mass forces. Assuming that the incident free-surface  $\zeta = \zeta_a \sin(\omega_e t - kx)$  is higher than  $\eta_B + h(x)$ , buoyancy force is given by

$$F_{3,buoy} = \rho g B \int_{a(t)}^{b(t)} [\zeta_a \sin(\omega_e t - kx) - \eta_B - h(x)] dx. \quad (21)$$



### 3.3.11 Three-body model

Ge et al. [55] studied numerically and experimentally wet deck slamming induced global loads on a catamaran in head sea deep-water regular waves. The model is shown in figure 21. Theoretically the pre-mentioned vessel can be modeled as three rigid bodies with longitudinal connections of elastic beams as shown in the figure 22 below.

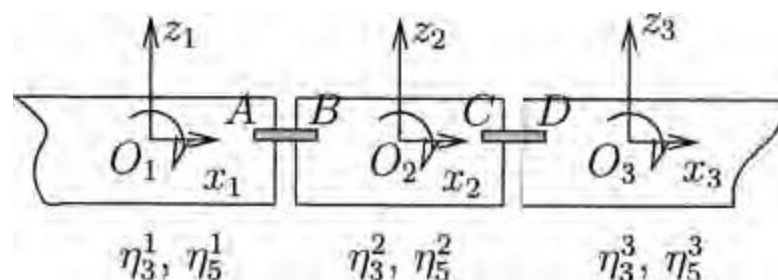


**Figure 22: Degrees of freedom of segmented model**

The general equation system for the motion of the hull segments can be expressed as

$$\mathbf{M}_{gen}\ddot{\mathbf{r}} + \mathbf{B}_{gen}\dot{\mathbf{r}} + \mathbf{K}_{gen}\mathbf{r} = \mathbf{F}_{gen}(\mathbf{r}, \dot{\mathbf{r}}, \ddot{\mathbf{r}}, t)$$

$\mathbf{r}$ = displacement matrix of this six degrees- of-freedom system, containing the heave and pitch for each segment

$\mathbf{M}_{gen}$ = Mass matrix, mass refers to both the segment mass and the added mass

$\mathbf{B}_{gen}$ = damping matrix

$\mathbf{K}_{gen}$ = restoring (stiffness) matrix, including the hydrostatic restoring terms from the ship segments as well as the coupling terms from the spring beams

$\mathbf{F}_{gen}$ = forces due to wet deck slamming and linear wave excitation loads on the side hulls

The static beam equation with zero loading is

$$EI \cdot d^4w/dx^4 = 0,$$

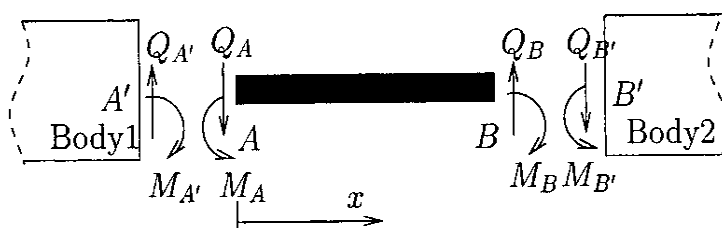


**Figure 23: Elastic connection between two adjacent rigid body segments**



The connecting beam AB between body 1 and body2 is used to illustrate the procedure (Figure 23).  $x=0$  and  $L$  correspond to, respectively, point A and point B. Integrating above equation

$$w(x) = \frac{1}{EI} \left( \frac{1}{6}ax^3 + \frac{1}{2}bx^2 + cx + d \right)$$

The boundary conditions of the beam require that the vertical and rotational displacements at the ends of A and B match those at the adjacent ends of body 1 and body 2, so

$$\begin{aligned} w|_A &= \eta_3^1 - \overline{O_1 A} \eta_5^1 \\ w|_B &= \eta_3^2 + \overline{O_2 B} \eta_5^2 \\ \left. \frac{\partial w}{\partial x} \right|_A &= -\eta_5^1 \\ \left. \frac{\partial w}{\partial x} \right|_B &= -\eta_5^2 \end{aligned}$$

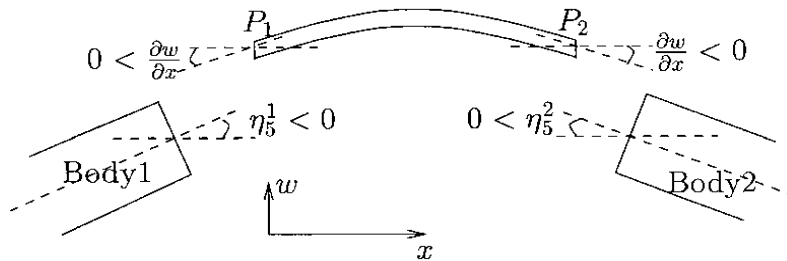


**Figure 24: Illustration of rotational sign for and adjacent bodies**

The longitudinal distribution of vertical shear force  $Q(x)$  and bending moment  $M(x)$  at the right hand side of the beam element

$$\begin{aligned} Q(x) &= -EI \frac{\partial^3 w}{\partial x^3} = -a \\ M(x) &= -EI \frac{\partial^2 w}{\partial x^2} = -ax - b \end{aligned}$$

at  $x=0$  and  $L$ , the loads acting on the three rigid bodies due to the connecting beams can then be expressed as

$$\begin{pmatrix} F_3^1 \\ F_5^1 \\ F_3^2 \\ F_5^2 \\ F_3^3 \\ F_5^3 \end{pmatrix} = \begin{pmatrix} Q_A \\ M_A - Q_A \overline{O_1 A} \\ Q_C - Q_B \\ M_C - M_B - Q_B \overline{O_2 B} - Q_C \overline{O_2 C} \\ -Q_D \\ -M_D - Q_D \overline{O_3 D} \end{pmatrix} = \mathbf{kr} \quad (22)$$



There are six degrees of freedom and thus six pairs of eigenmodes and frequencies. The two lowest modes with lowest natural frequencies are the coupled heave and pitch modes. The important stiffness of these modes are the result of the hydrostatic restoring coefficients.[1]

The third and fourth modes are the two node and three node bending modes in the longitudinal vertical plane and are illustrated in figure 25,

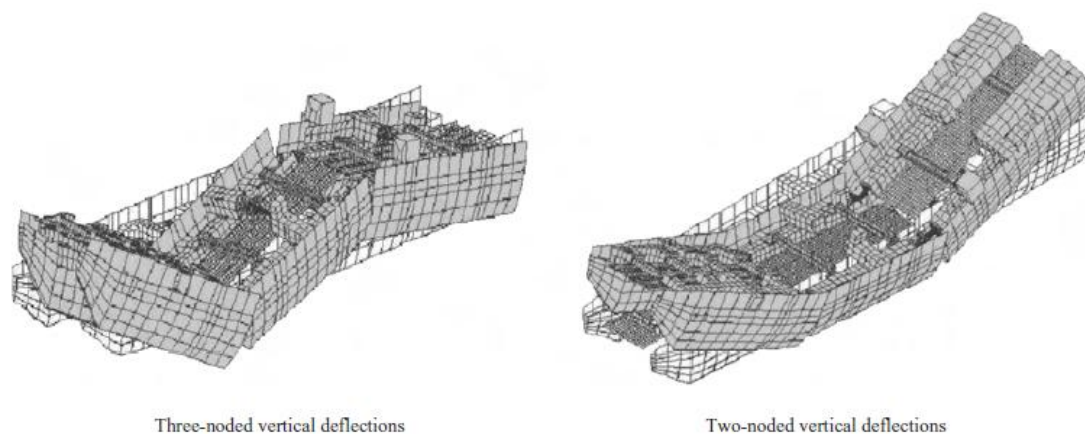


**Figure 25: Calculated shapes of eigen modes for 3-body model.**

The illustration is based on a finite element model, which is really not necessary for finding the required modes for a segmented model such as this. However a finite element model is needed to find the modes for a real ship. The fifth and sixth modes have very high natural frequencies relative to the other modes and are in reality highly structurally damped.

Steady-state experimental and numerical vertical shear force (VSF) and vertical bending moment (VBM) at cut 1 in regular head sea waves for the most severe slamming case obtained for the model presented in figure 26. . The dominant contributions are the result of the two node bending mode, but there are also noticeable rigid-body effects. The Froude number is  $Fn = 0.29$ , the wave period is  $T = 1.8$  s and the incident wave amplitude is 0.041 m.[1]



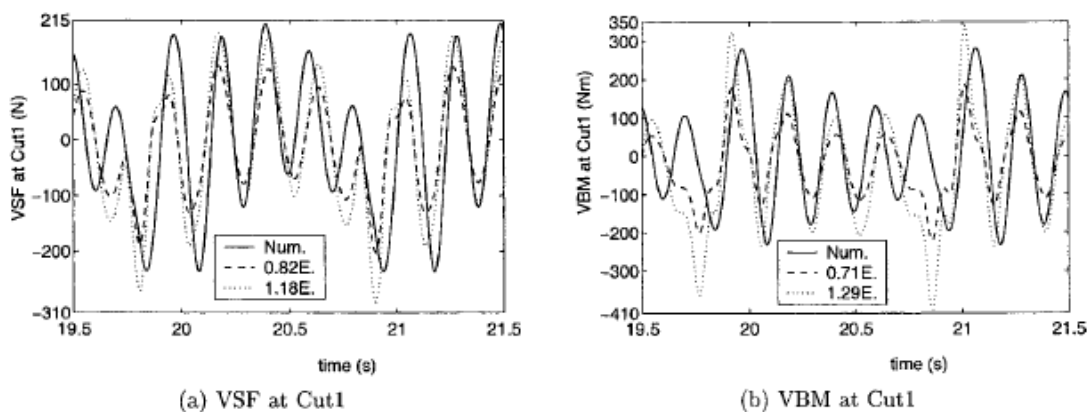


**Figure 26: Comparison between experimental and numerical value.**

### 3.3.12 Global Hydro-elastic effects on mono-hulls

Beam equations are considered to describe the global hydroelastic effects on monohulls. Timoshenko model accounts for the shear deformation and rotational inertia, but is more complicated than the Euler beam model and does not predict much difference when it comes to bending moments. The effect of shear deformation should be included, especially when higher modes are important.

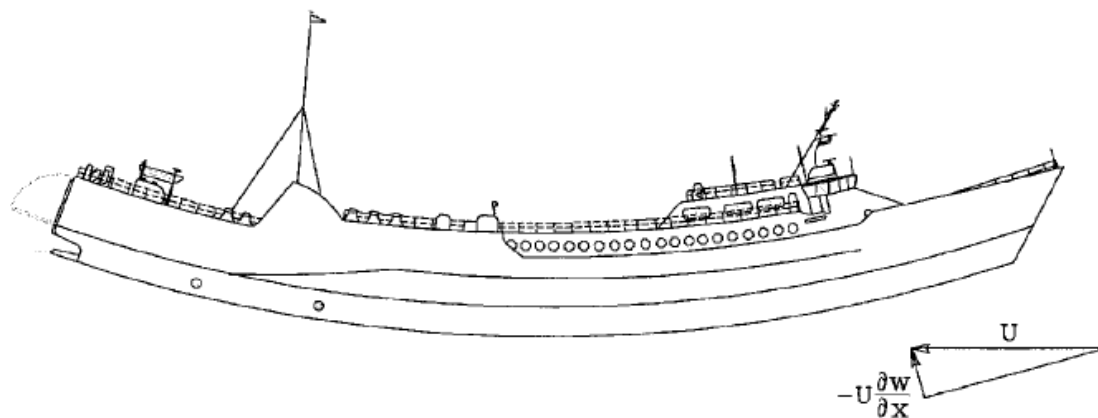


**Figure 27: Ship vibrating with two-node deformation.**

$w$  = deformation

The  $x$ -axis is in the direction of the inflow velocity  $U$ .  $U$  = ship speed.

Using Euler beam model

$$m(x) \frac{\partial^2 w}{\partial t^2} + \frac{\partial^2}{\partial x^2} \left[ EI(x) \frac{\partial^2 w}{\partial x^2} \right] = f_3(x, t) \quad (23)$$



Assuming that the deformation is small or rather that  $\partial w/\partial x \ll 1$ .  $m(x)$  is the body mass per unit length, and  $EI(x)$  is the bending stiffness and  $f_3$  is time-dependent vertical hydrodynamic force per unit length. The end conditions are zero shear force and bending moment at the forward and aft ends of the ship.

$$\frac{\partial^3 w}{\partial x^3} = 0 \quad \text{and} \quad \frac{\partial^2 w}{\partial x^2} = 0 \quad \text{at the end of the ship.}$$

First we neglect excitation and express the contributions to  $f_3$  due to linear hull vibrations. We are interested in oscillations with clearly higher frequencies than typical frequencies of encounter due to incident waves, it is appropriate to use the free-surface condition  $\phi = 0$  on the mean free surface  $z = 0$ .  $\phi$  satisfies the 2D Laplace equation in the transverse cross-sectional plane of the ship. The vibrations cause a local angle  $\partial w/\partial x$  of the ship relative to the  $x$  axis. This angle implies that the steady flow with velocity  $U$  along the  $x$ -axis has a velocity component  $-U\partial w/\partial x$  in the cross-sectional plane of the vibrating ship. we must account for the vibrating velocity  $\partial w/\partial t$  in formulating that there is no flow through the hull surface.[1] Linear body boundary condition is given by,

$$\frac{\partial \phi}{\partial n} = n_3 \left( \frac{\partial w}{\partial t} + U \frac{\partial w}{\partial x} \right) \quad \text{on } C(x) \quad (24)$$

$C(x)$ = mean submerged cross-sectional curve of the hull surface

$n = (n_1, n_2, n_3)$ , the normal vector to the hull surface with positive direction into the fluid

A normalized velocity potential  $\phi_3$  is given by

$$\phi = \phi_3 \left( \frac{\partial w}{\partial t} + U \frac{\partial w}{\partial x} \right)$$

Linear hydrodynamic pressure *on* the hull is given by

$$p = -\rho \frac{\partial \phi}{\partial t} - \rho U \frac{\partial \phi}{\partial x}$$

Hence The 2D vertical force  $f_3^{HD}$  on the hull due to the dynamic pressure

$$f_3^{HD} = - \left( \frac{\partial}{\partial t} + U \frac{\partial}{\partial x} \right) \left[ a_{33} \left( \frac{\partial w}{\partial t} + U \frac{\partial w}{\partial x} \right) \right]$$

$a_{33}$  = 2D infinite-frequency added mass in heave.

Introducing the change of buoyancy due to the beam deflection,



$$(m+a_{33}) \frac{\partial^2 w}{\partial t^2} + 2a_{33}U \frac{\partial^2 w}{\partial x \partial t} + U \frac{da_{33}}{dx} \frac{\partial w}{\partial t} + U^2 \frac{\partial}{\partial x} \left( a_{33} \frac{\partial w}{\partial x} \right) + \rho g b w + \frac{\partial^2}{\partial x^2} (EI \frac{\partial^2 w}{\partial x^2}) = f_3^{exc} \quad (25)$$

Here  $b$  means sectional beam and  $f_3^{exc}$  is the hydrodynamic excitation load per unit length. Lewis form technique is a simple way to estimate  $a_{33}$ . The expression for infinite frequency is

$$a_{33} = \rho 0.5\pi ((a + aa_1)^2 + 3(aa_3)^2)$$

Where

$$aa_1 = 0.5(0.5b - d)$$

$$aa_3 = -0.25(0.5b + d)$$

$$+ 0.25 \sqrt{(0.5b + d)^2 - 8(2A/\pi - 0.5bd)}$$

$$a = 0.5(0.5b + d) - aa_3$$

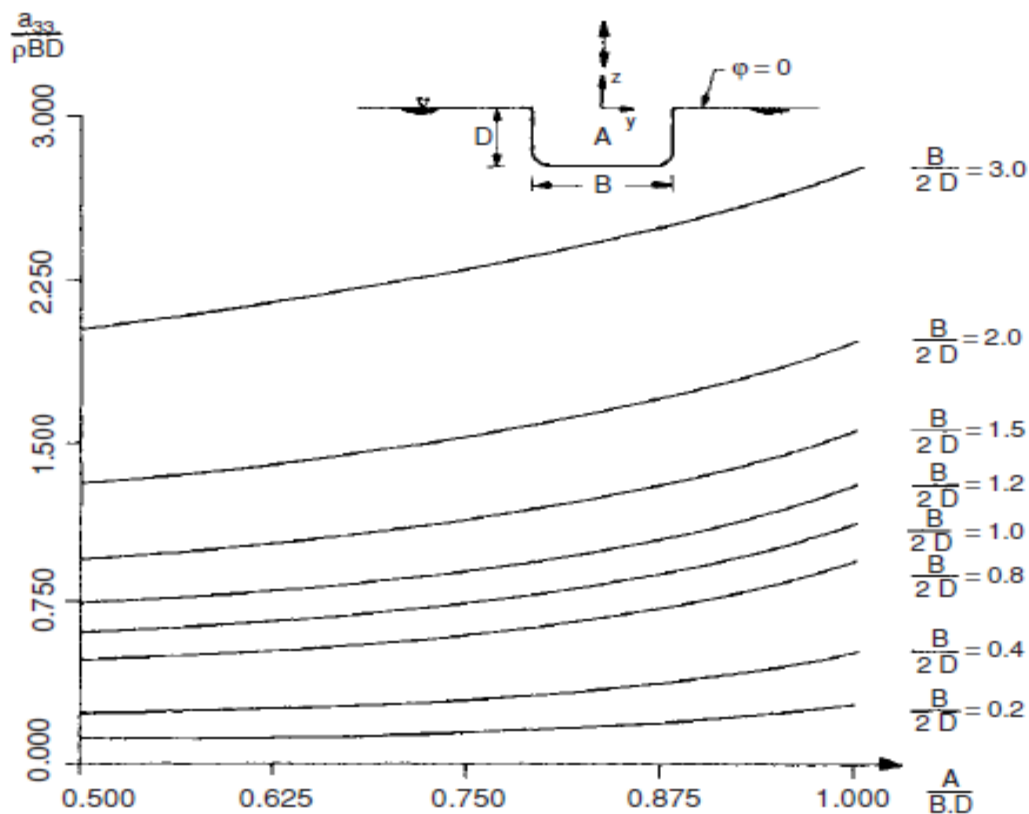


**Figure 28: 2D added mass in heave for Lewis form sections**

The diagram given above is considering the frequency of oscillation.[1]

$A$  = cross-sectional area,  $B$  = beam,  $D$  = draft,  $\phi$  = velocity potential.



## 4 Wave induced responses

The fundamental elements of a vibrating system include the basic mass-elastic properties as well as damping and exciting forces. In order to control or limit the vibratory response it is necessary to modify the mass-elastic properties by increasing the damping, reducing the exciting forces or changing the exciting frequencies. Increasing the damping may be useful in the solution of local structural vibration problems and in certain machinery and equipment problems but is not a practical solution for reducing hull girder vibration. The wave induced response of ships and floating offshore structures might occur in two different forms denoted as springing and whipping. Whipping is characterized by transient vibration response caused by slamming impulses, and springing represents a resonant periodic vibration response to high frequency harmonic wave excitation components. The analysis methods only for whipping vibration response are briefly discussed.

### 4.1 Hull Structural response

Structural model must reflect the hull's dynamic properties in the frequency range of interest, i.e. the natural frequencies, the associated mode shapes and, last but not least, the damping characteristics. Depending on the application a variety of methods is used for this purpose:

- a) Dynamic amplification factors in combination with quasi-static calculations,
- b) Analytical formulae valid for impulsively or harmonically excited vibrations of 1- or 2-DOF systems,
- c) Timoshenko beam FE models reflecting one or several hull girder vertical bending modes,
- d) As like as c) but extended to simulate also torsional and horizontal bending vibration modes,
- e) 3D FE models of the complete hull for more complex hull structures, f) as e) but with local FE mesh refinements for specific assessment purposes, e.g. stress concentration effects or local deck panel vibration. The prediction methods for wave induced vibration can be classified in coupled (hydro-elastic) and decoupled approaches. Decoupled methods neglect the influences of hull elasticity and hull vibration displacements on the magnitude of the impulsive or harmonic hydrodynamic pressure excitation forces.



Coupling between hydrodynamic analysis and structural response calculation is normally realised by integrating the structural model into the hydrodynamic excitation force analysis. Hull models according c), d), and e) are used for this purpose. In most applications the hull FE models are replaced by modal representations for the sake of computation efficiency. Normally, only a few of the first natural modes of the hull girder are required to describe the dynamic response of the hull with sufficient accuracy.

## 4.2 Whipping vibration analysis

Hull whipping response magnitude due to slamming impulses mainly depends on the strength and location of the slamming impulse. The ratio of the impulse duration to the natural period of the relevant hull girder vibration mode and the shape of the time history of the impulsive force determine the grade of dynamic magnification of the quasi-static response. In structural dynamics the dynamic amplification factor (DAF) is often used to estimate the dynamic response from the quasi-static response to avoid elaborate time domain transient response computations. Theoretically, the DAF can reach a maximum value of 2.0, but for slamming excited hull girder vibration values between approximately 1.1 and 1.4 are more typical. In order to point out the difference to the fully decoupled approaches, as, e.g., the DAF concept, some researchers use the term ‘1-way coupling’ for such a procedure as long as hydrodynamic and structural response analysis are performed independently, and ‘2-way coupling’, if also these computations are performed simultaneously, i.e. a hydro-elastic analysis is performed.[56]

Also the calculation of ship motions, wave loads and slamming pressures can be performed with simple and efficient or more elaborate and accurate methods. In combination with the different ways to perform the structural response prediction and to couple hydrodynamic and structural analysis, there exist a number of options for the definition of a meaningful overall analysis procedure. [56]

In practice, there will be always a need for a compromise between the accuracy of the respective approach and its computational efficiency. It goes without saying that the choice of the most suitable overall procedure will depend on the objective of the analysis, e.g., it must be differentiated between extreme load scenarios, the computation of stress range spectra or the prediction of design values based on long-term statistics.[56]

Whipping effect is currently very difficult to reliably calculate or model. Classification societies are therefore unable to predict its magnitude or effect on a ship’s structure, with any confidence, and as a consequence they are not generally calculated during the structural design process. [56]



### **4.3 Hull Frequency determination**

The most important requirement to minimize hull vibration is to limit the exciting forces, is to avoid resonance of the hull girder with the frequency of exciting forces. Here we focus on methods available to calculate hull natural frequencies and demonstrates a simplified, empirical method that can be used in the preliminary hull vibration analysis.

#### **4.3.1 Empirical Analysis**

In early 1894, Schlick [25] developed an empirical formula based on modification of an ordinary beam, which approximated fundamental bending frequency. By introducing empirical factors obtained by systematic shipboard vibration studies, it was possible to estimate the fundamental vertical frequency of a ship. A study by Disenbacher and Perkins [26] , demonstrates a further refinement of this simplified approach, which would provide the natural frequencies of a ship's hull, within  $\pm 5\%$  of that obtained by the more conventional 20-station beam model, which requires a complete distribution of ship parameters.

#### **4.3.2 20-Station Beam Model**

The 20-station beam model, frequently used for preliminary design purposes, was developed at the David Taylor Research Center [27]. For each station along the length of a hull, it is necessary to develop the weight, virtual mass, bending rigidity and shear rigidity. This of course, requires firm design data that is not necessarily available in the early stages of design, and considerable engineering time to assemble and calculate. An early digital computer program for solving the system of finite-difference equations that approximate the problem representing the steady-state motion of a vibrating beam-spring system, such as a ship hull in bending, was also developed at DTRC.

#### **4.3.3 Finite Element Model**

Primarily ship model is made of finite-elements of beam and plate, with large number of joints (or nodes) as inter-joining points. With each node having six degrees of freedoms (DOF), the mathematical model consists of mass and stiffness matrices of high order. Computations with matrices of such an order of magnitude are very costly



and not warranted to determine hull frequencies. Reduction of matrix size was therefore undertaken. For determination of the basic hull frequencies however, only the lowest frequencies are required. The use of the finite-element model analysis requires the geometry of the structure to be analyzed. In the early design phase, the detail required for a vibratory response analysis is generally not available. If it is necessary to make assumptions on the structural details and the boundary conditions, the accuracy expected of the finite-element analysis is lost and the expense is not warranted.

#### **4.4 Dynamic Analysis**

There are number of different computer programs are available in the market for dynamic analysis (Free vibration and forced response) of ships and offshore structures, for instance ABAQUS package, ANSYS, SESAM-DNV package, GL shipload etc. ABAQUS is one of the most widely used software by wide range of industries, including aircraft manufacturers, automobile companies, oil companies, shipbuilding industries and microelectronics industries, as well as national laboratories and research centers. For this thesis work, ABAQUS is also used for free vibration analysis and dynamic forced response analysis.

##### **4.4.1 Overview**

There are several methods for performing dynamic analysis of problems in which inertia effects are considered. Modal methods are usually chosen for linear analyses because in direct-integration dynamics the global equations of motion of the system must be integrated through time, which makes direct-integration methods significantly more expensive than modal methods. Subspace-based methods are provided in Abaqus/Standard and offer cost-effective approaches to the analysis of systems that are mildly nonlinear.

In Abaqus/Standard dynamic studies of linear problems are generally performed by using the eigen modes of the system as a basis for calculating the response. In such cases the necessary modes and frequencies are calculated first in a frequency extraction step. Eigen mode extraction can become computationally intensive if many modes are required for a large model. [45]



#### 4.4.2 Implicit Versus Explicit

The direct-integration dynamic procedure provided in Abaqus/Standard offers a number of implicit operators for integration of the equations of motion, while Abaqus/Explicit uses the central-difference operator. In an implicit dynamic analysis the integration operator matrix must be inverted and a set of nonlinear equilibrium equations that must be solved at each time increment. Displacements and velocities are calculated in terms of quantities that are known at the beginning of an increment in an explicit dynamic analysis; therefore, the global mass and stiffness matrices need not be formed and inverted, which means that each increment is relatively inexpensive compared to the increments in an implicit integration process. The size of the time increment in an explicit dynamic analysis is limited, however, because the central-difference operator is only conditionally stable; whereas the implicit operator options available in Abaqus/Standard are unconditionally stable and, thus, there is no such limit on the size of the time increment that can be used for most analyses. Abaqus/Explicit offers fewer element types than Abaqus/Standard. For example, only first-order, displacement method elements (4-node quadrilaterals, 8-node bricks, etc.) and modified second-order elements are used, and each degree of freedom in the model must have mass or rotary inertia associated with it. [45]

Dynamic, implicit step is used for the response analysis in the work. This step is used in the analysis because it provides suitable understanding for

- must be used when nonlinear dynamic response is being studied;
- can be fully nonlinear (general dynamic analysis) or can be based on the modes of the linear system (subspace projection method); and
- can be used to study a variety of applications, including
  - Dynamic responses requiring transient fidelity and involving minimal energy dissipation;
  - Dynamic responses involving nonlinearity, contact, and moderate energy dissipation; and
  - Quasi-static responses in which considerable energy dissipation provides stability and improved convergence behavior for determining an essentially static solution





### 4.4.3 Time integration methods

Abaqus/Standard uses the Hilber-Hughes-Taylor time integration by default unless it is specified that the application type is quasi-static. The Hilber-Hughes-Taylor operator is an extension of the Newmark  $\beta$ -method. Numerical parameters associated with the Hilber-Hughes-Taylor operator are tuned differently for moderate dissipation and transient fidelity applications. The backward Euler operator is used by default if the application classification is quasi-static.[41]

These time integration operators are implicit, which means that the operator matrix must be inverted and a set of simultaneous nonlinear dynamic equilibrium equations must be solved at each time increment. This solution is done iteratively using Newton's method. The principal advantage of these operators is that they are unconditionally stable for linear systems; there is no mathematical limit on the size of the time increment that can be used to integrate a linear system. Marching through a simulation with a finite time increment size generally introduces some degree of numerical damping. This damping differs from the material damping. [40]

Default parameters for the Hilber-Hughes-Taylor integrator.

Parameter	Application	
	Transient Fidelity	Moderate Dissipation
$\alpha$	-0.05	-0.41421
$\beta$	0.275625	0.5
$\gamma$	0.55	0.91421

**Table 1: Hilber- Hughes- Taylor integrator parameters[41]**

In this process time increment size is specified. This approach is not generally recommended but may be useful in special cases. The analysis terminates if convergence tolerances are not satisfied within the maximum number of iterations allowed.



#### 4.4.4 Damping in dynamic analysis

Every non-conservative system exhibits some energy loss that is attributed to material nonlinearity, internal material friction, or to external (mostly joint) frictional behavior. Conventional engineering materials used in ship building industry like steel and high strength aluminum alloys provide small amounts of internal material damping, not enough to prevent large amplification at or near resonant frequencies.

##### 4.4.4.1 Source of damping

There are four categories of damping sources: material and element damping, global damping, modal damping, and damping associated with time integration.

##### **Material damping**

Material Rayleigh damping is defined by two Rayleigh damping factors:  $\alpha_R$  for mass proportional damping and  $\beta_R$  for stiffness proportional damping. In general, damping is a material property specified as part of the material definition. For the cases of rotary inertia, point mass elements, and substructures, where there is no reference to a material definition, the damping can be defined in conjunction with the property references. Any mass proportional damping also applies to nonstructural features

Dashpots, springs with their complex stiffness matrix, and connectors that serves as dampers, all with viscous and structural damping factors. Viscous damping can be included in mass, beam, pipe, and shell elements with general section properties.

##### **Global Damping**

In cases where material or element damping is not appropriate or sufficient, abstract damping factors are used to an entire model. Abaqus allowsto specify global damping factors for both viscous (Rayleigh damping) and structural damping (imaginary stiffness matrix). [45]

##### **Modal Damping**

Modal damping applies only to mode-based linear dynamic analyses which are not used in the current work.



## **Damping in a linear dynamic analysis**

Damping applied to a linear dynamic system in two ways

- velocity proportional viscous damping
- Displacement proportional structural damping, which is for use in frequency domain dynamics. The exception is SIM-based transient modal dynamic analysis, where the structural damping is converted to the equivalent diagonal viscous damping.[45]

### **4.4.5 Frequency Extraction procedure**

- Eigen value are extracted to calculate the natural frequencies and the corresponding mode shapes of a system;
- include initial stress and load stiffness effects due to preloads and initial conditions if geometric nonlinearity is accounted for in the base state, so that small vibrations of a preloaded structure can be modeled;
- compute residual modes if requested;
- linear perturbation procedure; [45]

### **4.4.6 Eigen Extraction methods**

There are three eigen value extraction methods:

- Lanczos
- Automatic multi-level substructuring (AMS), an add-on analysis capability for Abaqus/Standard
- Subspace iteration

Lanczos method is used in the eigen value extraction method in the current work.

#### ***4.4.6.1 Lanczos Eigen Solver***

In Lanczos method it is needed to provide the maximum frequency of interest or the number of eigen values required. Abaqus/Standard determines a suitable block size. If you specify both the maximum frequency of interest and the number of eigen values



required and the actual number of eigenvalues is underestimated, In that case Abaqus/Standard issue a corresponding warning message; the remaining eigen modes can be found by restarting the frequency extraction. [45]

## 5 Input Data

This section contains the input from the benchmark committee to develop the ship model in GeniE. Afterwards exports from GeniE used as input for HydroD and ABAQUS analysis.

### 5.1 Ship data

The ship has been analysed in this thesis work is owned by Wagenborg which is a multi-purpose cargo/container ship. The bench mark committee has provided all the information about the ship and corresponding sea condition and mass distribution.

The input from the committee consist of

1. Body Plan
2. Load Condition
3. Structural drawings of the man structure of both fore body and aft body
4. Structural drawings of the prismatic section of the hull
5. Sea, state, heading and speed.

All the drawings and sketches used in the model is attached in the Appendix-A [9.1] section.

Committee has also provided with the Mass distribution for three different loading conditions.

- Light ship condition
- Ballast Condition
- Fully loaded condition

The information available in mass distribution for all loading condition is

- Component
- Weight[tons]
- Longitudinal center of gravity [m]



- Start position [m]
- End position [m]
- Weight/m
- Component width [m]
- Component height [m]
- $I_{XX}$  [Kgm<sup>2</sup>]
- $I_{YY}$  [Kg m<sup>2</sup>]

The start position and the end position for the components are measured from the position of the aft perpendicular [AP].

Detail mass distributions with all the properties mentioned above are given in the Appendix-A.

## 5.2 FE Model

For the complex shape in the bow [bulbous bow] and stern area ship is preliminary modeled in SESAM/GeniE. No wheelhouse, superstructure and forecastle has not been included in the model. The model contains Outer shell, inner shell Framming structure only. Small brackets and machinery part are not also included in the model.

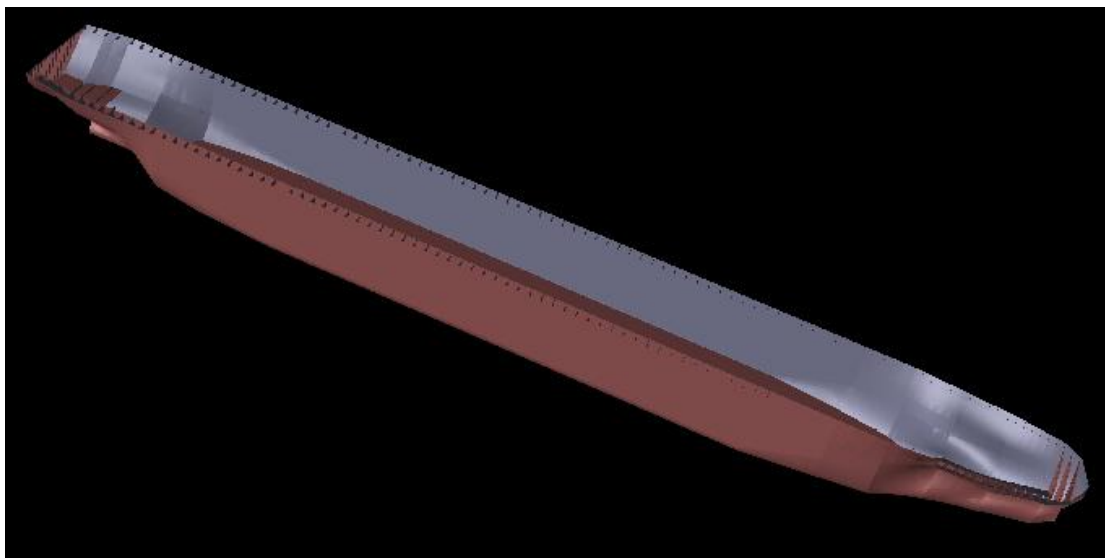


**Figure 29: Ship preliminary model in GeniE.**

This model only contains the geometry of the ship which was imported to ABAQUS afterwards. No properties and sections did not assign to the GeniE preliminary model.



### 5.3 Panel Model

A panel model developed in SESAM/GeniE which was used in another SESAM module called SESAM/HydroD. In HydroD all the relevant Environmental load condition and sea state are modeled properly. To find the added mass matrix and total damping matrix was the main purpose for HydroD analysis.

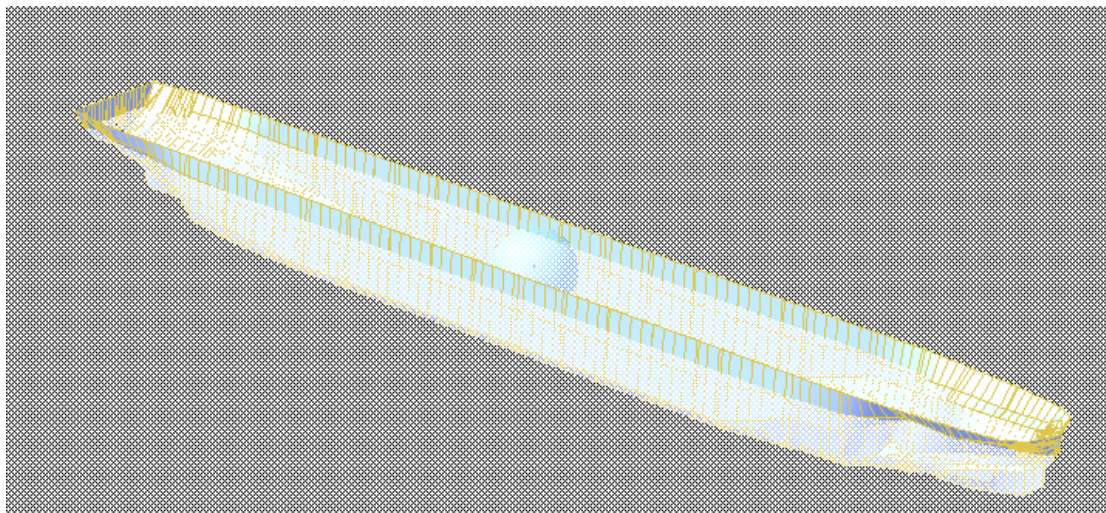


**Figure 30: Panel model in SESAM/HydroD**

A typical Added mass matrix and total damping matrix and the explanation of the results are given below.

```
+-----+
| WAVELENGTH      = 1.0697E+01 |
| WAVEPERIOD      = 2.6180E+00 |
+-----+
```

ADDED MASS MATRIX

	1	2	3	4	5	6
1	1.2788E-02	4.8186E-04	9.4406E-03	1.2852E-05	7.4410E-03	6.5607E-05
2	6.5382E-04	2.0984E-01	2.6559E-03	2.8506E-03	-3.2155E-04	1.0676E-01
3	8.9324E-03	2.1534E-03	1.0803E+00	6.7455E-05	-5.2688E-01	1.8313E-04
4	1.3832E-05	2.5501E-03	6.7448E-05	3.0454E-04	-1.1170E-05	1.5518E-03
5	8.1830E-03	-2.8654E-04	-5.2723E-01	-1.2556E-05	3.0752E-01	-3.6418E-05
6	9.5892E-05	1.0754E-01	2.3493E-04	1.6967E-03	-3.3362E-05	7.0983E-02



TOTAL DAMPING MATRIX

	1	2	3	4	5	6
1	5.4444E-02	8.2794E-04	8.1225E-03	1.8090E-05	2.3323E-02	1.6282E-04
2	3.6700E-04	9.8963E-01	3.0455E-03	7.8501E-03	-3.2148E-04	5.2061E-01
3	1.6522E-02	3.2268E-03	1.6417E-01	4.6541E-05	-4.5493E-02	3.6135E-04
4	1.0254E-05	8.7158E-03	1.1659E-05	1.6162E-04	9.8327E-07	5.6229E-03
5	1.6882E-02	-4.5378E-04	-4.8234E-02	-3.7007E-06	3.5059E-02	-5.4518E-05
6	1.2647E-04	5.1372E-01	1.7984E-04	5.1121E-03	2.6216E-06	3.4818E-01

4.1 EXPLANATION OF THE RESULTS

NON-DIMENSIONAL DEFINITIONS:

		I=1-3 J=1-3	I=1-3 I=4-6 J=4-6 J=1-3	I=4-6 J=4-6
MASS INERTIA MATRIX	NON-DIMENSIONALIZED BY:	RO*VOL,	RO*VOL*L	RO*VOL*L*L
ADDED MASS MATRIX	NON-DIMENSIONALIZED BY:	RO*VOL,	RO*VOL*L	RO*VOL*L*L
DAMPING MATRIX	NON-DIMENSIONALIZED BY:	RO*VOL*SQRT(G/L)	RO*VOL*SQRT(G*L)	RO*VOL*L*SQRT(G*L)
RESTORING MATRICES	NON-DIMENSIONALIZED BY:	RO*VOL*G/L,	RO*VOL*G	RO*VOL*G*L
		I=1-3	I=4-6	
EXCITING FORCES	NON-DIMENSIONALIZED BY:	RO*VOL*G*WA/L	RO*VOL*G*WA	
MOTIONS	NON-DIMENSIONALIZED BY:	WA	WA/L	(4-6 IN RADIANS)
SECTIONAL LOADS	NON-DIMENSIONALIZED BY:	RO*VOL*G*WA/L	RO*VOL*G*WA	
DRIFT FORCES	NON-DIMENSIONALIZED BY:	RO*G*L*WA*WA	RO*G*L*L*WA*WA	
		I=1-3		
PRESSURES	NON-DIMENSIONALIZED BY:	RO*G*WA		
VELOCITIES	NON-DIMENSIONALIZED BY:	WA*SQRT(G/L)		
ACCELERATIONS	NON-DIMENSIONALIZED BY:	WA*G/L		
2ND-ORDER FORCES	NON-DIMENSIONALIZED BY:	RO*G*L	RO*G*L*L	
2ND-ORDER PRESSURE	NON-DIMENSIONALIZED BY:	RO*G/L		
		I=1,2	I=6	
WAVE DRIFT DAMPING MATRIX	NON-DIMENSIONALIZED BY:	RO*G*L*WA*WA	RO*G*L*L*WA*WA	

NON-DIMENSIONALIZING FACTORS:

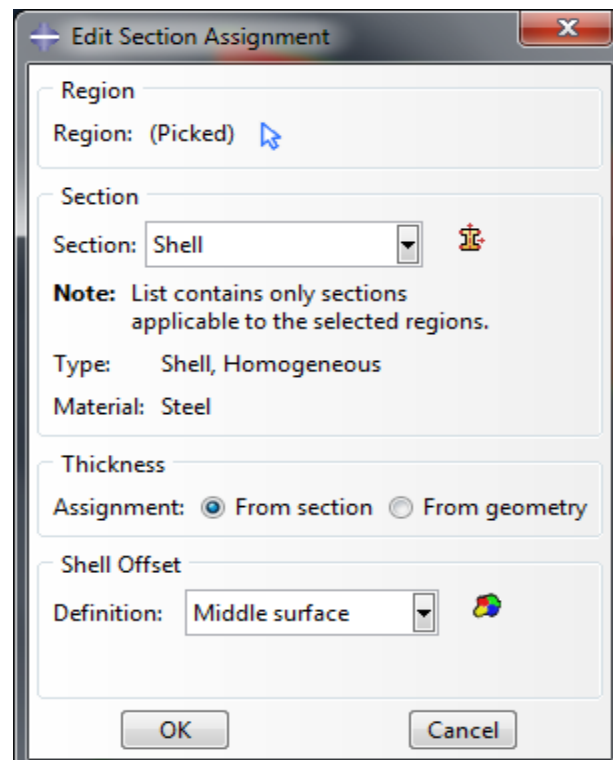
THE OUTPUT IS NON-DIMENSIONALIZED USING -

RO = DENSITY OF THE FLUID  
 G = ACCELERATION OF GRAVITY  
 L = CHARACTERISTIC LENGTH, AS GIVEN IN THE INPUT  
 VOL = DISPLACED VOLUME OF BODY 1 (COMBINED MORISON AND PANEL MODEL)  
 WA = WAVE AMPLITUDE OF THE INCOMING WAVES

RO = 0.1025E+04  
 G = 0.9807E+01  
 VOL = 0.1170E+05  
 L = 0.1300E+03

## 5.4 ABAQUS model

The Preliminary model that was made in GeniE, was imported in ABAQUS as part later on. There was three different model has been made, Lightship condition, Ballast condition and Fully Loaded condition. For the models apart from the mass distribution everything is exactly same. Assigned section to the model given below.



The material used in the model is the Steel with the properties given below:

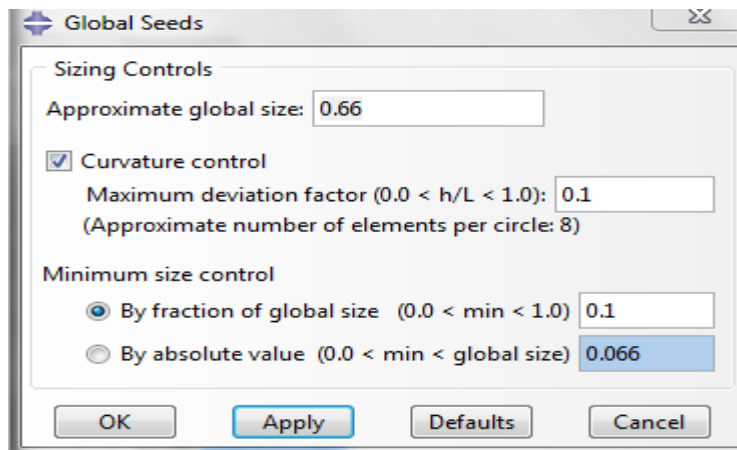
Steel:

- Elasticity modulus:  $2.1 \times 10^{11} \text{N/m}^2$
- Poisson ratio: 0.3
- Density:  $7850 \text{Kg/m}^3$

For these three different models total mass, rotational mass, position of longitudinal center of gravity and vertical center of gravity was obtained from the mass distribution provided by the benchmark committee. Table of mass distributions are provided in the appendix.

Another three modes has been made corresponding to Lightship model, Ballast condition and fully loaded model including Added mass for wet mode analysis. Hydrodynamic damping and water plane were also added to the wet mode models As dashpot/spring in ten different locations [ 4 on each side, 1 in stern and 1 in bow area] of the model. The Global seed used in the entire model is





Properties of the Elements used in the model given below

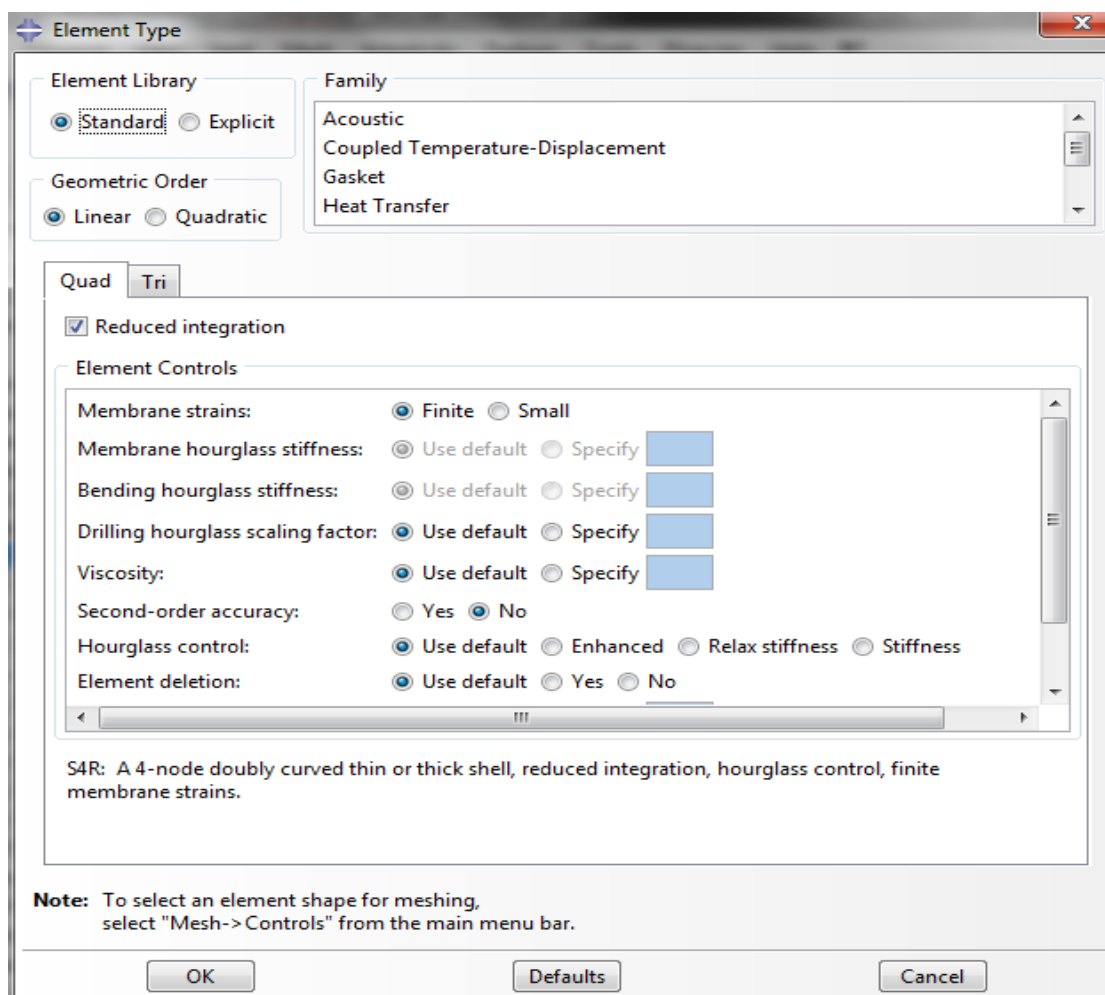


**Figure 31: Element properties**



Total number of nodes: 26707

Total number of elements: 31766

29721 linear quadrilateral elements of type S4R

2045 linear triangular elements of type S3

Conventional Shell Element S4R is used because it provide with

- Uniformly reduced integration to avoid shear and membrane locking.
- The element has several hourglass modes that may propagate over the mesh
- Converges to shear flexible theory for thick shells and classical theory for thin shells.
- S4R is a robust, general-purpose element that is suitable for a wide range of applications

Where it is not applicable to use S4R elements , S3 elements are used.

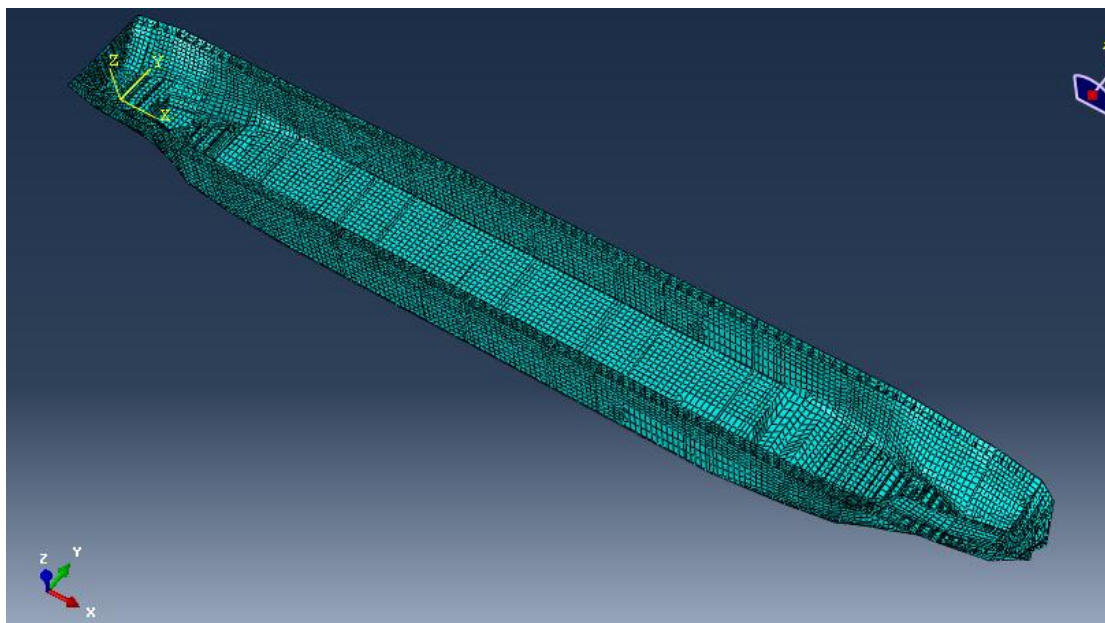


**Figure 32: Mesh model in ABAQUS**



This was the step that was used for Frequency analysis.

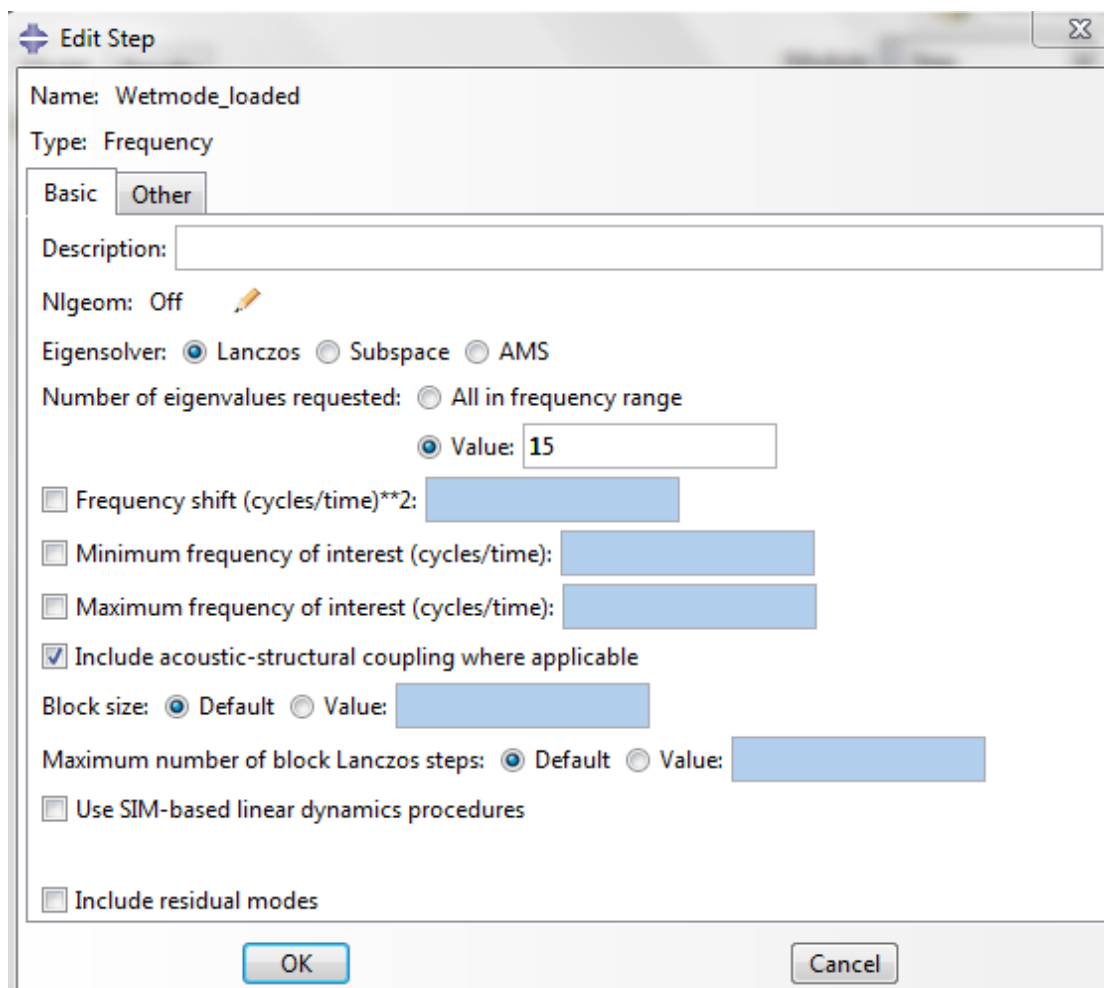


**Figure 33: Frequency Analysis Steo in ABAQUS**

Rayleigh damping and structural damping is also added to the dynamic analysis model. Dynamic implicit analysis is used as analysis process with used direct time integration. Total time period for analysis was used 15 second as the highest natural period was close to 2 second. Fixed increment is used in the analysis which was 0.01 second.



## 6 Analysis and Results

### 6.1 Natural frequency and vibration modes

Linear perturbation analysis step is used for Natural frequency extraction for the system.. Linear perturbation analyses can be performed from time to time during a fully nonlinear analysis by including the linear perturbation steps between the general response steps. The linear perturbation response has no effect as the general analysis is continued. Lanczos eigen solver has been chosen for frequency extraction. First 15 eigen values are requested for the analysis.

The first six mode shapes are rigid body modes. These six rigid body mode shapes, which are Surge, Sway, Heave, Roll, Pitch and Yaw, are not to display elastic distortion. For these cases, Frequency is generally very low, well below the first elastic natural mode. Any mixing of rigid body modes and/or missing rigid body mode(s) would be a good indication of an erroneous FE modeling, especially when incorrect multi-point constraints are applied to the FE model.

Three different loading conditions were considered in the frequency analysis. Loading conditions were Lightship condition, Ballast condition and Fully Loaded Condition. Both the Dry mode frequencies and Wet mode frequencies were calculated.

Only the wet mode frequencies and vibration modes are given below. Dry mode frequencies and vibration modes are given in the appendix.



## 6.1.1 Wet mode frequencies and mode shapes

### Lightship Condition

The screenshot shows a software window titled "Step/Frame" with a close button (X) in the top right corner. The window contains a table with two columns: "Step Name" and "Description". The first row is highlighted in blue and contains "Wetmode\_Light". Below this is a section labeled "Frame" containing a table with two columns: "Index" and "Description". The "Description" column contains detailed information for each mode, including its index, value, and frequency in cycles/time. The first row of the "Frame" table is also highlighted in blue.

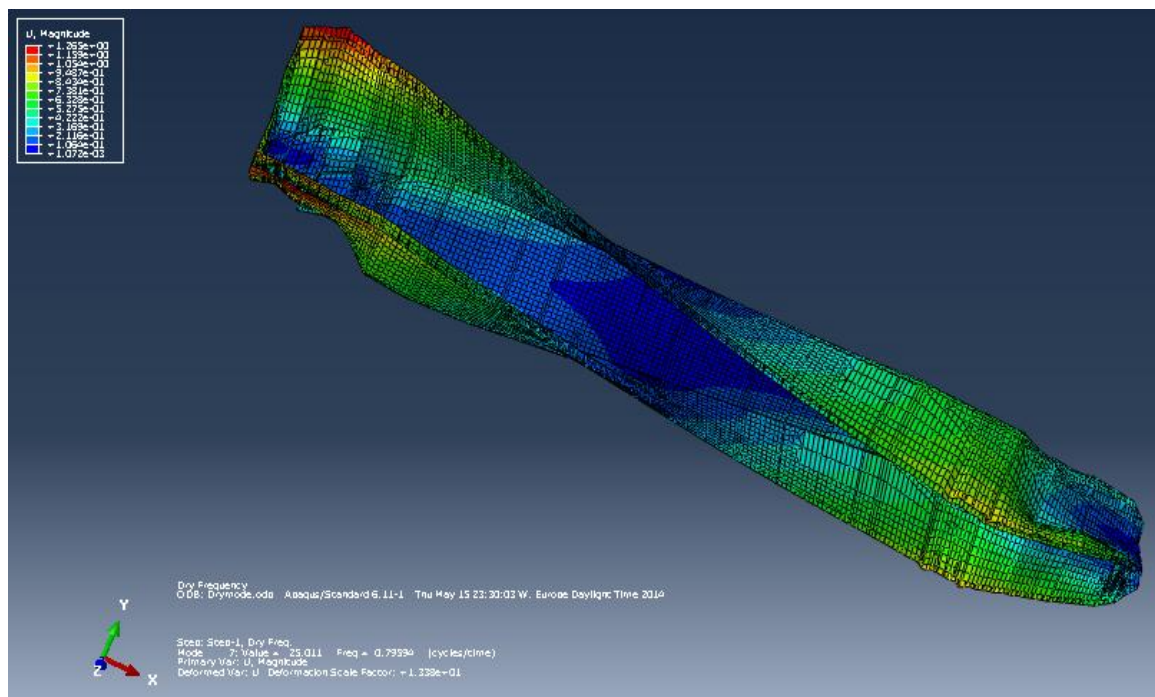
Step Name	Description
Wetmode_Light	

Index	Description
0	Increment 0: Base State
1	Mode 1: Value = -1.43405E-10 Freq = 0.0000 (cycles/time)
2	Mode 2: Value = -2.24743E-11 Freq = 0.0000 (cycles/time)
3	Mode 3: Value = 3.53068E-12 Freq = 2.99054E-07 (cycles/time)
4	Mode 4: Value = 3.38160E-11 Freq = 9.25510E-07 (cycles/time)
5	Mode 5: Value = 9.97369E-11 Freq = 1.58945E-06 (cycles/time)
6	Mode 6: Value = 1.97555E-04 Freq = 2.23699E-03 (cycles/time)
7	Mode 7: Value = 7.1620 Freq = 0.42593 (cycles/time)
8	Mode 8: Value = 23.520 Freq = 0.77186 (cycles/time)
9	Mode 9: Value = 24.658 Freq = 0.79031 (cycles/time)
10	Mode 10: Value = 68.666 Freq = 1.3188 (cycles/time)
11	Mode 11: Value = 80.300 Freq = 1.4262 (cycles/time)
12	Mode 12: Value = 94.014 Freq = 1.5432 (cycles/time)
13	Mode 13: Value = 102.15 Freq = 1.6085 (cycles/time)
14	Mode 14: Value = 108.78 Freq = 1.6600 (cycles/time)
15	Mode 15: Value = 122.24 Freq = 1.7596 (cycles/time)

At the bottom of the window, there are four buttons: "OK", "Apply", "Field Output...", and "Cancel".

**Table 2: Wet mode natural frequencies [Lightship]**



**Figure 34: Global Torsion Mode at 0.42593 Hz.**

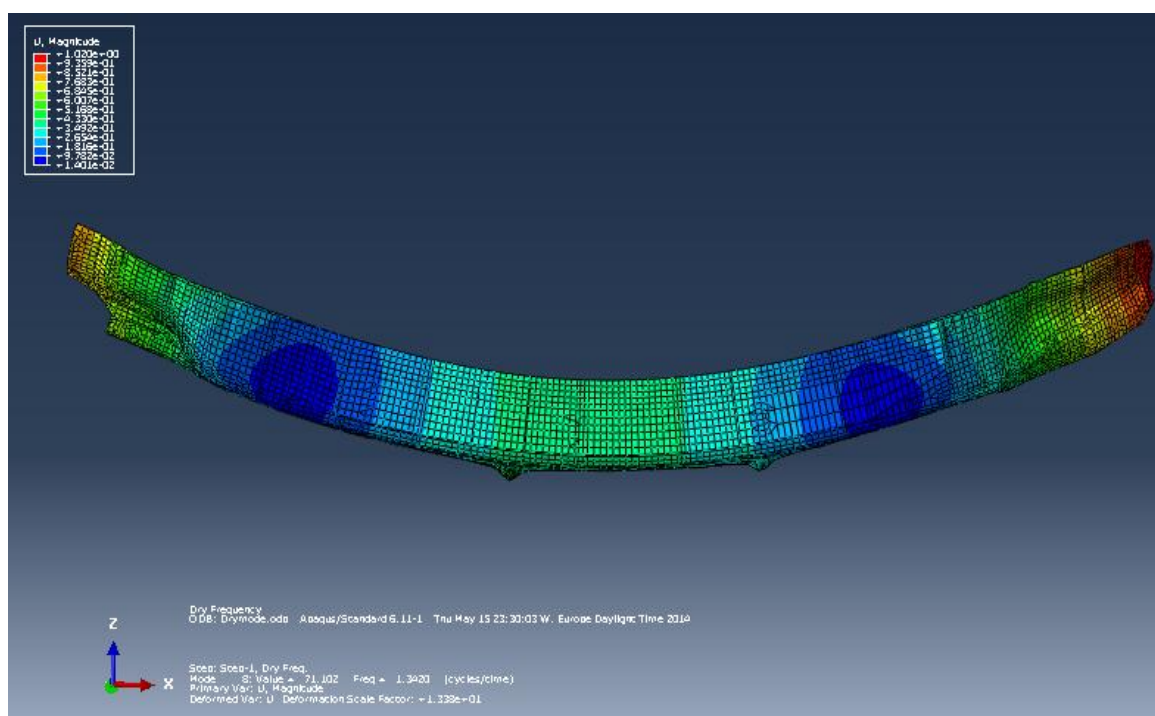




Figure 35: 2-node Vertical Bending Mode at 0.77186 Hz

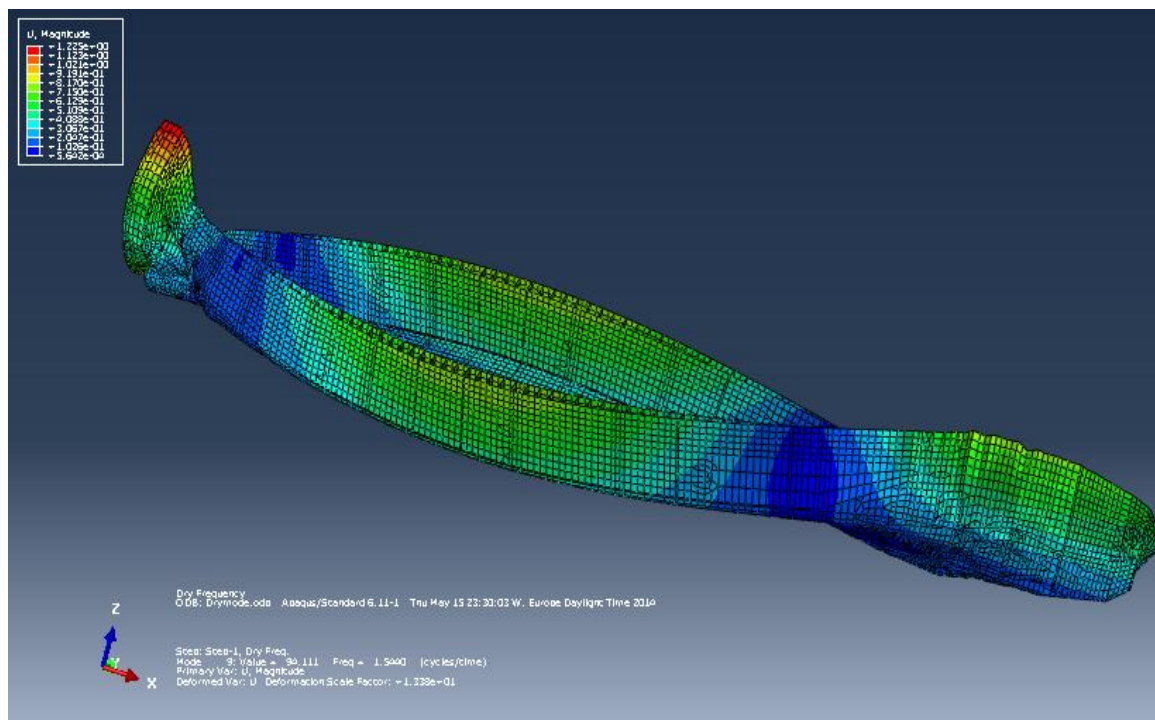


Figure 36: Global Torsion and Horizontal Bending Mode at 0.79031 Hz

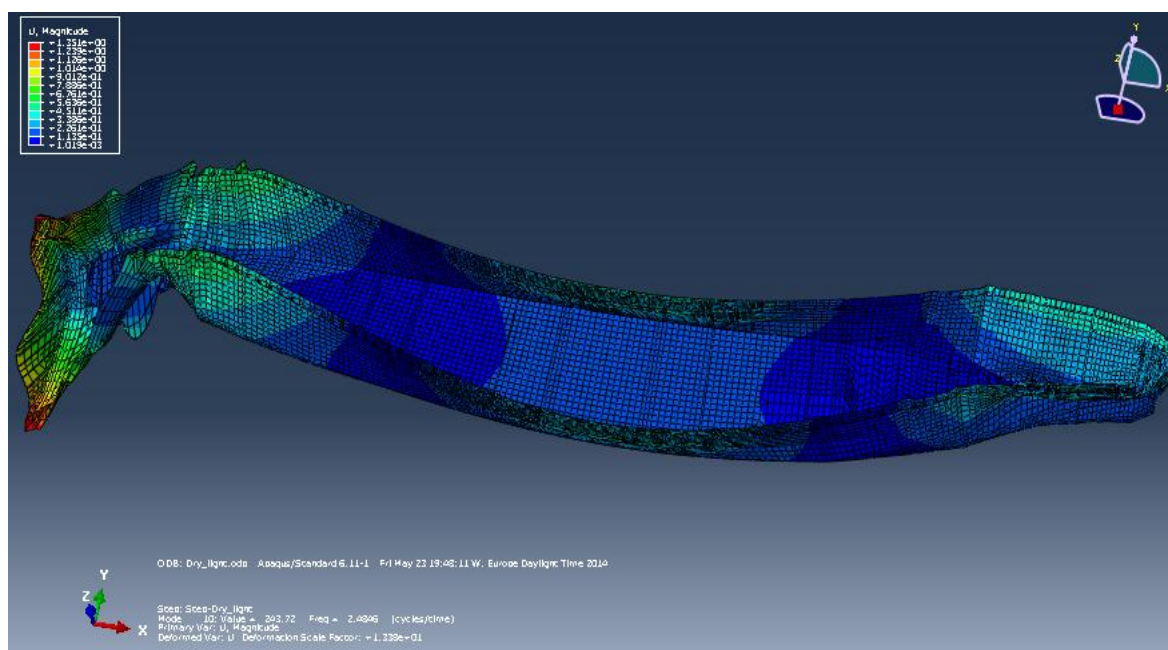




Figure 37: 3- node horizontal bending at 1.3188 Hz

### Ballast Condition

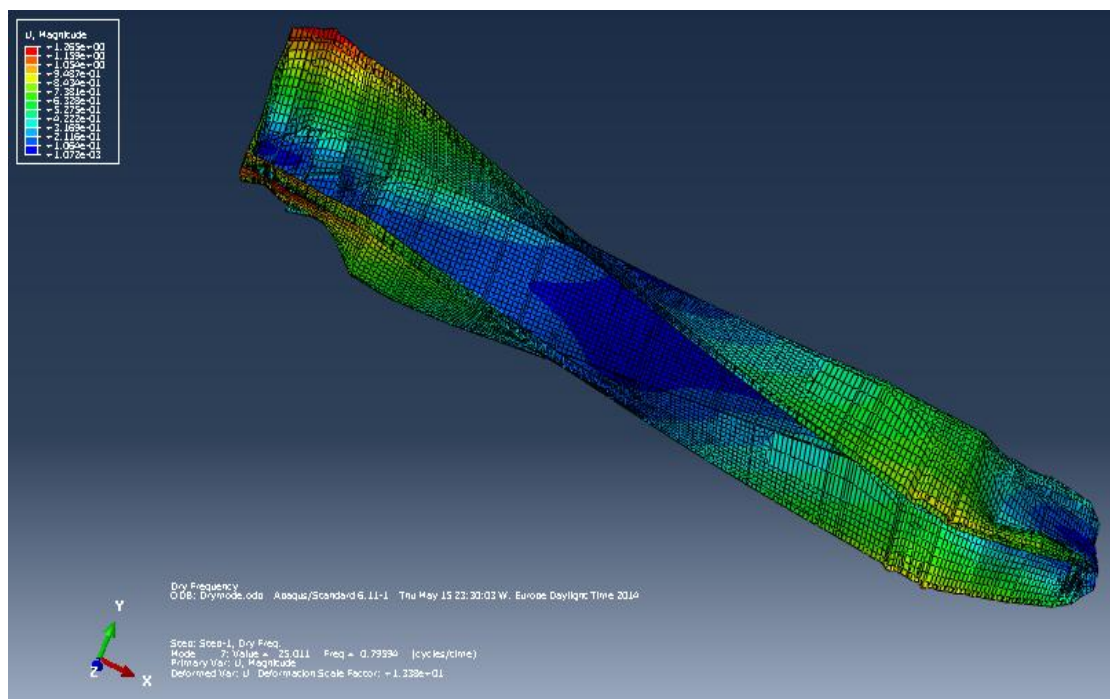
Step Name	Description
Wetmode_ballast	

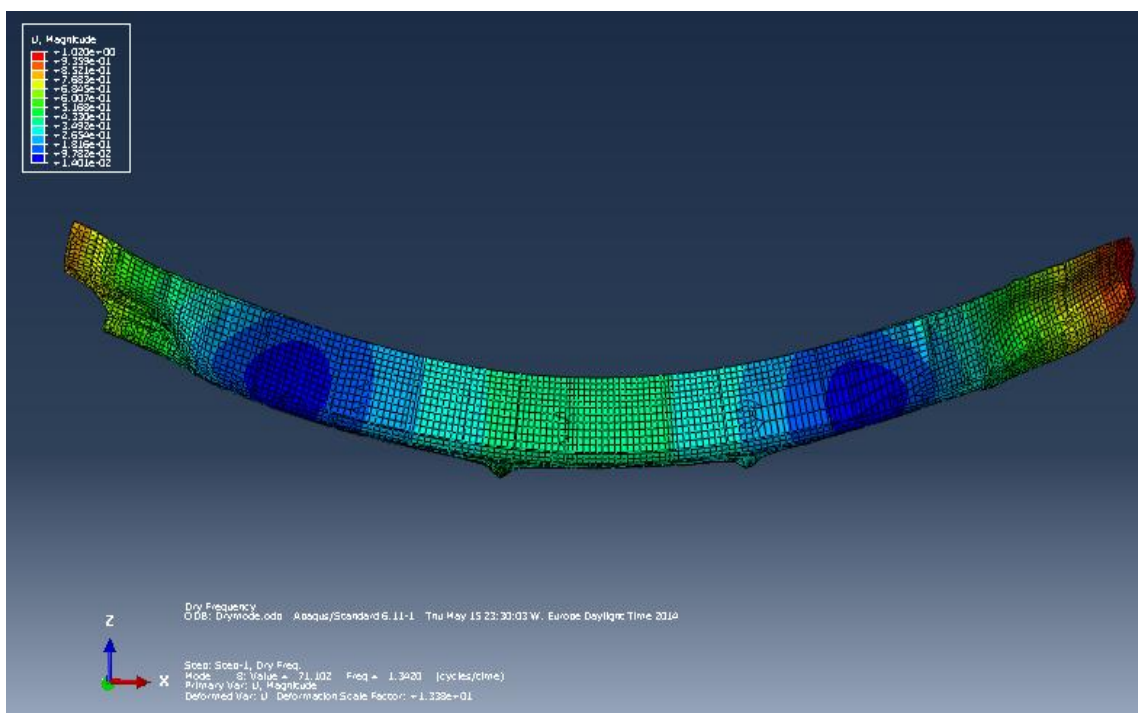
Index	Description
0	Increment 0: Base State
1	Mode 1: Value = -7.28830E-11 Freq = 0.0000 (cycles/time)
2	Mode 2: Value = -1.56970E-11 Freq = 0.0000 (cycles/time)
3	Mode 3: Value = 1.64417E-11 Freq = 6.45347E-07 (cycles/time)
4	Mode 4: Value = 4.86640E-11 Freq = 1.11026E-06 (cycles/time)
5	Mode 5: Value = 1.62129E-10 Freq = 2.02652E-06 (cycles/time)
6	Mode 6: Value = 1.78268E-04 Freq = 2.12499E-03 (cycles/time)
7	Mode 7: Value = 6.8023 Freq = 0.41509 (cycles/time)
8	Mode 8: Value = 21.547 Freq = 0.73877 (cycles/time)
9	Mode 9: Value = 23.721 Freq = 0.77515 (cycles/time)
10	Mode 10: Value = 67.289 Freq = 1.3055 (cycles/time)
11	Mode 11: Value = 79.411 Freq = 1.4183 (cycles/time)
12	Mode 12: Value = 84.588 Freq = 1.4638 (cycles/time)
13	Mode 13: Value = 95.178 Freq = 1.5527 (cycles/time)
14	Mode 14: Value = 102.07 Freq = 1.6079 (cycles/time)
15	Mode 15: Value = 106.95 Freq = 1.6459 (cycles/time)

Table 3: Wet mode natural frequencies [Ballast condition]





**Figure 38: Global Torsion Mode at 0.41509 Hz.**



**Figure 39: 2-node Vertical Bending Mode at 0.73877 Hz**

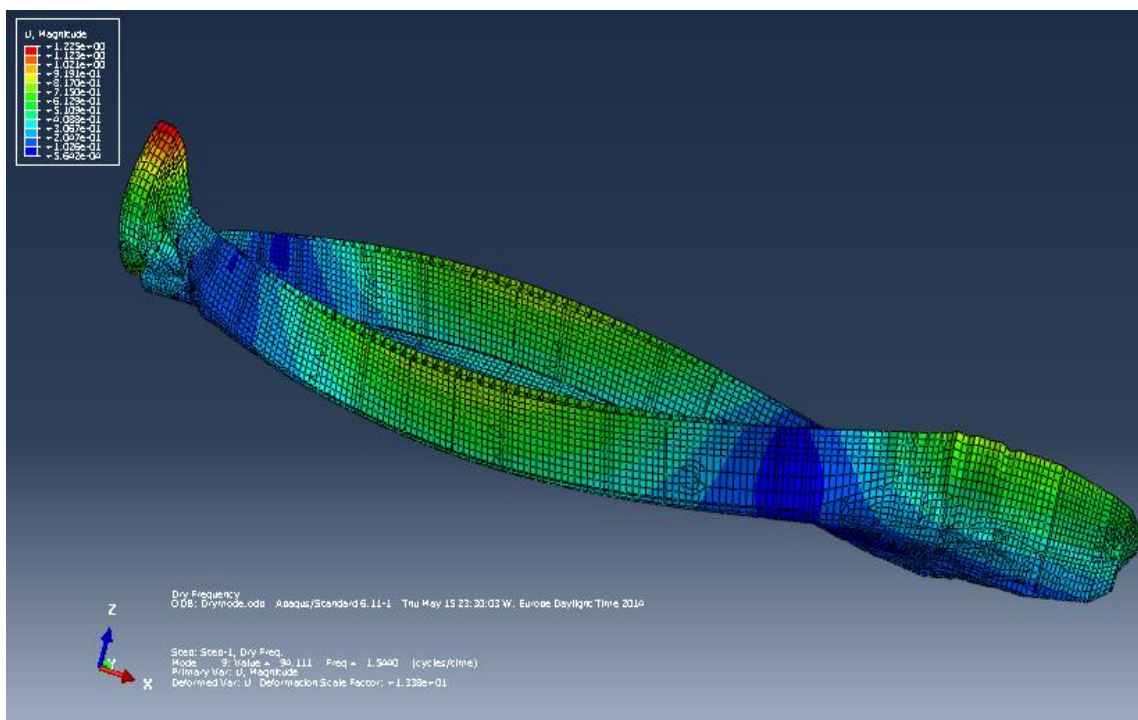


**Figure 40: Global Torsion and Horizontal Bending Mode at 0.77515 Hz**

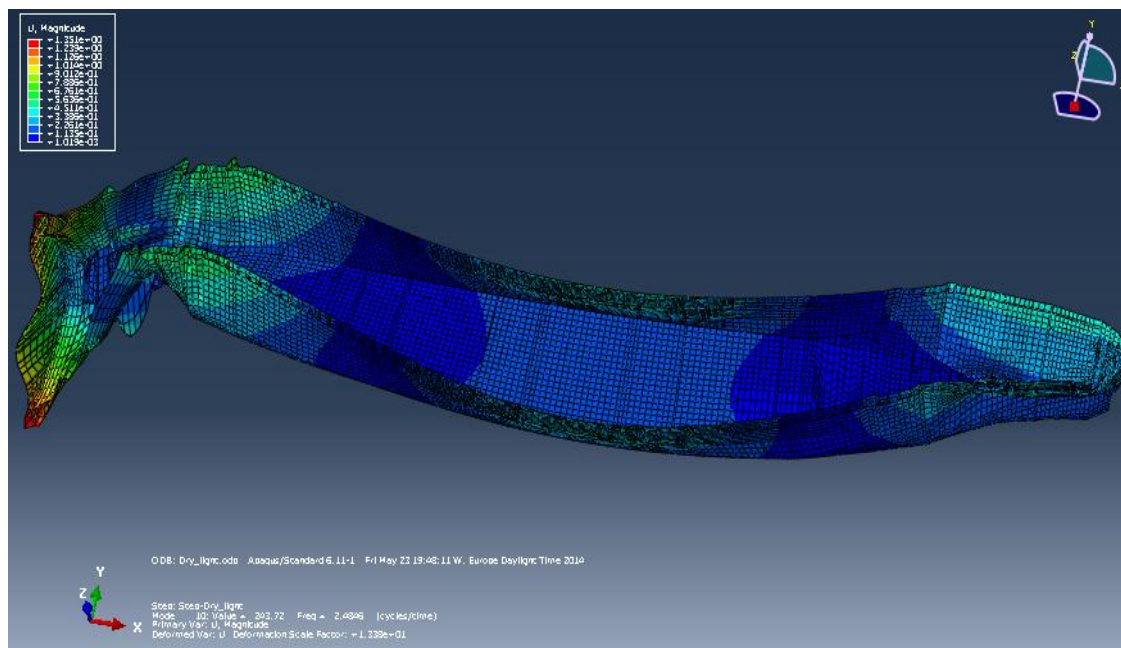


**Figure 41:3- node horizontal bending at 1.3055 Hz**

### **Loaded Condition**



Step/Frame

Step Name	Description
Wetmode_loaded	

Frame

Index	Description
0	Increment 0: Base State
1	Mode 1: Value = -1.40119E-10 Freq = 0.0000 (cycles/time)
2	Mode 2: Value = -5.62390E-11 Freq = 0.0000 (cycles/time)
3	Mode 3: Value = 5.75650E-13 Freq = 1.20753E-07 (cycles/time)
4	Mode 4: Value = 1.71617E-11 Freq = 6.59326E-07 (cycles/time)
5	Mode 5: Value = 3.37999E-11 Freq = 9.25290E-07 (cycles/time)
6	Mode 6: Value = 1.68562E-04 Freq = 2.06633E-03 (cycles/time)
7	Mode 7: Value = 5.8181 Freq = 0.38389 (cycles/time)
8	Mode 8: Value = 19.887 Freq = 0.70975 (cycles/time)
9	Mode 9: Value = 20.190 Freq = 0.71513 (cycles/time)
10	Mode 10: Value = 59.492 Freq = 1.2276 (cycles/time)
11	Mode 11: Value = 78.695 Freq = 1.4119 (cycles/time)
12	Mode 12: Value = 80.293 Freq = 1.4261 (cycles/time)
13	Mode 13: Value = 102.06 Freq = 1.6079 (cycles/time)
14	Mode 14: Value = 108.39 Freq = 1.6569 (cycles/time)
15	Mode 15: Value = 113.11 Freq = 1.6927 (cycles/time)

OK Apply Field Output... Cancel

**Table 4: Wet mode natural frequencies [Loaded]**

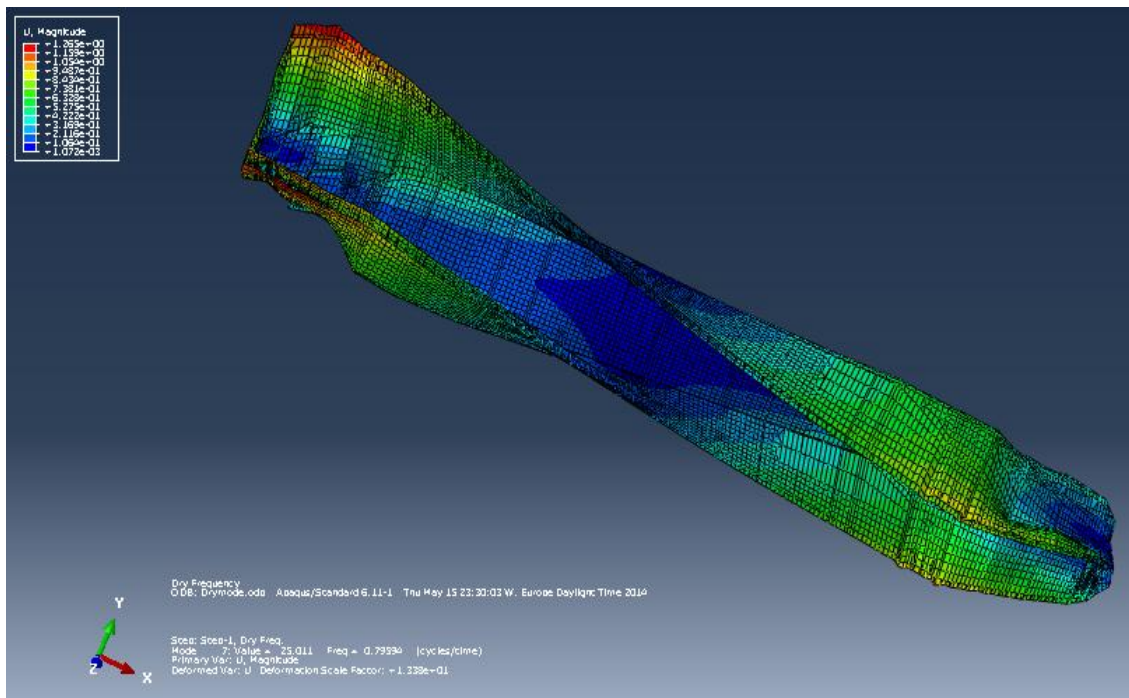


**Figure 42: Global Torsion Mode at 0.38389 Hz**

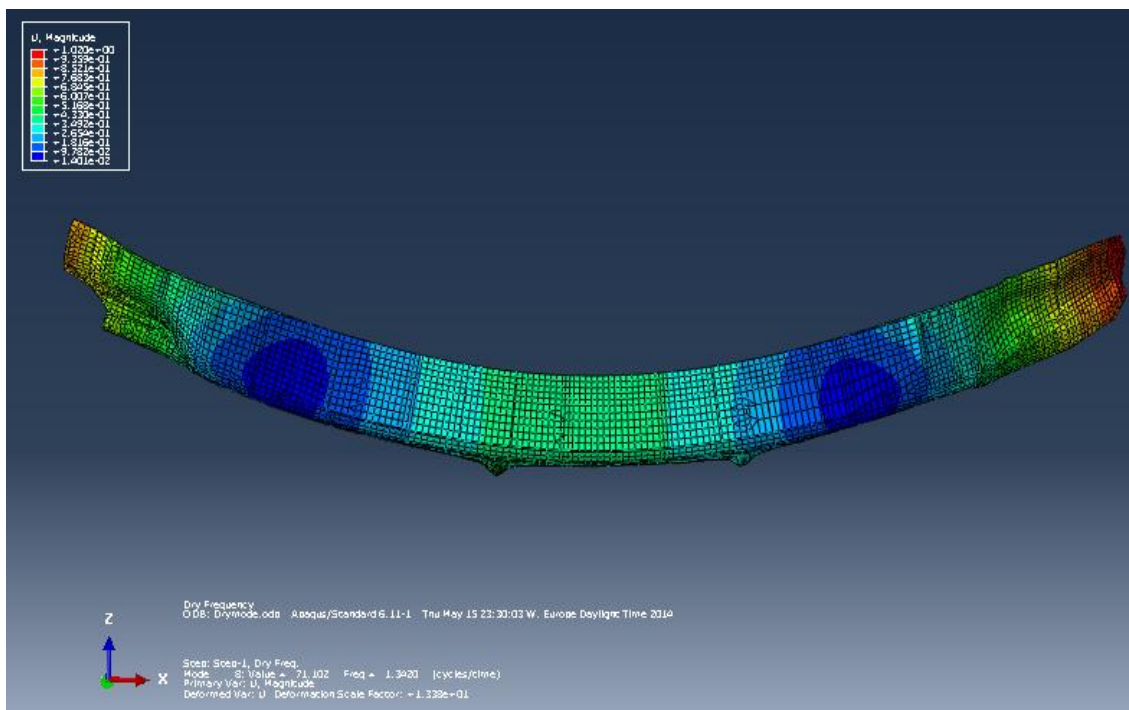


**Figure 43: 2-node Vertical Bending Mode at 0.70975 Hz**

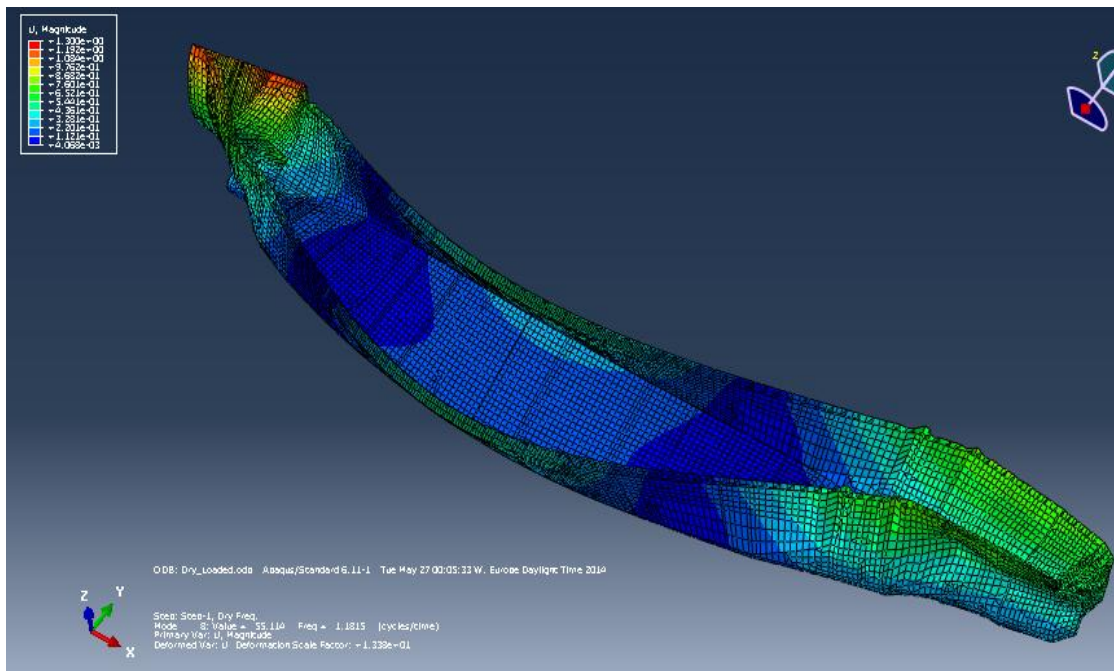


**Figure 44: Horizontal bending /torsion mode at 0.71513 Hz**

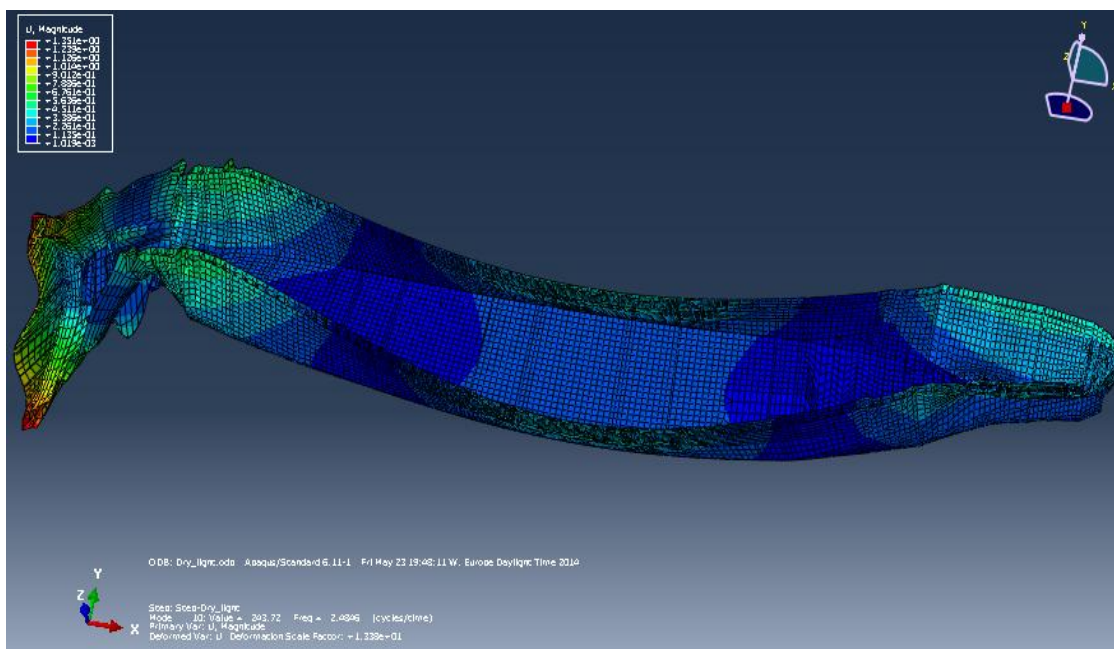


**Figure 45:3- node horizontal bending at 1.2276 Hz**

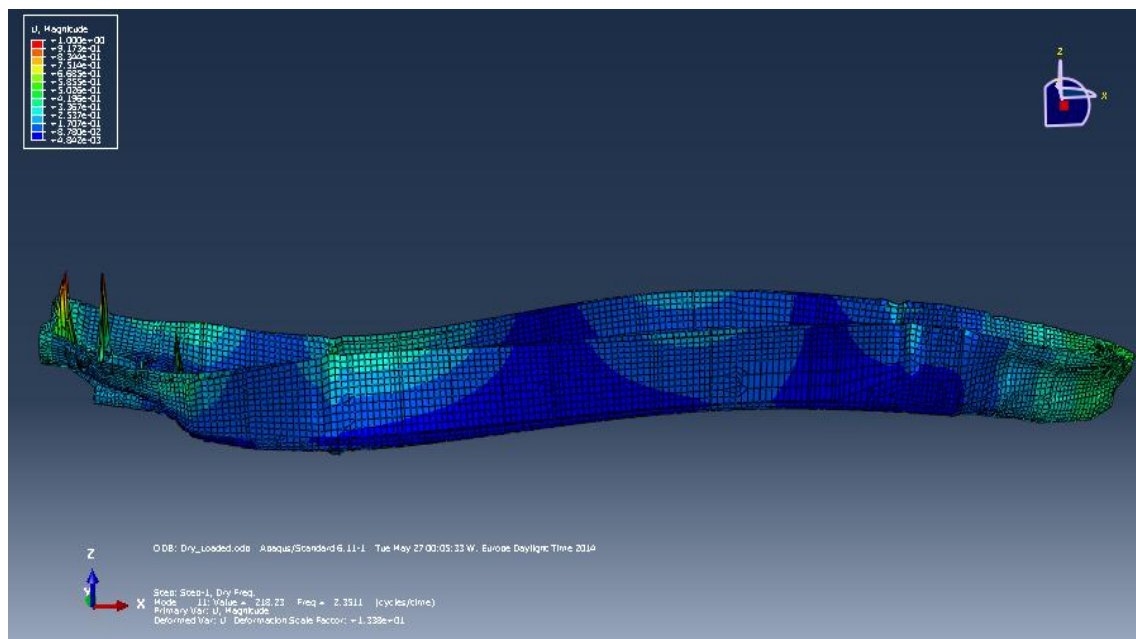


**Figure 46:3- node vertical bending at 1.4119 Hz**

Comparison between dry mode and wet mode frequencies are given below for pre mentioned three loading conditions.

#### Light ship

Mode Shape	Dry mode[Hz]	Wet mode[Hz]
Global torsion	0.86080	0.42593
2-node VB	1.6229	0.77186
Torsion/Hor. Bending	1.6419	0.79031
3-node Hor. Bending	2.4846	1.3188

#### Ballast condition

Mode Shape	Dry mode[Hz]	Wet mode[Hz]
Global torsion	0.77608	0.41509
2-node VB	1.3189	0.73877
Torsion/Hor. Bending	1.5123	0.77515
3-node Hor. Bending	2.3763	1.3055
3-node VB	2.1229	



## Loaded Condition

Mode Shape	Dry mode[Hz]	Wet mode[Hz]
Global torsion	0.61398	0.38389
2-node VB	1.2281	0.70975
Torsion/Hor. Bending	1.1815	0.71513
3-node Hor. Bending	2.0107	1.2276
3-node VB	2.3511	1.4119

**Table 5: Comparison between dry mode and wet mode natural frequencies**

## 6.2 Response time traces

Time traces of the calculated accelerations and strains at the locations as specified in the figure 48 is one of the requested output from the benchmark committee. Specified locations are given below.

1. Frame. 35 [Deck]
2. Frame, 100.5 [Deck, Bottom]
3. Frame, 154.4 [Deck]
4. Frame, 161 [Bottom]
5. Frame, 161.5 [Deck]
6. Frame, 164.5 [Deck]
7. Frame 170 [Deck]
8. Frame 170.5 [Deck]

Figure 48 shows a side view of the vessel under consideration. The location and the type of the sensors are indicated.

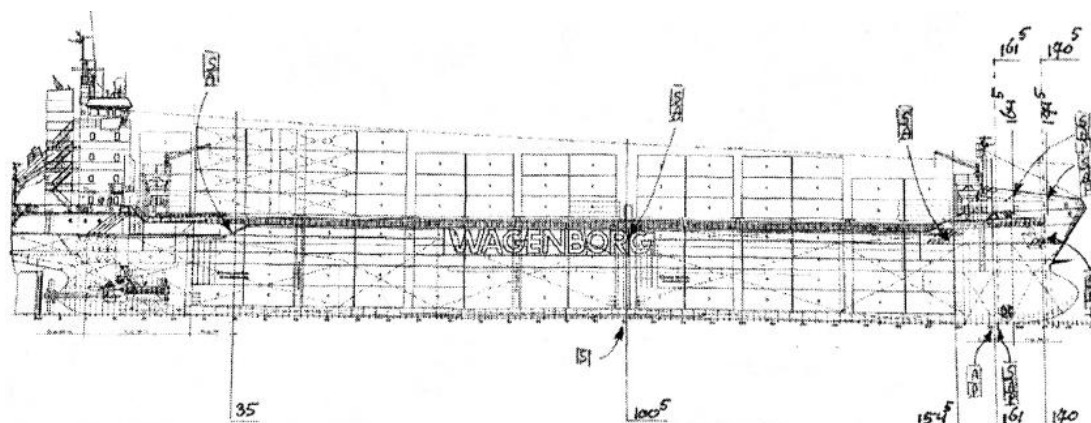






**Figure 47: 135 m dry cargo vessel, sensor locations indicated.**

There are three types of sensors available. [Strain (s), Acceleration (A) and Pressure (P)].

Bottom pressure time traces used that were used as the impulse load have been included in the appendix. Load is applied at the bow area [at five nodal points] as concentrated upward vertical force with amplitude- tabular. That means impulse from slamming press modeled as triangular impulse. [See Appendix]

### 6.2.1 Acceleration time traces

Dynamic response analysis was done for each three Wet mode model [Lightship, Ballast, and Loaded]. In this section results only for wet mode- loaded condition are given.

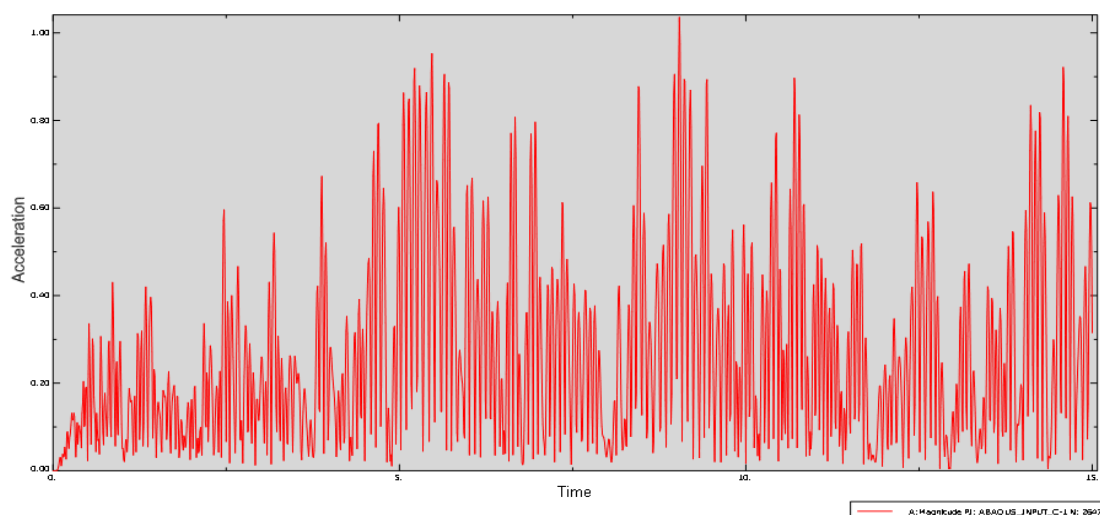


**Figure 48: Acceleration time traces Frame 35 [Deck, SB]**

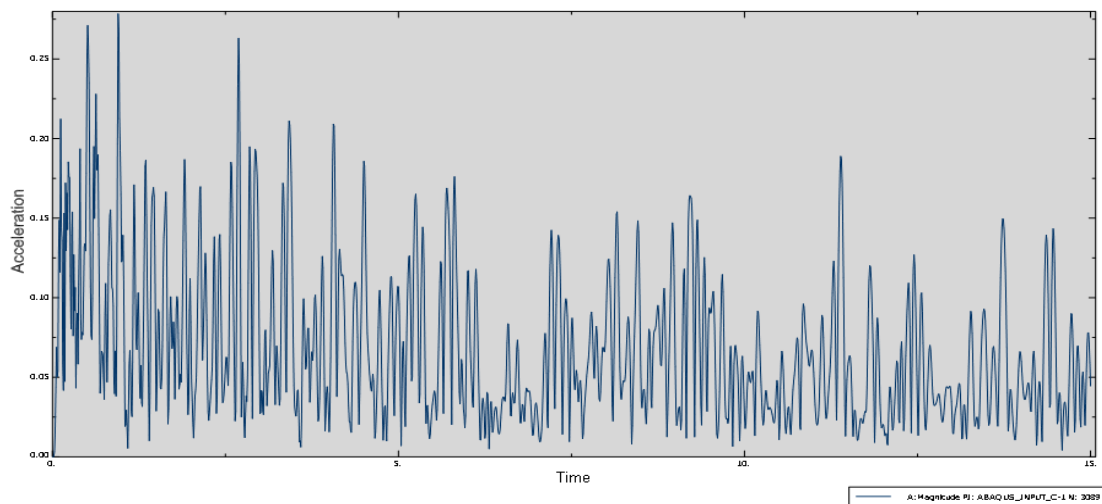


**Figure 49: Acceleration time traces frame 100.5 [Deck, SB]**

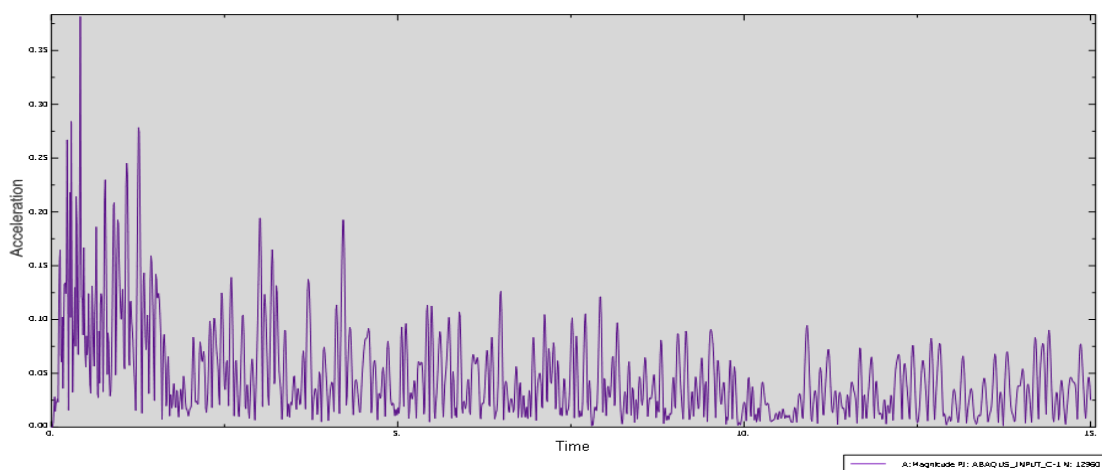


**Figure 50: Acceleration time traces, Frame 100.5 [Bottom, CL]**

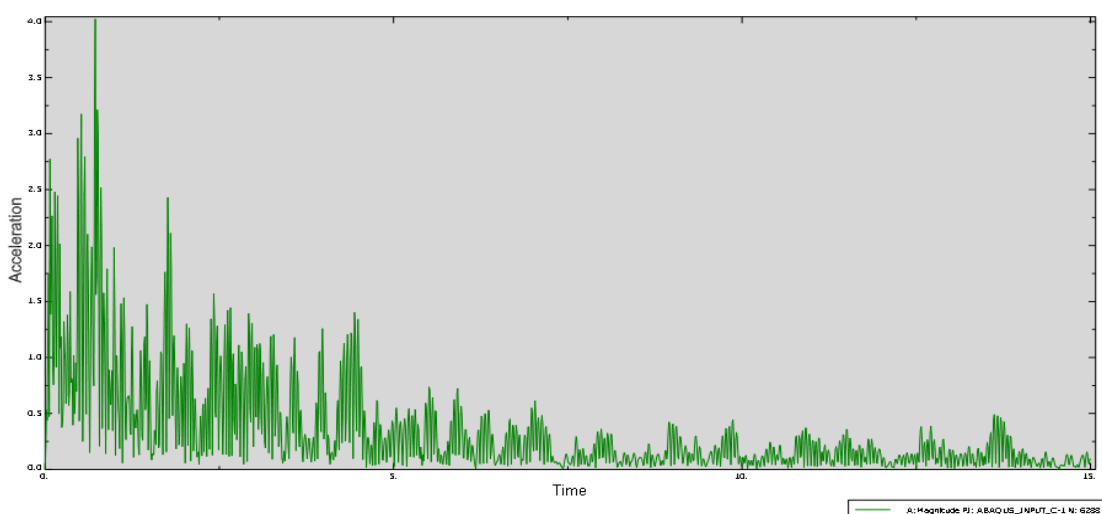


**Figure 51: Acceleration time traces, frame 154.5 [Deck, SB]**

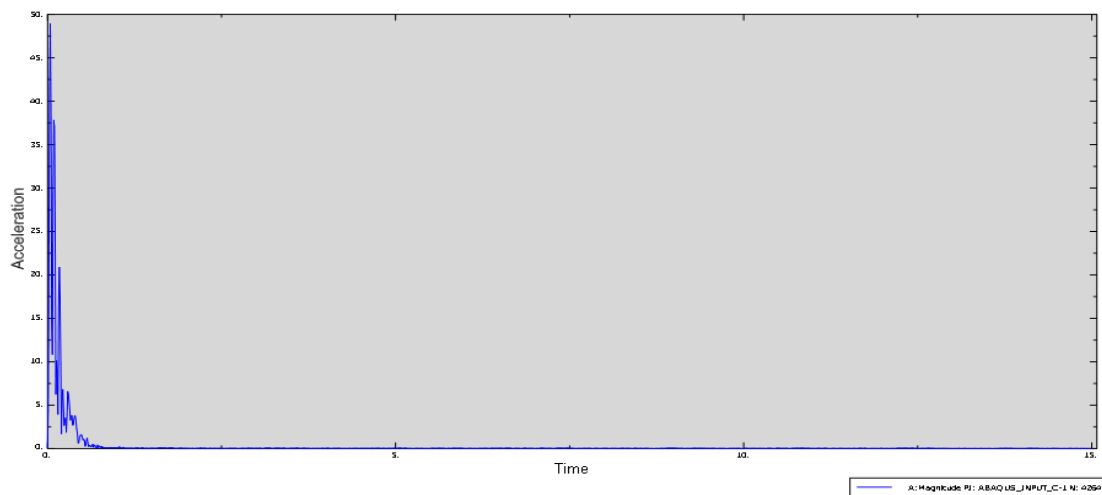


**Figure 52: Acceleration time traces, Frame 161[Bottom, CL]**

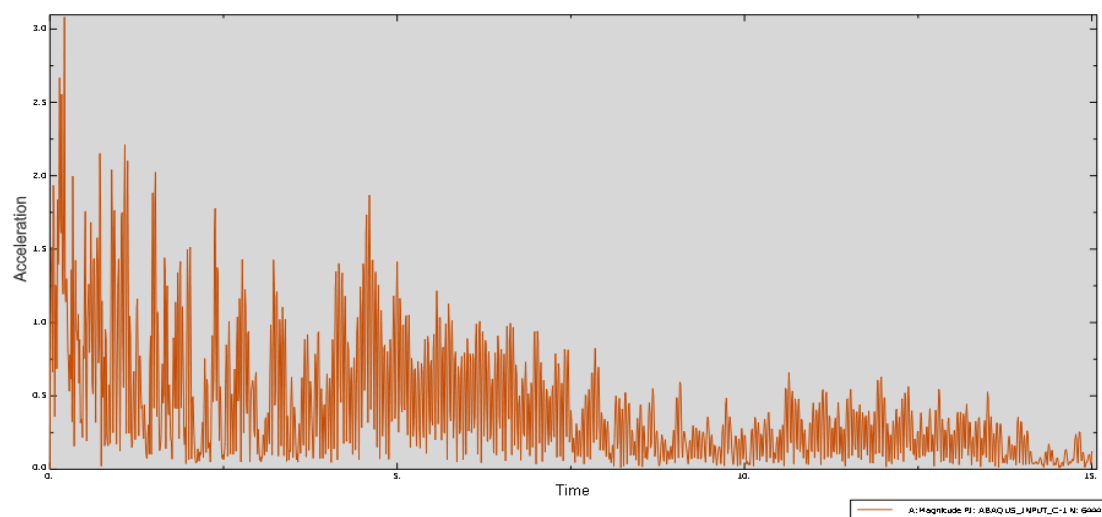


**Figure 53: Acceleration time traces, Frame 161.5[Deck, SB]**

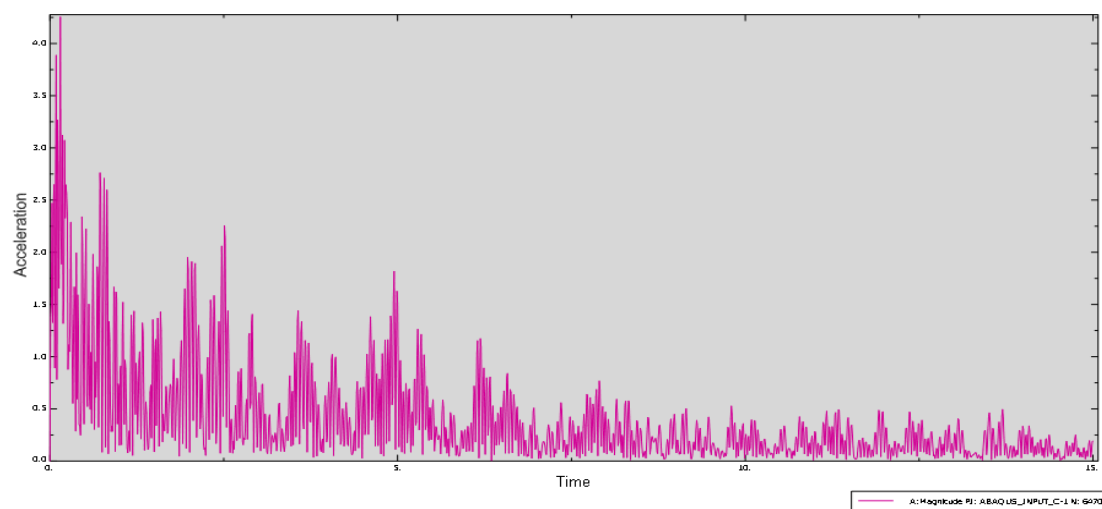


**Figure 54: Acceleration time traces, Frame 164.5 [Deck, SB]**

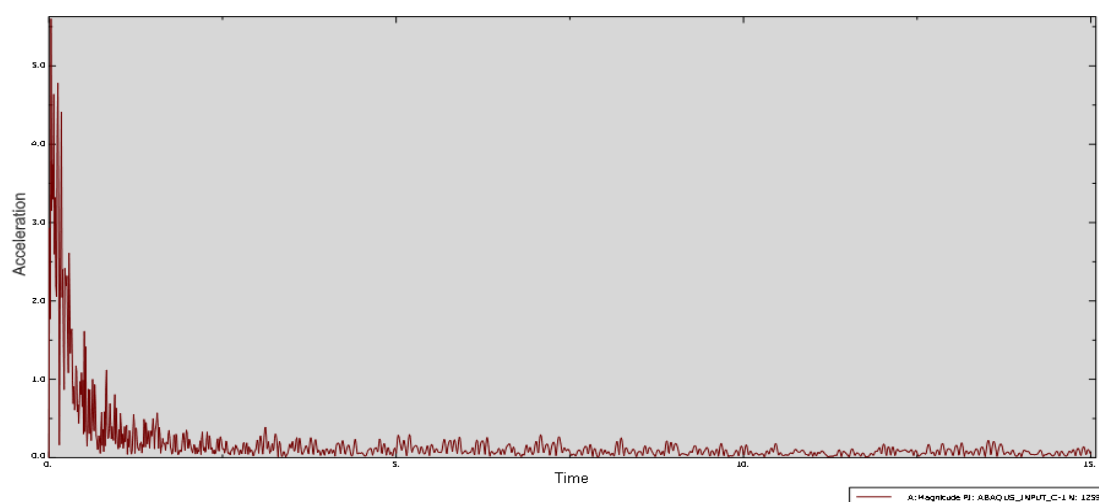


**Figure 55: Acceleration time traces, Frame 170 [Deck, SB]**

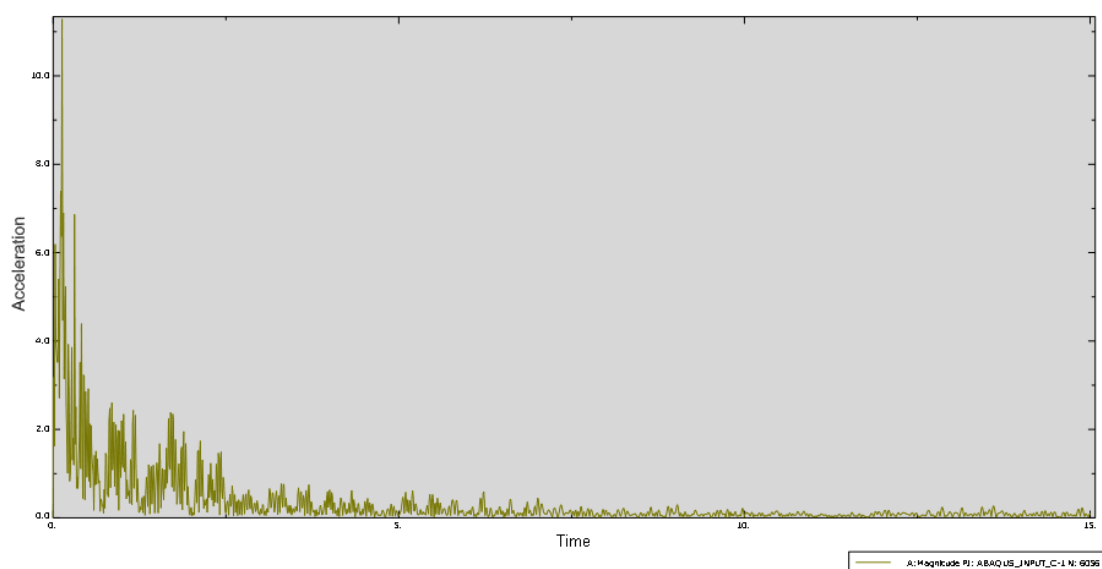


**Figure 56: Acceleration time traces, frame 170.5 [Deck, SB]**

In the amidships area and area aft to mid ship area acceleration during the entire period looks quite stable. In the areas close to the bow acceleration damps out as the time passes.

## 6.2.2 Strain time traces

Dynamic response analysis was done for each three Wet mode model [Lightship, Ballast, and Loaded]. In this section results only for wet mode- loaded condition are given.

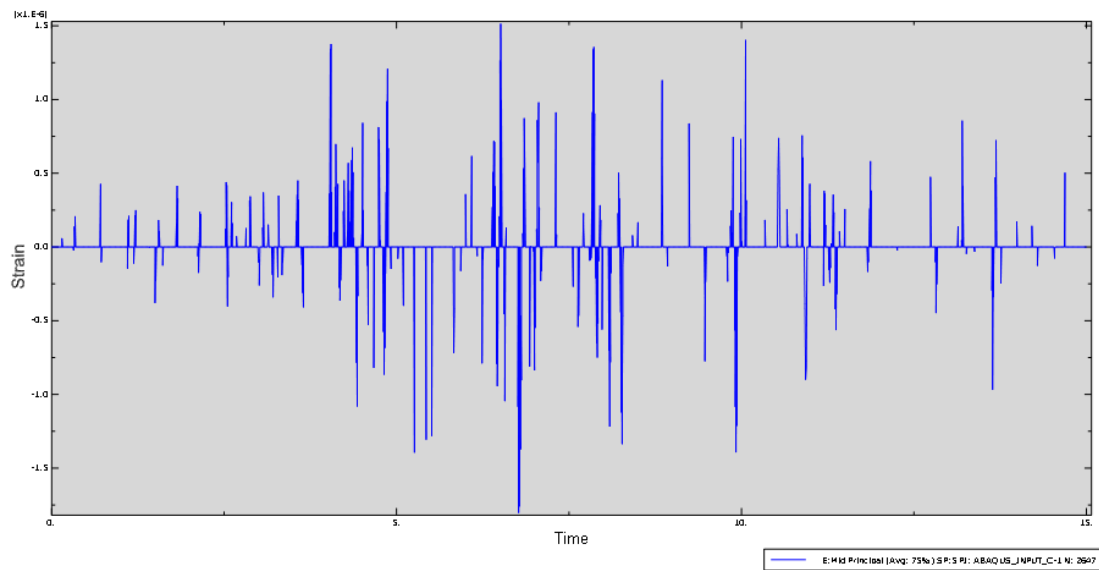


**Figure 57: Strain time traces, Frame 35[Deck, SB]**

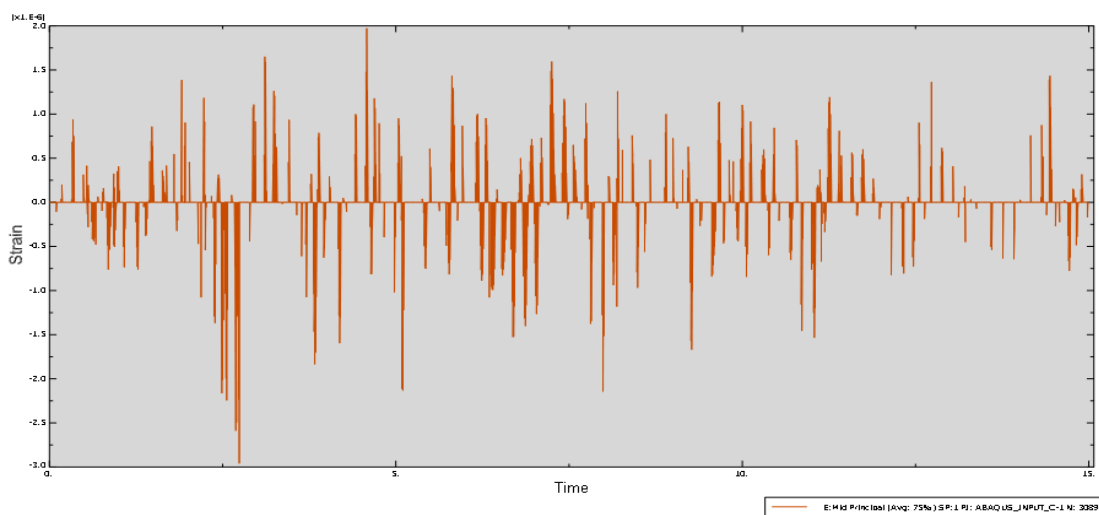


**Figure 58: Strain time traces, Frame 100.5 [Deck, SB]**

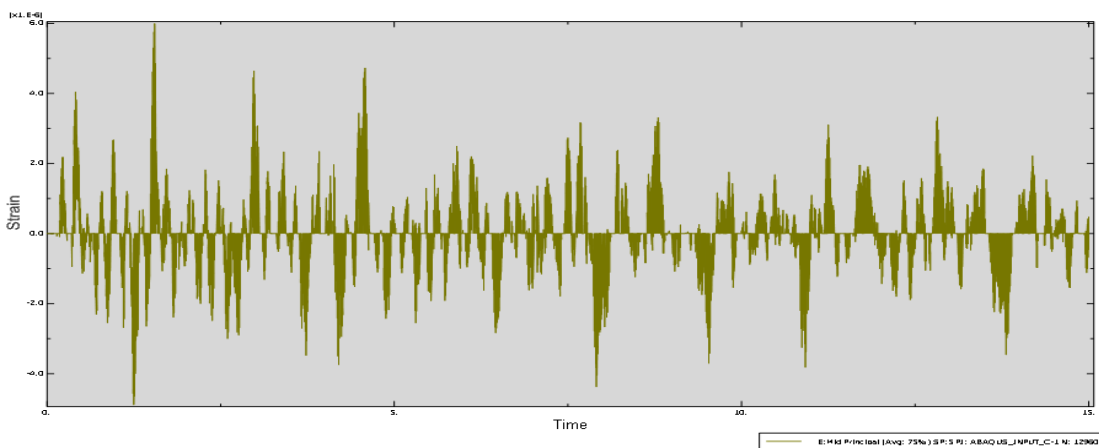


**Figure 59: Strain time traces, Frame 100.5 [Bottom, CL]**

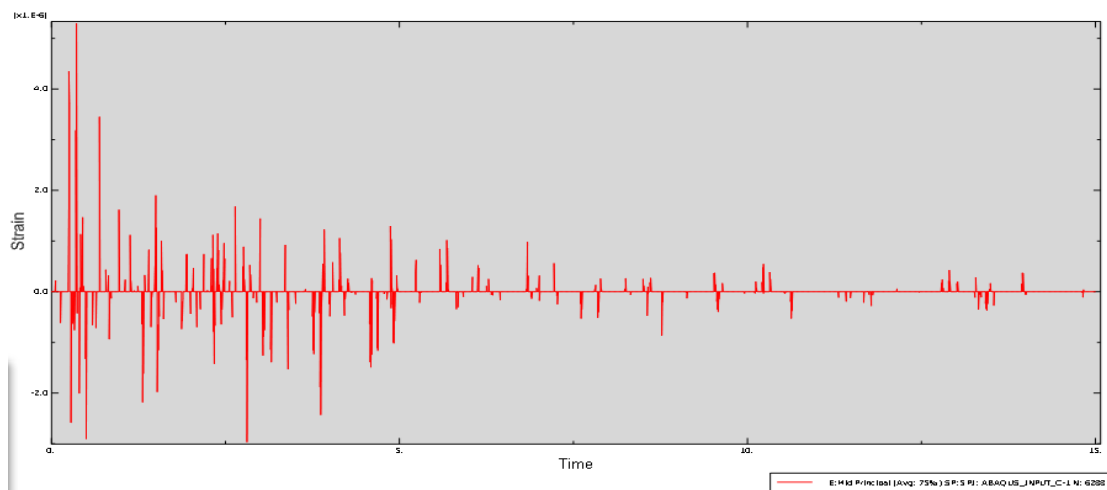


**Figure 60: Strain time traces, Frame 154.5 [Deck, SB]**

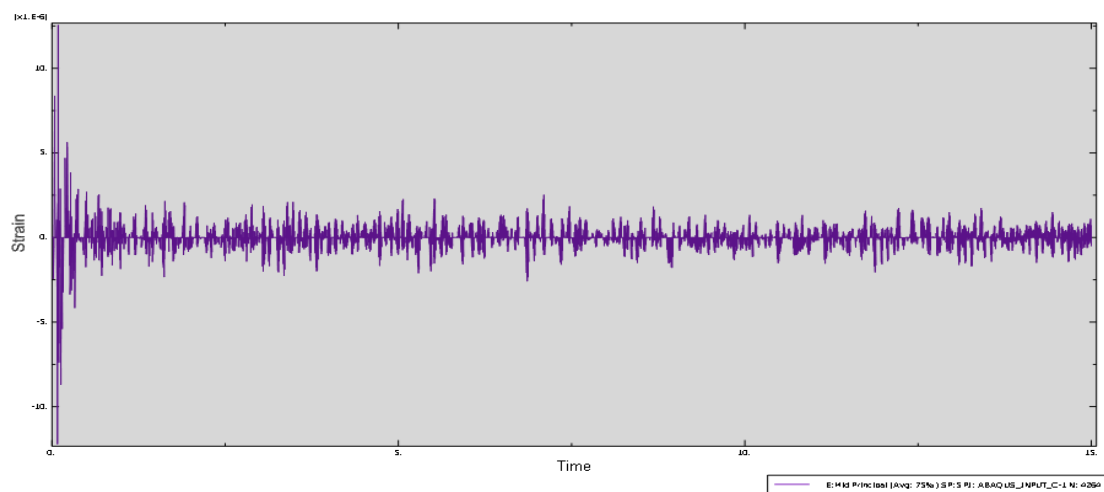


**Figure 61: Strain time traces, Frame 161 [Bottom, CL]**

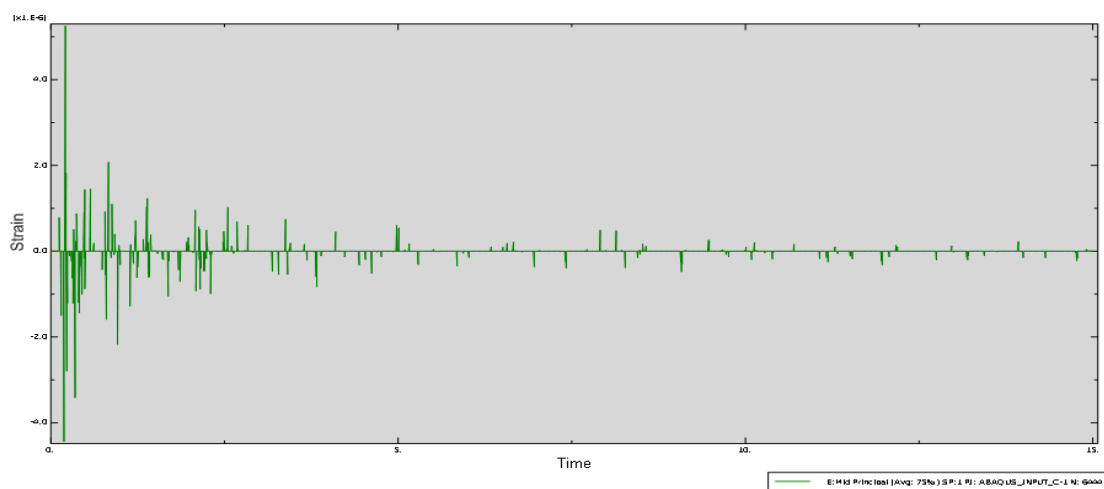


**Figure 62: Strain time traces, frame 161.5 [Deck, SB]**

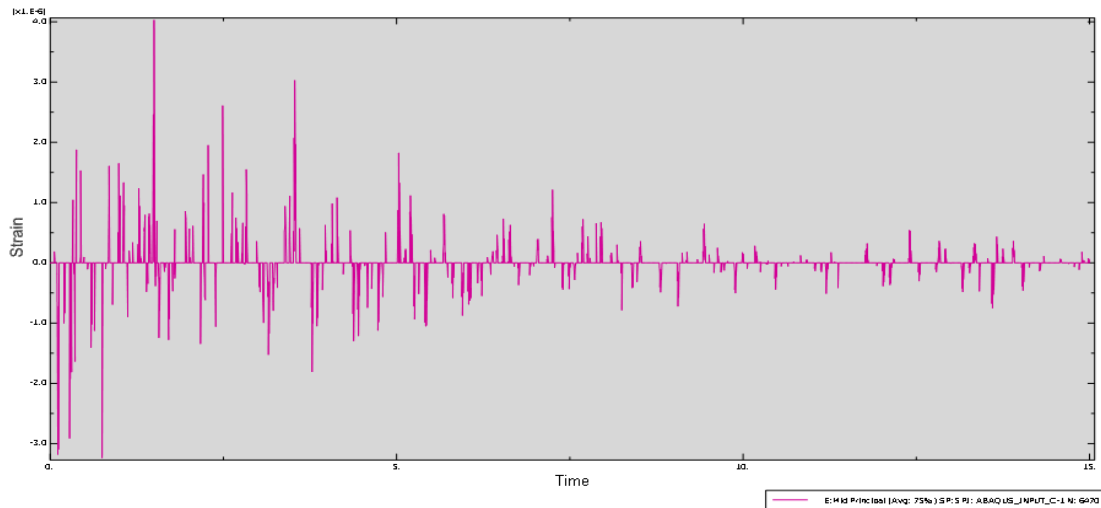


**Figure 63: Strain time traces, Frame 164.5 [Deck, SB]**

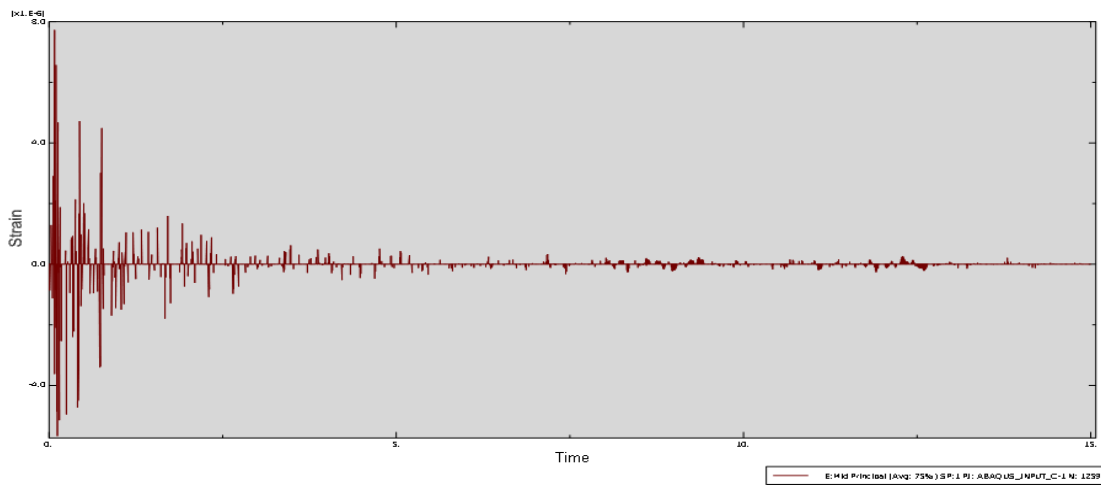


**Figure 64: Strain time traces, Frame 170 [Deck, SB]**

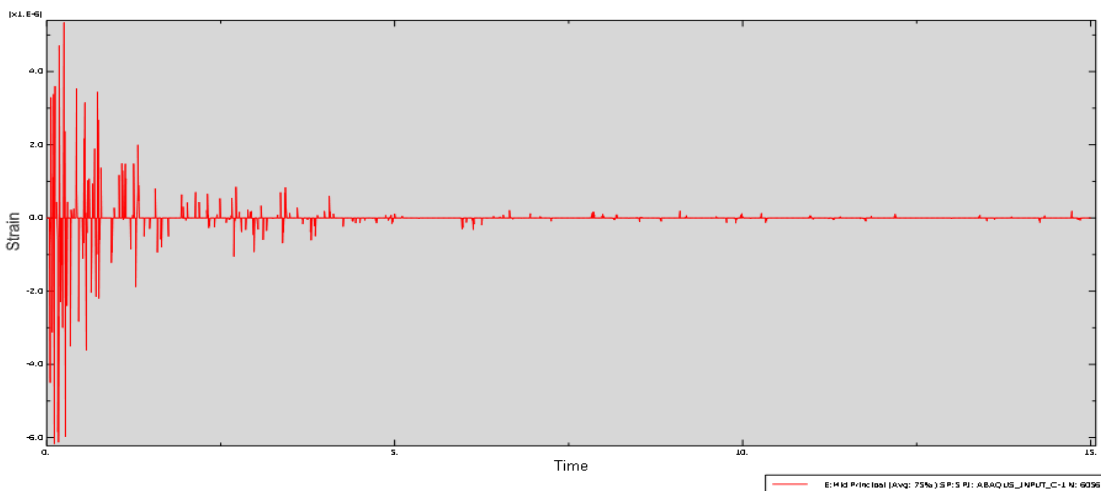


**Figure 65: Strain time traces, Frame 170.5 [Deck, SB]**



Time traces for strain in different location of ship show different characteristics due to slamming load. In the Area aft of amidships and amidships strain traces are almost same and maximum response at the middle of the period. However it looks as the location move to bow direction response damps out quickly.





## 7 Discussion and Conclusions

One of the main approximations of this study is related to the development of the model. Only the transverse frames, longitudinal frames, outer shell and inner shell were modeled. For light ship model, all the non-structural mass was distributed on the entire ship part [uniformly distributed on each node]. Position of longitudinal center of gravity was perfectly obtained but as there was no structural member above the inner bottom, vertical center of gravity position quite roughly estimated. Results might be influenced by the method of application of the slamming load. Dynamic, implicit analysis was used with fixed increment of 0.01 second. A lot of studies done before, low the increment size give better result. Another approximation was made for the wet mode model. Calculated added mass applied to the model as distributed on each node. Buoyancy stiffness added to the model as dashpot in ten location of the entire model which may create some disturbance from the actual result.

For both acceleration and strain time traces aft of the mid ship show that the magnitude is higher in the middle of the time period. In the bow area, there is a sudden increase in the peak value and damps out quite quickly as the time passes. Response is quite influenced by the Fluid structure Interaction (FSI). In this study FSI is accounted in terms of added mass and water plane stiffness but in real life scenario FSI problems are related to lot of other factors. Acceleration and strain results for each specified location of the have been presented in the result chapter. For the physical interpretation of the results, calculated results are compared with ISO 6954 standard “Guide lines for overall evaluation of vibration in merchant ships”.

For the same loading condition natural frequencies reduces around 40 percent for the wet mode ( In case of 2- node vertical mode in loaded condition, dry mode frequency is 1.2281 Hz and corresponding wet mode frequency 0.70975 Hz). From the work of Gul and Levent [57] it has been seen that for similar loading condition wetted frequency reduced almost 35 percent from the dry frequency. In their [57] work, surrounding water was modeled with acoustic finite element. For loaded condition wet mode model, there is overlap in appearance of mode shapes between wet and dry mode. (For instance lateral bending mode appears before vertical bending mode for wet mode).

A typical velocity trace in bow area is given below. It shows that, in the bow area during the time of impulse response amplitude is very high, after wards velocity in somewhere in forecandle deck is significantly low.

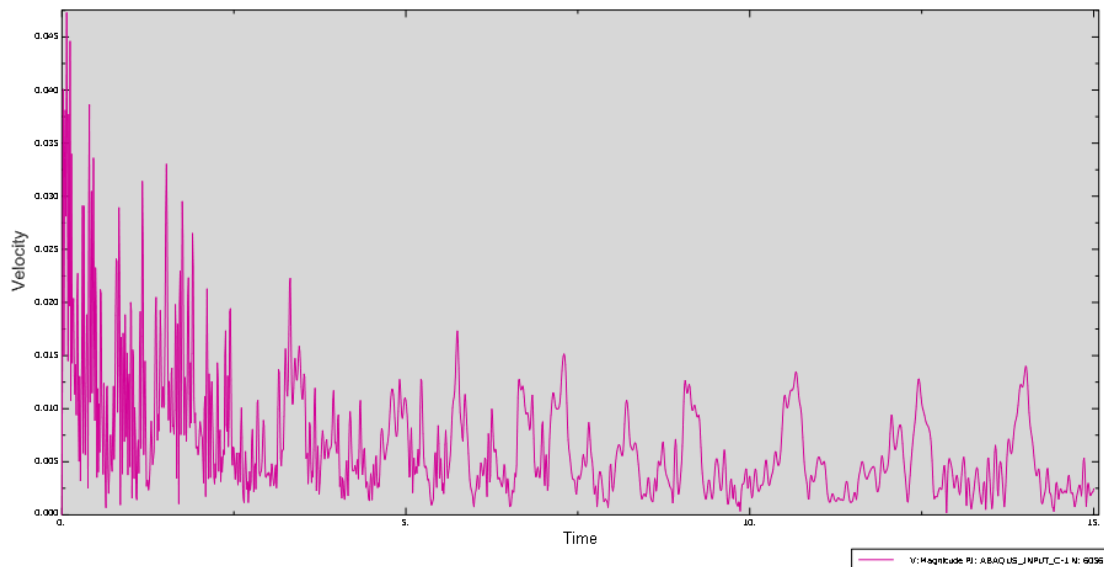


**Figure 66: Velocity trace in the bow area , Frame 170, SB**

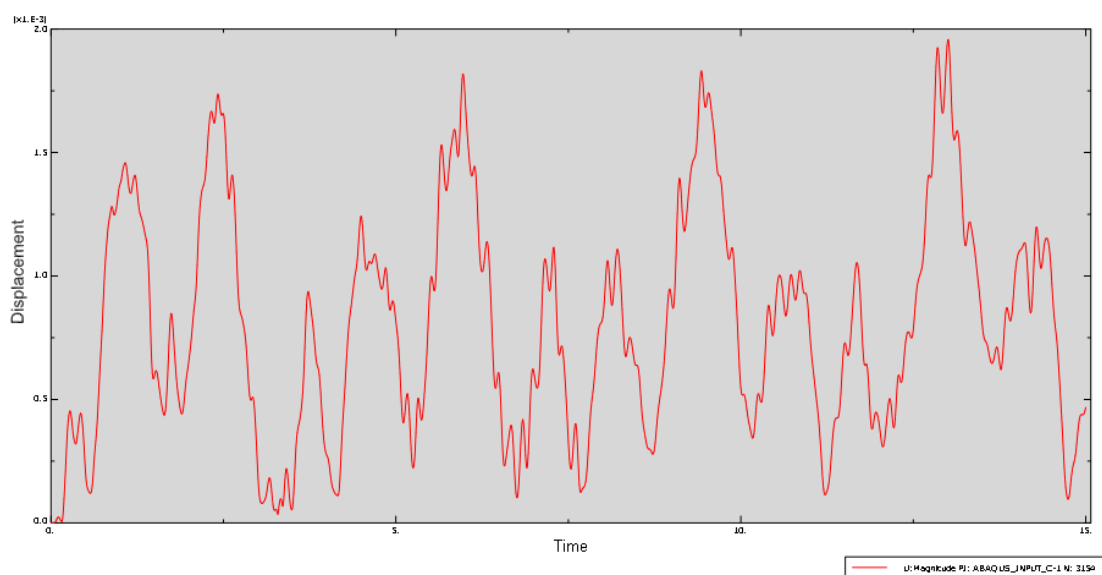


**Figure 67: Displacement trace in amidship., SB**

From the above time traces, the peak value for displacement repeats at a period of 2.25 second. Generally maximum force is applied at one time step and the maximum vertical bending moment occurs at another time step. Analysis shows that model shows some responses at a random time step even though the impulse is applied earlier.

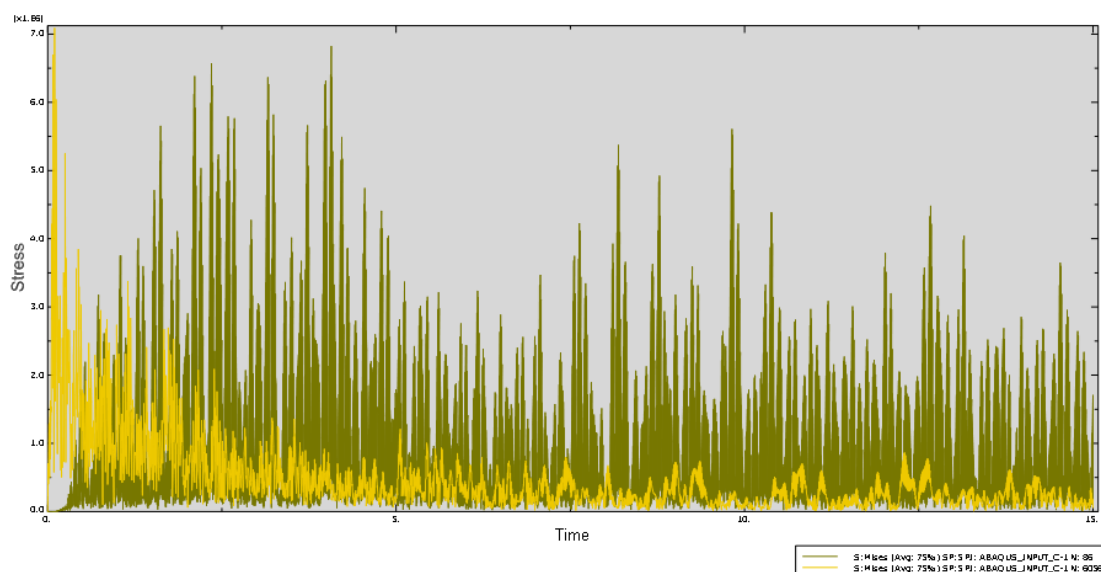


**Figure 68: Stress [mises] plot in bow and stern area, SB**

In the bow area [Yellow], stress level falls very quickly just after the slamming occurrence. In the stern area all through the time period, the variation of stress level with respect to time is low. So it can be said that for local structure fatigue damage in the deckhouse and superstructure slamming load has to be tackled carefully.

First possible way to improve the result is to put more effort on the development of model. All the structure including machinery and installations need to be modeled to get the proper mass distribution. To account the hydrodynamic effects properly, surrounding seawater around the ship is also need to be modeled as acoustic medium. Hull vibratory responses to waves are important in other modes than the 2-node or 3-node vertical bending mode for instance lateral bending, torsion or combination of bending and torsion in case of oblique sea or quartering sea. Exact prediction of hull whipping response is complex process because of the stochastic nature of the sea way, the non-linear character of the response transfer functions and the impossibility to exactly predict the ship's operational parameters.

Damping still remains a literally uncertain parameter in ship girder vibration study. Until today a generally applicable approach for damping estimation has not been found. Recent works set that measured damping constants can vary significantly depending on the type of ship and the vibration frequency and mode shape.

Slamming is a rarely occurring phenomenon. For developing a reliable statistical analysis, it is necessary to accumulate a large number of occurrences in long time investigation both numerically and experimentally.

Development of standard methodologies for ship vibration study is needed to be tackled considering the diversity of ship types, propulsion plants and comfort requirements.



## **8 Recommendation for future work**

In recent years lot of effort has been given predicting the nature and magnitude of loads related to slamming. From global hull strength point of view, translation of these loads to structural response has to be considered with significant attention. This thesis work was a part of ISSC 2015 Committee II and concern of the committee is the dynamic structural response of ship and offshore structure from environmental loads, machinery and propeller excitation. Influence of propeller and other rotating machinery on board are important sources of hull vibration. Coupling between different sources of hull girder vibration may provide the whole picture.



## 9 References

- [1] Odd M. Faltinsen, Hydrodynamics of High-Speed Marine Vehicles, Chapter 8, 2005
- [2] Kazuhiro Iijima, Tetsuya Yao, Torgeir Moan, Structural response of a ship in severe seas considering global hydro-elastic vibrations, 2008, Marine Structures 21, 420-445
- [3] 17<sup>th</sup> international ship and offshore structure congress 16-21 august, 2009, seoul, korea, Dynamic response committee II.2
- [4] 18<sup>th</sup> international ship and offshore structure congress ,09-13 september 2012, rostock, Germa, Dynamic response committee II.2
- [5] Gaidai, O.; Storhaug, G. and Naess, A. Extreme value statistics of Whipping response for large ships. PRADS 2010.
- [6] Lee, Y.; Wang, Z. and White, N. Time domain analysis of springing and Whipping Response Acting on a Large Container Ship, ASME, OMAE, 2011.
- [7] Ochi MK, Motter LE. A method to estimate the slamming characteristics for ship design. Mar. Technol 1971; 8:219}32
- [8] Kawakami M, Michimoto J, Kobayashi K. Prediction of long term whipping vibration stress due to slamming of large full ships in rough seas. Int. Shipbuild Prog 1977; 24:83}110.
- [9] Belik O, Bishop RED, Price WG. Influence of bottom and #are slamming on structural responses. Trans RINA 1988;130:325}37
- [10] Belik O, Price WG. Comparison of slamming theories in the time simulation of ship responses in irregular waves. Int Shipbuild Prog 1982;29:173}87.
- [11] Yamamoto Y, Sugai K, Inoue H, Yoshida K, Fujino M, Ohtsubo H. Wave loads and response of ships and offshore structures from the viewpoint of hydroelasticity. Advances in marine structures, Amsterdam: Elsevier, 1986, pp. 26}40
- [12] Ramos J, Guedes Soares C. On the assessment of hydrodynamic coefficient in heaving. Ocean Engng 1997;24(8):743}64
- [13] Guedes Soares C. Transient response of ship hulls to wave impact. Int Shipbuild Prog 1989;36:137}56.
- [14] Salvesen N, Tuck E, Faltiseu O. Ship motions and sea loads. Trans SNAME 1970;78:250}87.
- [15] Molin B, Cointe R, Fontaine E. On energy arguments applied to slamming force. Proceedings of the 11th International Workshop on Water Waves and Floating Bodies, Hamburg, Germany, 1996.
- [16] Tao Z, Incecik A. Large amplitude ship motions and bow Flare slamming pressures. Proceedings of the 15th International Conference on Offshore Mechanics and Arctic Engineering, OMAE'96, Florence, Italy, 1996



- [17] Sames PC, Schellin TE, Muzaferija S, Peric M. Application of a two-Fluid finite volume method to ship slamming. Proceedings of the 17th International Conference on Offshore Mechanics and Arctic Engineering, OMAE'98, Lisboa, Portugal, 1998.
- [18] Aksu S, Price WG, Temarel P. A comparative study of the dynamic behaviour of a fast patrol boat in rough seas. *Mar Struct* 1993;6:421-41
- [19] Ramos J, Guedes Soares C. Vibratory response of ship hulls to wave impact loads. *Int Shipbuild Prog* 1998;45(441):71-87
- [20] Todd, F. M., *Ship Hull Vibration*, Edward Arnold (Publishers) Ltd., London, 1961
- [21] Lewis, F. M., "Hull Vibration of Ships," Chapter X, S.N.A.M.E. Principles of Naval Architecture, 1967
- [22] Boylston, J. W. and Leback, W. G., "Toward Responsible Shipbuilding," S.N.A.M.E. Transactions, 1975.
- [23] Taggart, R., "Ship Design and Construction," S.N.A.M.E., 1980
- [24] Noonan, E.F., "An Assessment of Current Shipboard Vibration Technology," Ship Structures Symposium 1975, S.N.A.M.E. Publication SY-5.
- [25] Schlick, O., "Further Investigations of Vibration of Steamers," R.I.N.A. 1894
- [26] Dinsenbaker, A. L. and Perkins, R. L., "A Simplified Method for Computing Vertical Hull Natural Frequencies and Mode Shapes in Preliminary Design Stage," D.T.R.C. Report 3881, January, 1973.
- [27] Leibowitz, R. and Kennard, E., "Theory of Freely Vibrating Nonuniform Beams, Including Methods of Solution and Application to Ships," DTMB Report 1317, May, 1961.
- [28] Bruck, H. A., "Procedure for Calculating Vibration Parameters of Surface Ships," NSRDC Report 2875, December, 1968.
- [29] Cuthill, E. H. and Henderson, F. M., "Description and Usage of General Bending Response Code 1, (GBRCI)," DTMB Report 1925, July, 1965.
- [30] Noonan, E. F., "Design Considerations for Shipboard Vibration," S.N.A.M.E., Marine Technology, January, 1971
- [31] "124,000 CM LNG Carrier, F-D Hull Vibration Analysis Using 20-Station Beam Model," NKF Technical Note 7321-9, August, 1975.
- [32] MRI/Stardyne 3, "Static and Dynamic Structural Analysis Systems, User Information," developed by Mechanics Research, Inc., available through Control Data Corp
- [33] MRI/Stardyne, Static and Dynamic structural System, Theoretical Manual, available through Control Data Corp.
- [34] Guyan, R. J., "Reduction of Stiffness and Mass Matrices," AIAA Journal, Vol . 3, No. 2, February, 1965.



- [35] "Avondale Hull Vibration Analysis by Finite-Element Method Including Comparison with Conventional Beam Method on 125,000 CM LNG Carrier," NKF Technical Note 7321-8, August, 1975.
- [36] MacNeal, R. H., "The NAS' RAN Theoretical Manual, Level 15," a NASA Publication, April 1972.
- [37] Noonan, E. F., 'Prclininnry !hull nmd Machinery Vibration Analysis for DD 963 Class Destroyer Desig' N. Fcprt No. 7105-I, to Litton Systems, Inc., February, 1971.
- [38] Ali, H. B. "Calculated Natral Frequencies and Normal Modes of Vibration of *USS Brumby*, (DE- 1044)," NSRDC Report 2619, March, 1968.
- [39] Horn, F., "Horizontal and Torsionschwingurigen and Frachtschiffen," Werft Reederie Hafen, 1925.
- [40] Czekanski, A., N. El-Abbasi, and S. A. Meguid, "Optimal Time Integration Parameters for Elastodynamic Contact Problems," Communications in Numerical Methods in Engineering, vol. 17, pp. 379–384, 2001.
- [41] Hilber, H. M., T. J. R. Hughes, and R. L. Taylor, "Improved Numerical Dissipation for Time Integration Algorithms in Structural Dynamics," Earthquake Engineering and Structural Dynamics, vol. 5, pp. 283–292, 1977
- [42] American National Standard, Guidelines for the measurement and evaluation of vibration of ship propulsion machinery, ANSI S2.27 (2002)
- [43] Guide to measurement and evaluation of human exposure to whole-body mechanical vibration and repeated shock, BS 6841 (1987)
- [44] Yasar gul, Levent Kaydihan, Global Vibration analysis of a 1900 TEU capacity container ship.
- [45] ABAQUS/CAE 6.11-1 user manual.
- [46] SESAM/GeniE 64 V6.3-06 user manual
- [47] SESAM/HydroD V4.5-08
- [48] SNAME, Principles of Naval Architecture, Second Revision, Volume III, Motions in Waves and Controllability, 1989
- [49] O. M. Faltinsen, Sea Loads on Ships and Offshore Structure, 1990
- [50] TMR 4215:Sea Loads, Lecture Note, NTNU.
- [51] Flatinsen, O.M, Zhao, R, Water entry of ship sections and axisymmetric bodies, AGARD report 827, High speed body motion in water., 1998
- [52] Divities . N, de, Socio, L.M.de, Impact of floats on water, 2002
- [53] Wagner, H, U"ber Stoss- und Gleitvorga"nge an der Oberfl"ache von Fl"ussigkeiten., 1932
- [54] Zhang, R, Flatinsen, O.M, Slamming loads on High speed Vessel, 1996
- [55] Ge, C., Faltinsen, O.M, Moan, T, Global Hydro elastic response of catamarans due to wetdeck slamming, 2005
- [56] Sabera Khatoon, Transient dynamic response of ship hull, 2011



[57] Yasar Gul, Levent Kaydihan, Global vibration of a 1900 TEU capacity containership, 2005.





# Appendices

## 9.1 Appendix A

Input data from ISSC Committee II.2 Dynamic Response

The mass distributions of light weight and deadweight are given in this document

<b>Given</b>											
Displacem	98	tons									
LCG	61.49	m									
Neutral	4.00	m									
<b>Lightweig</b>											
Lightweig	29	tons									
LCG	51.88	m	Check	LSW							
			63.525	LCG FA		61.722					
Compone	Weight	LCG [m]	Start [m]	End [m]	VC	Weight/m	com	com	$I_{v,y} [km^2]$	$I_{v,z} [km^2]$	
Engine	51.0	13.00	10.20	15.45	3.00	9.71	3.00	4.00	157	120070	
Engineeroo	200.0	13.70	6.00	18.60	2.50	15.87	10.0	5.50	2620	461089	
Hull 1	34.5	3.00	-4.80	6.00	9.00	3.19	15.0	5.00	1579	118883	
Hull 2	29.5	7.80	6.00	9.50	5.00	8.43	15.8	12.7	1045	85664	
Hull 3	125.4	16.29	9.50	23.04	4.50	9.26	15.8	12.7	4347	260722	
Hull 4	113.4	29.01	23.04	34.88	4.00	9.58	15.8	12.7	3904	123315	
Hull 5	363.9	53.38	34.88	71.88	4.00	9.83	15.8	12.7	12527	73080	
Hull 6	145.5	79.28	71.88	86.68	4.00	9.83	15.8	12.7	5011	51775	
Hull 7	210.0	98.51	86.68	11	4.00	8.35	15.8	12.7	7231	303408	
Hull 8	40.3	11	111	11	4.00	7.78	15.8	12.7	1387	114332	
Hull 9	20.3	11	117	11	4.50	9.14	15.8	12.7	703	65557	
Hull 10	30.9	12	119	12	5.00	8.60	15.0	12.7	1027	110092	
Hull 11	4.4	12	122	12	6.00	7.27	14.0	12.7	147	16637	
Hull 12	30.6	12	123	13	6.00	3.46	12.0	10.0	745	129665	
Wheelhou	146.9	8.10	3.00	11.60	16.0	17.08	13.5	10.5	24734	421873	
Forecastle	200.0	11	112	13	13.0	9.85	12.0	5.00	19016	670748	
Rest	11	60.38	-4.80	12	2.00	8.90	15.8	5.00	31421	1669543	
Total	29	58.80									

<b>Deadweig</b>											
Deadweig	698	tons									
LCG	65.49	m									
Compone	Weight	LCG [m]	Start [m]	End [m]	VC	Weight/m	com	comp	$I_{v,y} [km^2]$	$I_{v,z} [km^2]$	
Ballast 1	168.4	121	116	126	0.55	16.84	8.00	1.10	2919	613401	
Ballast 2	135.4	115	110	120	0.55	13.54	8.00	1.10	2347	393320	
Ballast 3	84.5	103	98.97	108	0.58	8.45	4.00	1.10	1109	153301	
Ballast 4	84.8	104	99.00	109	0.58	8.48	4.00	1.10	1113	154061	
Ballast 5	161.9	105	100	110	6.34	16.19	1.30	1.80	953	321974	
Ballast 6	161.9	105	100	110	6.34	16.19	1.30	1.80	953	321974	
Ballast 7	168.8	88.9	83.9	93.9		16.88					
Ballast 8	100.4	83.1	78.1	88.1		10.04					
Ballast 9	100.4	83.1	78.1	88.1		10.04					
Ballast 10	156.3	84.54	79.54	89.54		15.63					
Ballast 11	156.3	84.54	79.54	89.54		15.63					
Ballast 12	71.4	75.21	70.21	80.21		7.14					
Ballast 13	109.6	58.16	53.16	63.16		10.96					
Ballast 14	109.6	58.16	53.16	63.16		10.96					
Ballast 15	240.2	57.45	52.45	62.45		24.02					
Total	200	88.60									
Fuel 1	99.0	27.79	22.79	32.79	2.29	9.90	1.30	4.00	435	113272	
Fuel 2	55.0	16.20	11.20	21.20	2.29	5.50	1.30	4.00	241	113281	
Fuel 3	17.1	17.50	12.50	22.50	5.96	1.71	1.60	3.00	82164	33236	
Fuel 4	16.6	17.38	12.38	22.38	5.57	1.66	1.60	3.00	56909	32440	
Fuel 7	2.6	10.20	5.20	15.20	7.95	0.26	2.00	1.00	41650	68622	
Fuel 8	15.0	7.54	2.54	12.54	7.77	1.50	2.00	1.50	221	43789	
To	205.3	21.28									



Remain. 1	29.4	2.98	-2.02	7.98	6.27	2.94	1.30	4.00	194836	100897691
Remain. 2	33.3	2.84	-2.16	7.84	6.28	3.33	1.30	4.00	222196	114828279
Remain. 3	2.3	12.17	7.17	17.17	8.64	0.23	1.50	2.00	50716	5614261
Remain. 4	1.0	13.72	8.72	18.72	7.03	0.10	1.50	2.00	9702	2290494
Remain. 5	0.9	15.13	10.13	20.13	8.29	0.09	2.50	3.00	17707	1942293
Remain. 6	0.5	9.15	4.15	14.15	7.63	0.05	4.00	3.50	7766	1374571
Remain. 7	0.6	9.16	4.16	14.16	0.95	0.06	5.00	1.10	6892	1649307
Remain. 8	3.4	5.41	0.41	10.41	7.00	0.34	1.50	1.50	31875	10721857
Remain. 9	13.3	7.09	2.09	12.09	8.61	1.33	2.00	1.50	289580	39474755
Remain.	6.5	13	8	18		0.65				
Remain.	1.1	14.51	9.51	19.51		0.11				
Remain.	0.9	8.46	3.46	13.46		0.09				
Remain.	1.3	8.45	3.45	13.45		0.13				
Total	94.5	5.07								
Cargo 1	50.0	40.00	18.60	113.32	4.00	0.53	13.00	6.00	854167	61177998
Cargo 2	40.0	98.51	98.18	98.84	6.39	60.61	13.00	8.50	1032651	55384001
Cargo 3	40.0	25.58	25.25	25.91	6.39	60.61	13.00	8.50	1032651	52145909
Cargo 4	1504.0	85.61	73.36	98.18	5.10	60.60	13.00	15.00	51201173	973379425
Cargo 5	2707.0	48.52	25.91	71.14	6.50	59.85	13.00	18.00	128131333	954985318
Cargo 6	331.0	21.92	18.60	25.25	5.60	49.77	13.00	18.00	14445943	524156189
Total	4672.0	58.72								

**Table 6: Mass data**

Drawing used as the basis of model development given below.

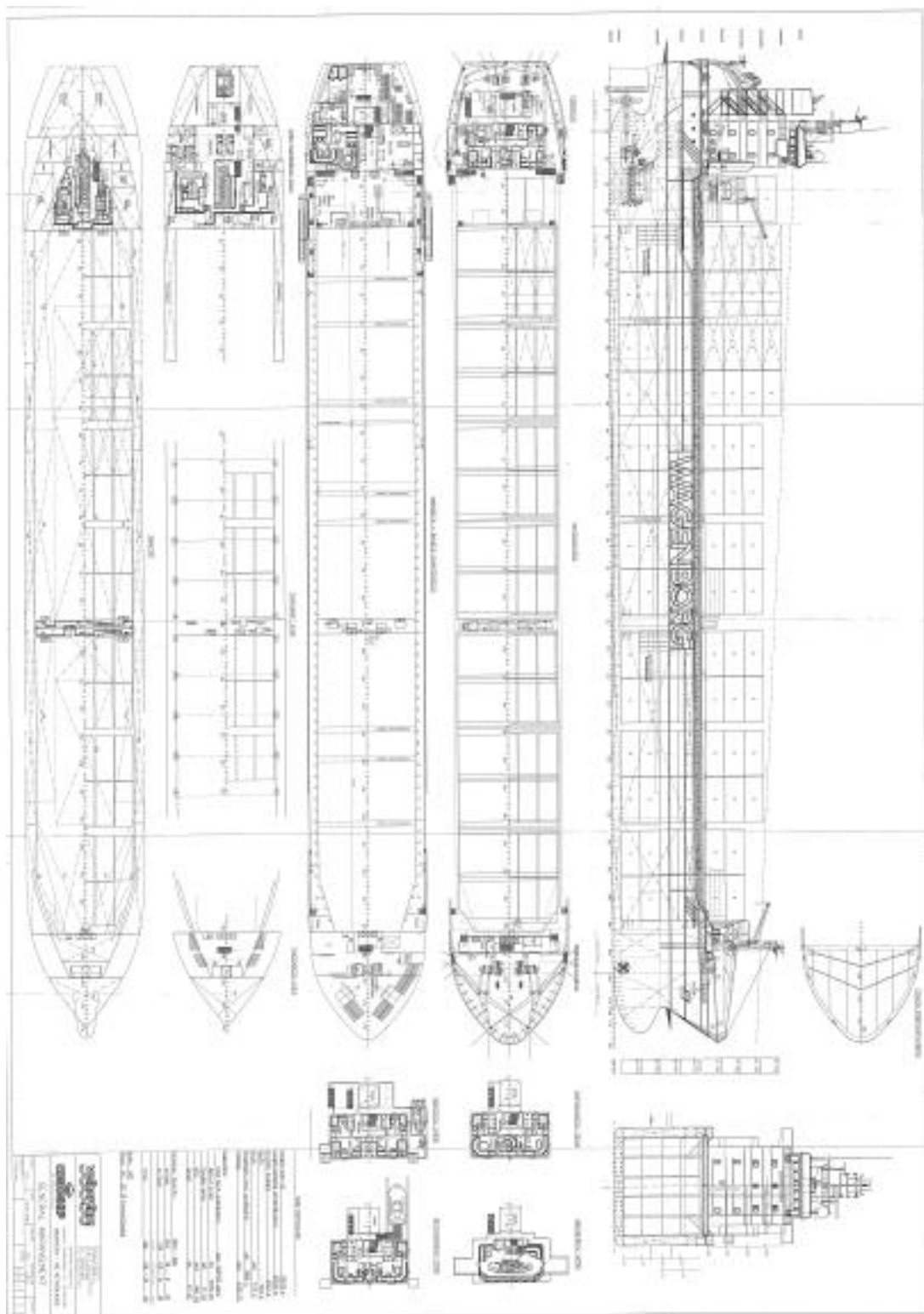


**Figure 69: General Arrangement**

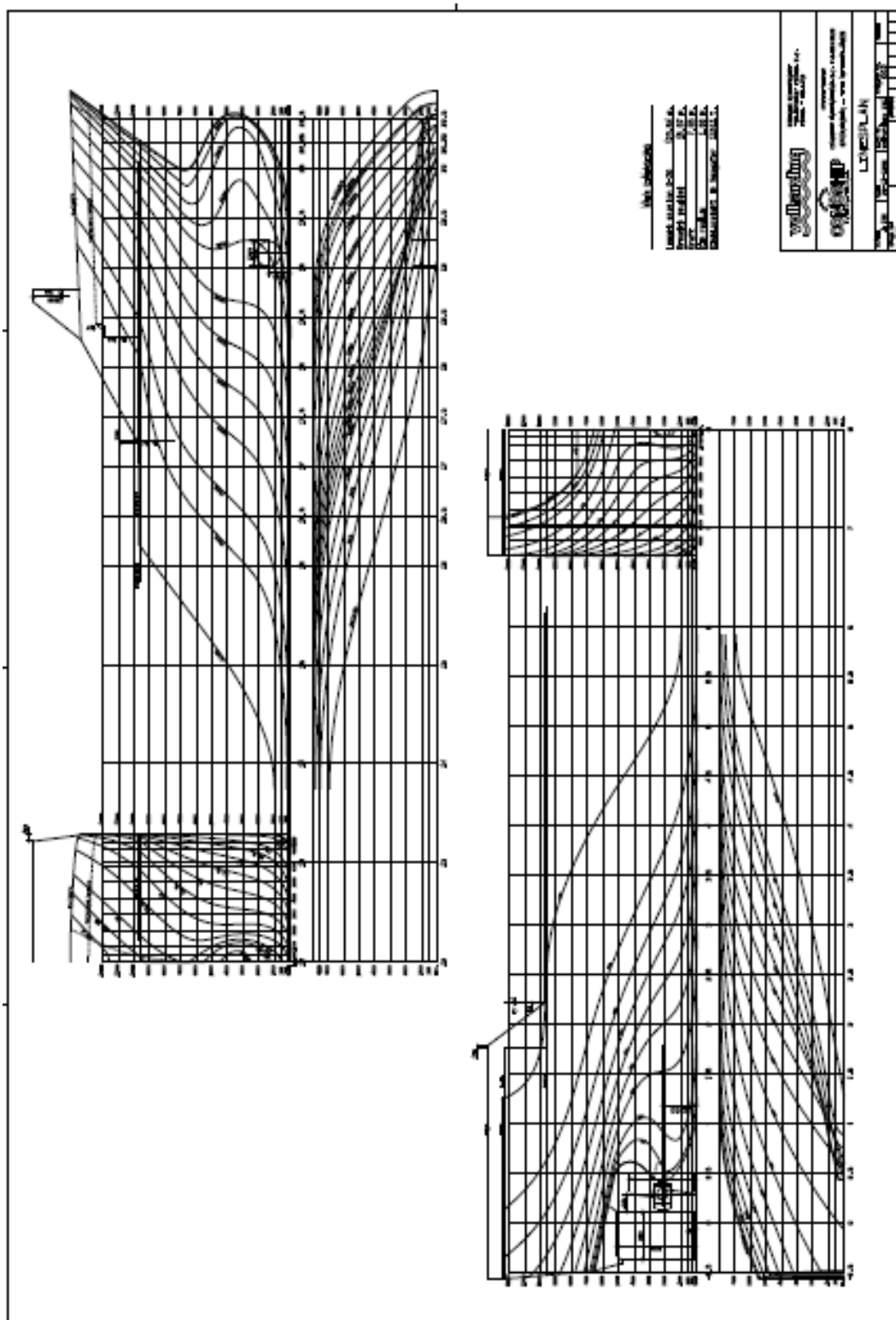


Figure 70: Lines Plan



## Sailing Condition

Ship speed = 14.0 knots  
Significant wave height = 3.50 meters  
Peak period = 8.5 seconds

**Headings = between bow quartering and head waves**

## Typical measured time traces

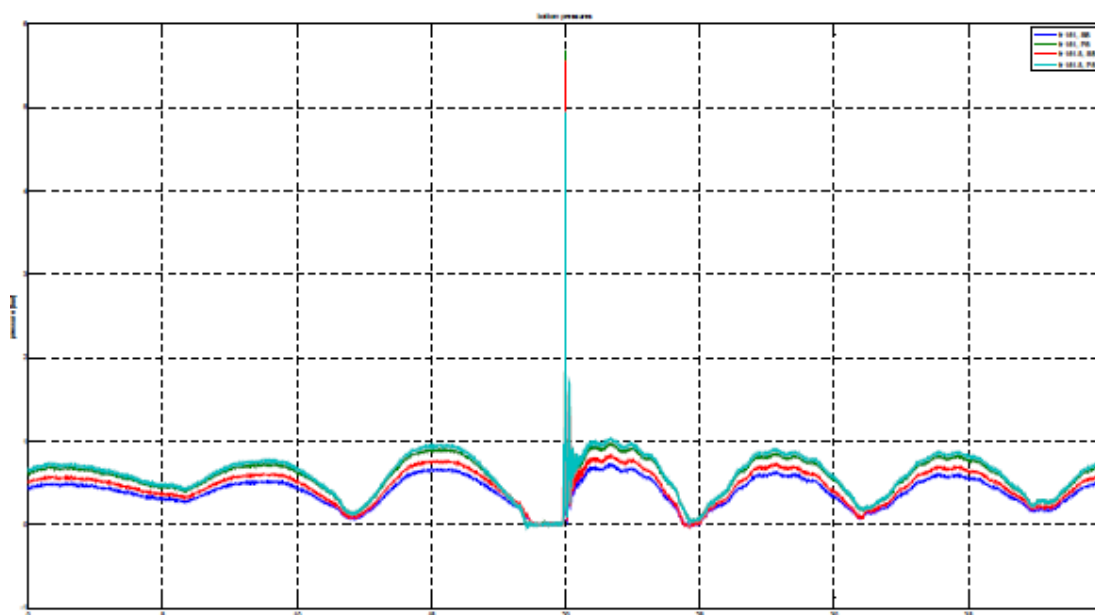


**Figure 71: Typical pressure trace fr.161 and 161.5 (measure 5)**

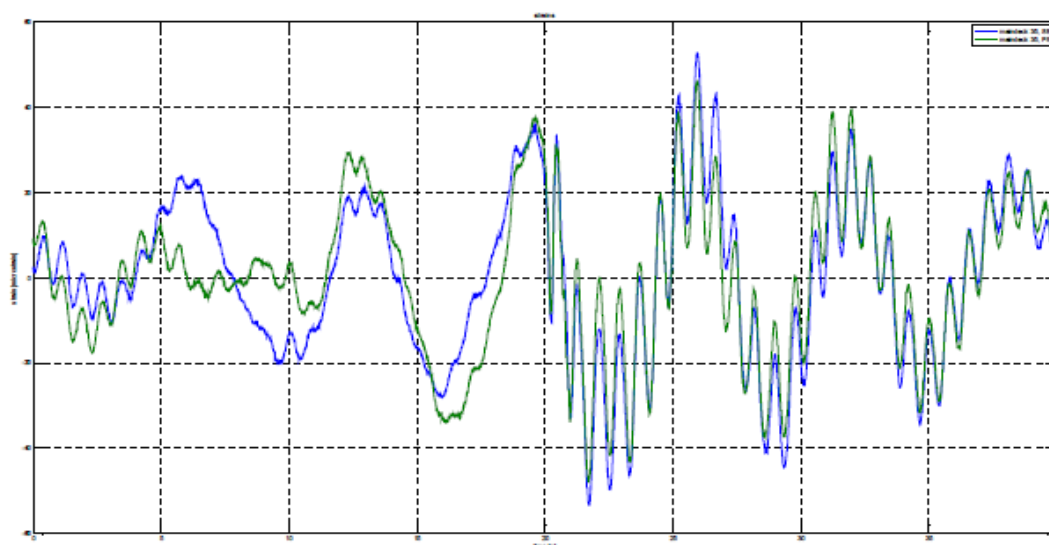




**Figure 72: Typical strain trace Frame 35 (measure 5)**

## 9.2 Appendix B

Added mass matrices and Total damping matrices for relevant are given below

### 4.1 EXPLANATION OF THE RESULTS

#### NON-DIMENSIONAL DEFINITIONS:

		I=1-3 J=1-3	I=1-3 I=4-6 J=4-6 J=1-3	I=4-6 J=4-6
MASS INERTIA MATRIX	NON-DIMENSIONALIZED BY:	RO*VOL,	RO*VOL*L	RO*VOL*L*L
ADDED MASS MATRIX	NON-DIMENSIONALIZED BY:	RO*VOL,	RO*VOL*L	RO*VOL*L*L
DAMPING MATRIX	NON-DIMENSIONALIZED BY:	RO*VOL*SQRT(G/L)	RO*VOL*SQRT(G*L)	RO*VOL*L*SQRT(G*L)
RESTORING MATRICES	NON-DIMENSIONALIZED BY:	RO*VOL*G/L,	RO*VOL*G	RO*VOL*G*L
		I=1-3	I=4-6	
EXCITING FORCES	NON-DIMENSIONALIZED BY:	RO*VOL*G*WA/L	RO*VOL*G*WA	
MOTIONS	NON-DIMENSIONALIZED BY:	WA	WA/L	(4-6 IN RADIANS)
SECTIONAL LOADS	NON-DIMENSIONALIZED BY:	RO*VOL*G*WA/L	RO*VOL*G*WA	
DRIFT FORCES	NON-DIMENSIONALIZED BY:	RO*G*L*WA*WA	RO*G*L*L*WA*WA	
		I=1-3		
PRESSURES	NON-DIMENSIONALIZED BY:	RO*G*WA		
VELOCITIES	NON-DIMENSIONALIZED BY:	WA*SQRT(G/L)		
ACCELERATIONS	NON-DIMENSIONALIZED BY:	WA*G/L		
2ND-ORDER FORCES	NON-DIMENSIONALIZED BY:	RO*G*L	RO*G*L*L	
2ND-ORDER PRESSURE	NON-DIMENSIONALIZED BY:	RO*G/L		
		I=1,2	I=6	
WAVE DRIFT DAMPING MATRIX	NON-DIMENSIONALIZED BY:	RO*G*L*WA*WA	RO*G*L*L*WA*WA	

#### NON-DIMENSIONALIZING FACTORS:

THE OUTPUT IS NON-DIMENSIONALIZED USING -

RO = DENSITY OF THE FLUID  
 G = ACCELERATION OF GRAVITY  
 L = CHARACTERISTIC LENGTH, AS GIVEN IN THE INPUT  
 VOL = DISPLACED VOLUME OF BODY 1 (COMBINED MORISON AND PANEL MODEL)  
 WA = WAVE AMPLITUDE OF THE INCOMING WAVES

RO = 0.1025E+04  
 G = 0.9807E+01  
 VOL = 0.1170E+05  
 L = 0.1300E+03



```
+-----+
+-----+
:
: W A V E L E N G T H      =  1.0697E+01
:
: W A V E P E R I O D    =  2.6180E+00
:
+-----+
+-----+
```

ADDED MASS MATRIX

```
-----
          1          2          3          4          5          6
1  1.2788E-02  4.8186E-04  9.4406E-03  1.2852E-05  7.4410E-03  6.5607E-05
2  6.5382E-04  2.0984E-01  2.6559E-03  2.8506E-03 -3.2155E-04  1.0676E-01
3  8.9324E-03  2.1534E-03  1.0803E+00  6.7455E-05 -5.2688E-01  1.8313E-04
4  1.3832E-05  2.5501E-03  6.7448E-05  3.0454E-04 -1.1170E-05  1.5518E-03
5  8.1830E-03 -2.8654E-04 -5.2723E-01 -1.2556E-05  3.0752E-01 -3.6418E-05
6  9.5892E-05  1.0754E-01  2.3493E-04  1.6967E-03 -3.3362E-05  7.0983E-02
```

TOTAL DAMPING MATRIX

```
-----
          1          2          3          4          5          6
1  5.4444E-02  8.2794E-04  8.1225E-03  1.8090E-05  2.3323E-02  1.6282E-04
2  3.6700E-04  9.8963E-01  3.0455E-03  7.8501E-03 -3.2148E-04  5.2061E-01
3  1.6522E-02  3.2268E-03  1.6417E-01  4.6541E-05 -4.5493E-02  3.6135E-04
4  1.0254E-05  8.7158E-03  1.1659E-05  1.6162E-04  9.8327E-07  5.6229E-03
5  1.6882E-02 -4.5378E-04 -4.8234E-02 -3.7007E-06  3.5059E-02 -5.4518E-05
6  1.2647E-04  5.1372E-01  1.7984E-04  5.1121E-03  2.6216E-06  3.4818E-01
```

```
+-----+
+-----+
:
: W A V E L E N G T H      =  3.1827E+00
:
: W A V E P E R I O D    =  1.4280E+00
:
+-----+
+-----+
```

ADDED MASS MATRIX

```
-----
          1          2          3          4          5          6
1  1.6987E-02  5.1353E-04  1.0613E-02  1.3044E-05  8.7902E-03  6.7841E-05
2  7.8138E-04  4.1055E-01  2.9010E-03  6.5099E-03 -3.3354E-04  2.1302E-01
3  1.0894E-02  2.2913E-03  1.0992E+00  7.5018E-05 -5.3505E-01  2.0750E-04
4  1.5675E-05  5.3205E-03  7.0416E-05  3.5208E-04 -1.1068E-05  3.0193E-03
5  1.0297E-02 -3.8059E-04 -5.3508E-01 -1.6656E-05  3.1242E-01 -6.4282E-05
6  1.2134E-04  2.1300E-01  2.6277E-04  3.5992E-03 -2.9604E-05  1.3683E-01
```



TOTAL DAMPING MATRIX

	1	2	3	4	5	6
1	4.7244E-03	3.5933E-04	7.1601E-04	-6.0402E-06	4.3414E-03	4.1729E-05
2	4.6035E-04	-3.0634E-02	-1.4595E-04	-2.0025E-03	-2.6714E-07	-2.3396E-02
3	4.9534E-03	-1.0306E-03	3.0562E-02	2.6812E-05	-9.1532E-03	-6.9347E-05
4	-1.2300E-05	-6.2196E-04	9.4285E-06	4.4551E-06	-1.3804E-06	-1.9383E-04
5	-2.0712E-03	1.9263E-04	-9.0340E-03	-2.5808E-06	6.8243E-03	6.4488E-05
6	-5.6998E-06	-2.3510E-02	4.8166E-05	-1.0522E-03	-7.1108E-06	-1.5531E-02

```
+-----+
|+-----+
|: W A V E L E N G T H   =   3.0428E+00 |:
|: W A V E P E R I O D   =   1.3963E+00 |:
|:-----+
+-----+
```

ADDED MASS MATRIX

	1	2	3	4	5	6
1	1.7097E-02	5.0630E-04	1.0555E-02	1.2779E-05	8.8578E-03	6.6982E-05
2	7.7620E-04	4.0132E-01	2.9083E-03	6.2359E-03	-3.3360E-04	2.0858E-01
3	1.0911E-02	2.3056E-03	1.0988E+00	7.4447E-05	-5.3486E-01	2.0648E-04
4	1.6004E-05	5.2900E-03	6.9865E-05	3.5111E-04	-1.1053E-05	3.0084E-03
5	1.0359E-02	-3.8284E-04	-5.3488E-01	-1.6950E-05	3.1234E-01	-6.5367E-05
6	1.2254E-04	2.0853E-01	2.6348E-04	3.4660E-03	-3.0227E-05	1.3452E-01

TOTAL DAMPING MATRIX

	1	2	3	4	5	6
1	4.1988E-03	5.0262E-04	2.3569E-04	-5.7695E-06	4.4018E-03	5.5465E-05
2	3.7148E-04	2.3670E-01	6.4683E-05	3.4347E-03	-9.1025E-05	1.1153E-01
3	5.5160E-03	4.0567E-04	3.0212E-02	9.6664E-06	-8.2662E-03	8.3155E-05
4	-5.0072E-06	1.2617E-03	7.9999E-06	3.6031E-05	1.0833E-06	6.6555E-04
5	-2.4680E-03	1.0270E-04	-8.0534E-03	-1.3064E-06	6.1276E-03	4.1745E-05
6	3.3298E-05	1.1265E-01	8.1939E-05	1.6306E-03	-7.2955E-06	6.1426E-02





```
+-----+
+-----+
: W A V E L E N G T H   =  2.3690E+00 :
: W A V E P E R I O D   =  1.2320E+00 :
+-----+
+-----+
```

ADDED MASS MATRIX

```
-----
          1          2          3          4          5          6
1    1.7903E-02  4.8115E-04  1.0499E-02  1.3142E-05  8.9198E-03  6.4118E-05
2    7.6005E-04  4.2646E-01  2.8482E-03  6.7719E-03 -3.2695E-04  2.2159E-01
3    1.0731E-02  2.3025E-03  1.0938E+00  7.7753E-05 -5.3238E-01  2.1278E-04
4    1.6477E-05  5.6151E-03  7.1271E-05  3.5925E-04 -1.1090E-05  3.1904E-03
5    1.0876E-02 -4.2884E-04 -5.3245E-01 -1.7977E-05  3.1115E-01 -7.5098E-05
6    1.1898E-04  2.2154E-01  2.6366E-04  3.7502E-03 -3.2452E-05  1.4266E-01
```

TOTAL DAMPING MATRIX

```
-----
          1          2          3          4          5          6
1    2.2291E-03  1.1282E-04 -2.7283E-03 -1.8291E-06  3.8225E-03  4.5052E-05
2    2.9538E-05 -7.4340E-02  5.7351E-04 -2.7761E-03 -6.7078E-05 -3.8208E-02
3   -2.0551E-04  6.9533E-04  2.1112E-02 -1.6308E-05 -9.2589E-03  1.0173E-04
4   -1.8280E-06 -5.9863E-04 -1.2362E-05 -1.0160E-05  7.3795E-07 -2.4829E-04
5    5.9893E-04 -5.6450E-05 -9.2244E-03  3.8318E-06  6.6709E-03  3.1946E-05
6   -6.3097E-05 -3.8892E-02 -1.1519E-04 -1.4345E-03  8.9193E-06 -2.1311E-02
```



```
+-----+
+-----+
: W A V E L E N G T H   =   2.1131E+00 :
: W A V E P E R I O D   =   1.1636E+00 :
:-----:
+-----+
```

ADDED MASS MATRIX

	1	2	3	4	5	6
1	1.8222E-02	4.6591E-04	1.0548E-02	1.3079E-05	8.8707E-03	6.0862E-05
2	7.7541E-04	4.3945E-01	2.8986E-03	7.0448E-03	-3.2958E-04	2.2838E-01
3	1.0680E-02	2.2564E-03	1.0904E+00	8.0571E-05	-5.3073E-01	2.1852E-04
4	1.6418E-05	5.7891E-03	6.9835E-05	3.6320E-04	-1.0817E-05	3.2804E-03
5	1.1096E-02	-4.3974E-04	-5.3081E-01	-1.8920E-05	3.1031E-01	-8.0720E-05
6	1.2268E-04	2.2835E-01	2.6434E-04	3.8894E-03	-3.1417E-05	1.4683E-01

TOTAL DAMPING MATRIX

	1	2	3	4	5	6
1	1.8935E-03	1.4767E-04	-3.1424E-03	-1.9676E-09	3.8294E-03	3.9605E-05
2	2.0314E-04	2.1538E-02	7.3849E-04	-2.8606E-04	-1.2705E-04	1.0586E-02
3	6.5198E-04	6.2152E-04	1.5818E-02	-4.8507E-06	-7.7030E-03	2.3220E-05
4	-4.5027E-06	1.7606E-04	-1.5785E-05	2.3159E-06	2.4633E-06	7.1062E-05
5	1.6913E-04	5.5391E-05	-8.0216E-03	5.1250E-07	6.4086E-03	3.2495E-05
6	1.7746E-05	1.1097E-02	4.8532E-05	-2.1833E-04	-1.5168E-05	5.9498E-03

```
+-----+
+-----+
: W A V E L E N G T H   =   1.7116E+00 :
: W A V E P E R I O D   =   1.0472E+00 :
:-----:
+-----+
```

ADDED MASS MATRIX

	1	2	3	4	5	6
1	1.8710E-02	4.5164E-04	1.0454E-02	1.2822E-05	8.7276E-03	5.5707E-05
2	7.9044E-04	4.7193E-01	2.8290E-03	7.7794E-03	-3.1769E-04	2.4484E-01
3	1.0666E-02	2.2903E-03	1.0817E+00	8.2705E-05	-5.2667E-01	2.1857E-04
4	1.6397E-05	6.1684E-03	7.0370E-05	3.7273E-04	-1.0726E-05	3.4816E-03
5	1.1331E-02	-4.8023E-04	-5.2672E-01	-2.0430E-05	3.0816E-01	-9.0520E-05
6	1.2923E-04	2.4480E-01	2.6680E-04	4.2603E-03	-3.4573E-05	1.5660E-01

TOTAL DAMPING MATRIX

	1	2	3	4	5	6
1	4.5852E-04	2.3641E-04	-1.9691E-03	-4.2583E-06	2.5760E-03	1.2165E-05
2	7.1487E-05	6.7698E-02	3.8982E-04	1.2040E-03	-4.6334E-06	3.2265E-02
3	-2.2181E-04	4.6906E-04	7.5305E-03	-5.6074E-06	-4.6860E-03	4.7585E-05
4	-1.7158E-06	4.4641E-04	-9.2783E-06	1.0137E-05	4.7208E-07	2.1795E-04
5	-1.4802E-04	-3.2541E-05	-4.3284E-03	3.0528E-07	3.9755E-03	5.3854E-06
6	1.3571E-05	3.2496E-02	1.2613E-05	5.1901E-04	1.7962E-05	1.7302E-02



### 9.3 Appendix C

Dry mode Natural frequencies and Vibration modes

#### Lightship Condition

The screenshot shows a dialog box titled "Step/Frame" with a close button in the top right corner. The dialog contains two main sections: "Step Name" and "Frame".

The "Step Name" section has a table with two columns: "Step Name" and "Description". The only entry is "Step-Dry\_light".

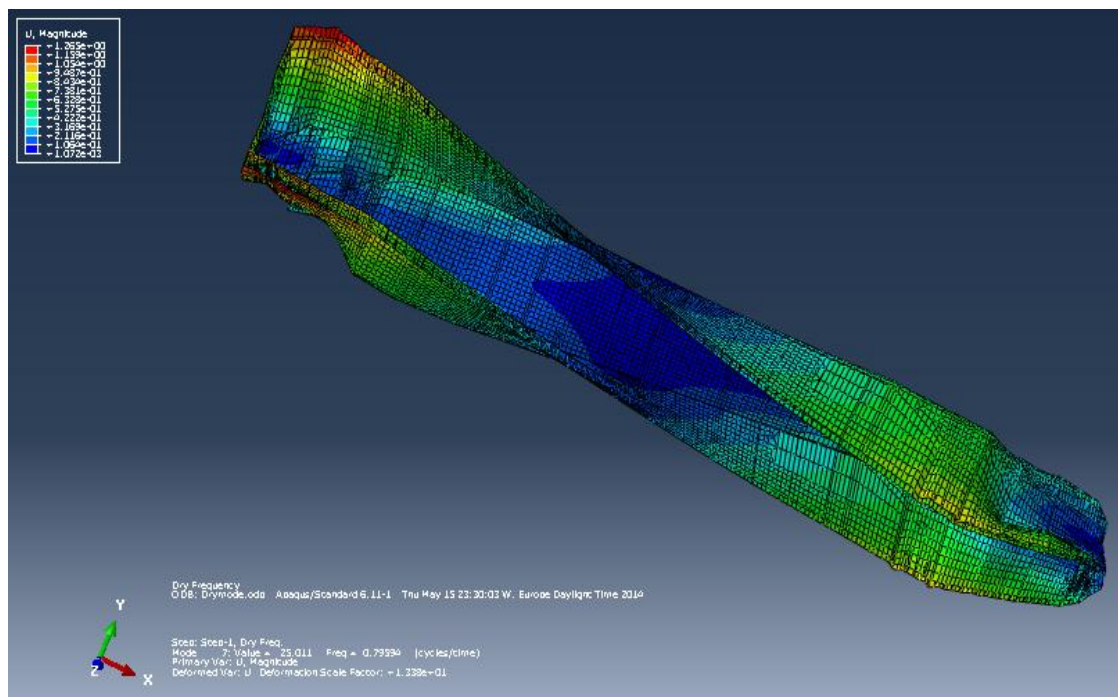
The "Frame" section has a table with two columns: "Index" and "Description". The table lists 16 modes (Index 0 to 15). Mode 0 is the "Base State". Modes 1 through 15 are "Mode" entries, each showing a value and a frequency in cycles/time.

Step Name	Description
Step-Dry_light	

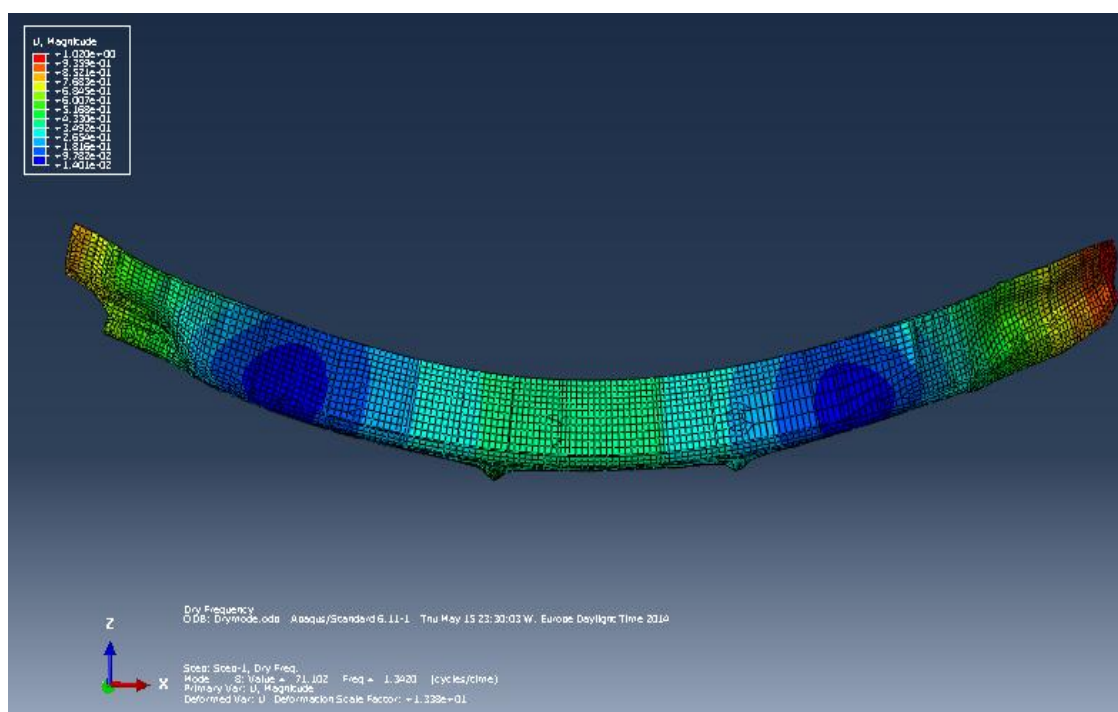
  

Index	Description
0	Increment 0: Base State
1	Mode 1: Value = -7.48933E-10 Freq = 0.0000 (cycles/time)
2	Mode 2: Value = -2.60867E-11 Freq = 0.0000 (cycles/time)
3	Mode 3: Value = 1.23495E-10 Freq = 1.76866E-06 (cycles/time)
4	Mode 4: Value = 2.80779E-10 Freq = 2.66688E-06 (cycles/time)
5	Mode 5: Value = 1.26499E-09 Freq = 5.66062E-06 (cycles/time)
6	Mode 6: Value = 1.77028E-09 Freq = 6.69639E-06 (cycles/time)
7	Mode 7: Value = 29.252 Freq = 0.86080 (cycles/time)
8	Mode 8: Value = 103.98 Freq = 1.6229 (cycles/time)
9	Mode 9: Value = 106.42 Freq = 1.6419 (cycles/time)
10	Mode 10: Value = 243.72 Freq = 2.4846 (cycles/time)
11	Mode 11: Value = 283.71 Freq = 2.6808 (cycles/time)
12	Mode 12: Value = 331.84 Freq = 2.8993 (cycles/time)
13	Mode 13: Value = 353.40 Freq = 2.9919 (cycles/time)
14	Mode 14: Value = 380.81 Freq = 3.1058 (cycles/time)
15	Mode 15: Value = 415.77 Freq = 3.2452 (cycles/time)

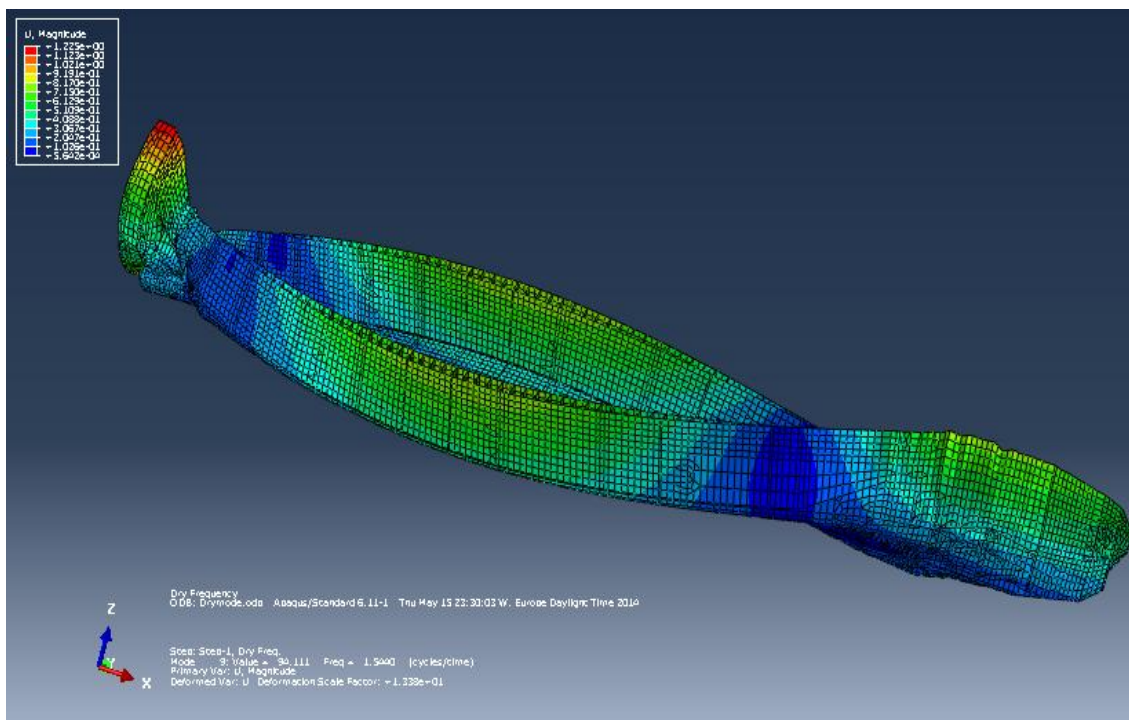
At the bottom of the dialog, there are four buttons: "OK", "Apply", "Field Output...", and "Cancel".



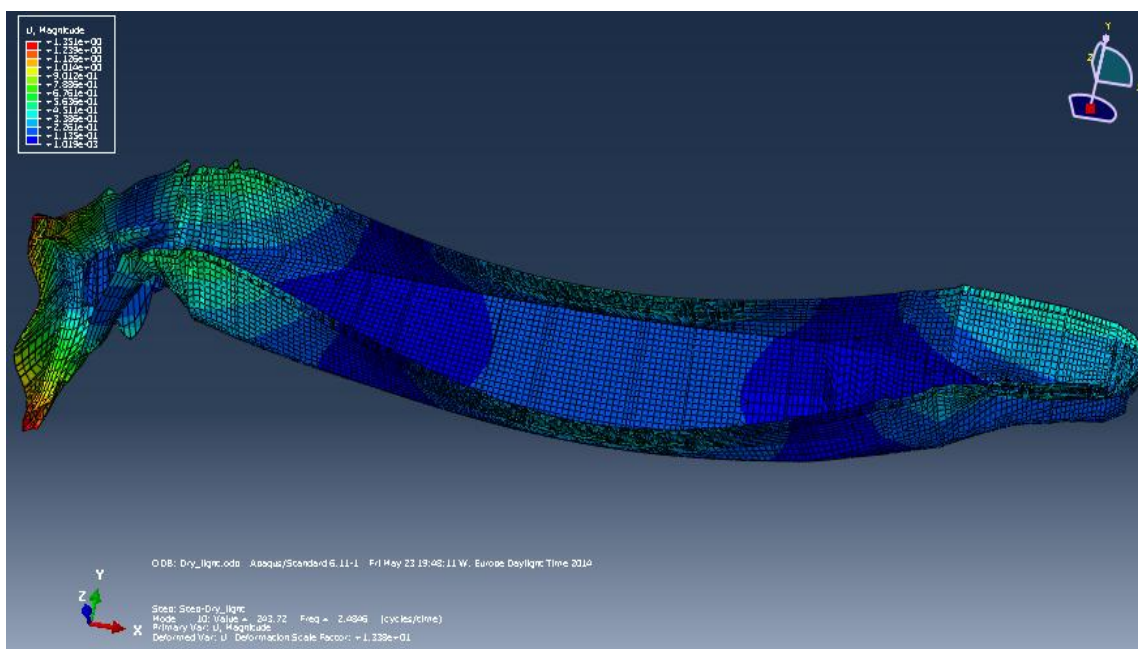
Global Torsion Mode at 0.86080 Hz.



2-node Vertical Bending Mode at 1.6229 Hz



Global Torsion and Horizontal Bending Mode at 1.6419 Hz



3-node horizontal bending at 2.4846 Hz



## Ballast Condition

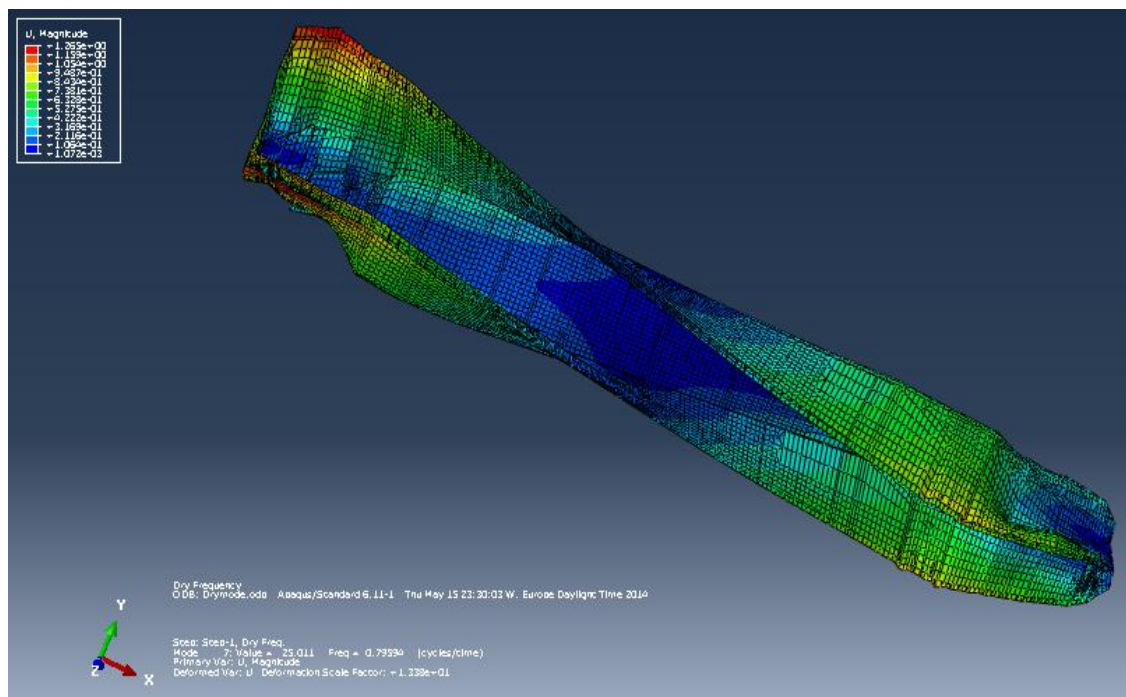
Step/Frame

Step Name	Description
Step-dry_ballast	

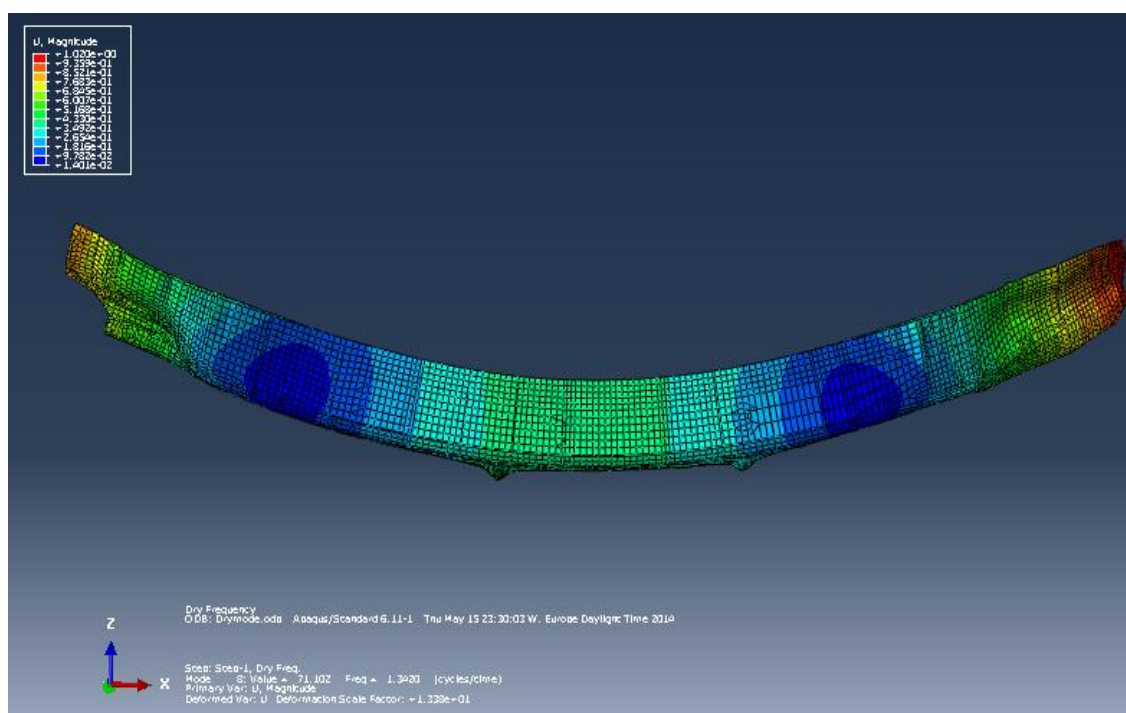
Frame

Index	Description
0	Increment 0: Base State
1	Mode 1: Value = -1.42084E-09 Freq = 0.0000 (cycles/time)
2	Mode 2: Value = -8.12537E-11 Freq = 0.0000 (cycles/time)
3	Mode 3: Value = 2.83060E-12 Freq = 2.67769E-07 (cycles/time)
4	Mode 4: Value = 7.72786E-11 Freq = 1.39910E-06 (cycles/time)
5	Mode 5: Value = 2.11338E-10 Freq = 2.31371E-06 (cycles/time)
6	Mode 6: Value = 1.07602E-09 Freq = 5.22071E-06 (cycles/time)
7	Mode 7: Value = 23.778 Freq = 0.77608 (cycles/time)
8	Mode 8: Value = 68.668 Freq = 1.3189 (cycles/time)
9	Mode 9: Value = 90.294 Freq = 1.5123 (cycles/time)
10	Mode 10: Value = 177.92 Freq = 2.1229 (cycles/time)
11	Mode 11: Value = 222.93 Freq = 2.3763 (cycles/time)
12	Mode 12: Value = 283.68 Freq = 2.6806 (cycles/time)
13	Mode 13: Value = 288.69 Freq = 2.7042 (cycles/time)
14	Mode 14: Value = 317.32 Freq = 2.8351 (cycles/time)
15	Mode 15: Value = 323.69 Freq = 2.8634 (cycles/time)

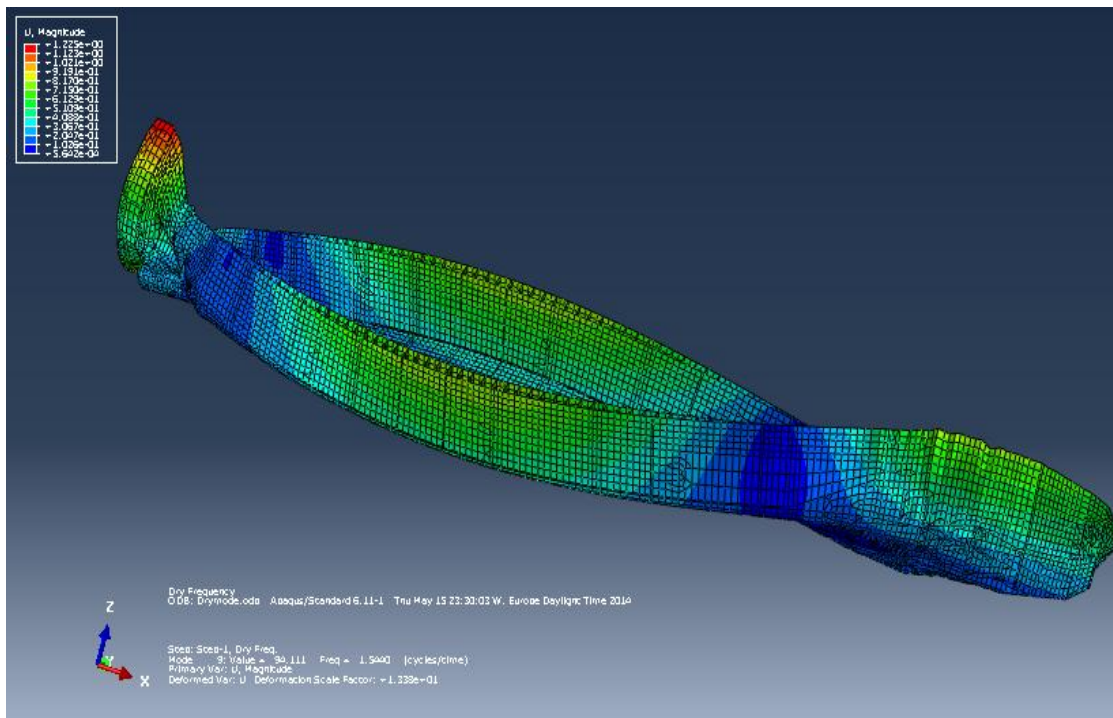
OK Apply Field Output... Cancel



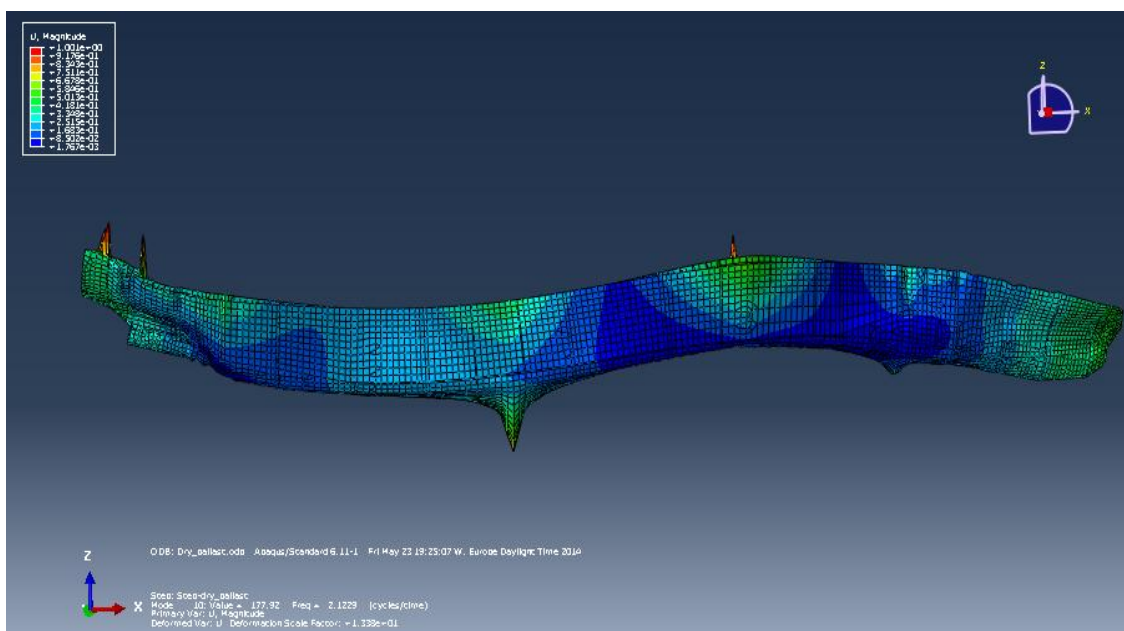
Global Torsion Mode at 0.77608 Hz.



2-node Vertical Bending Mode at 1.3189 Hz

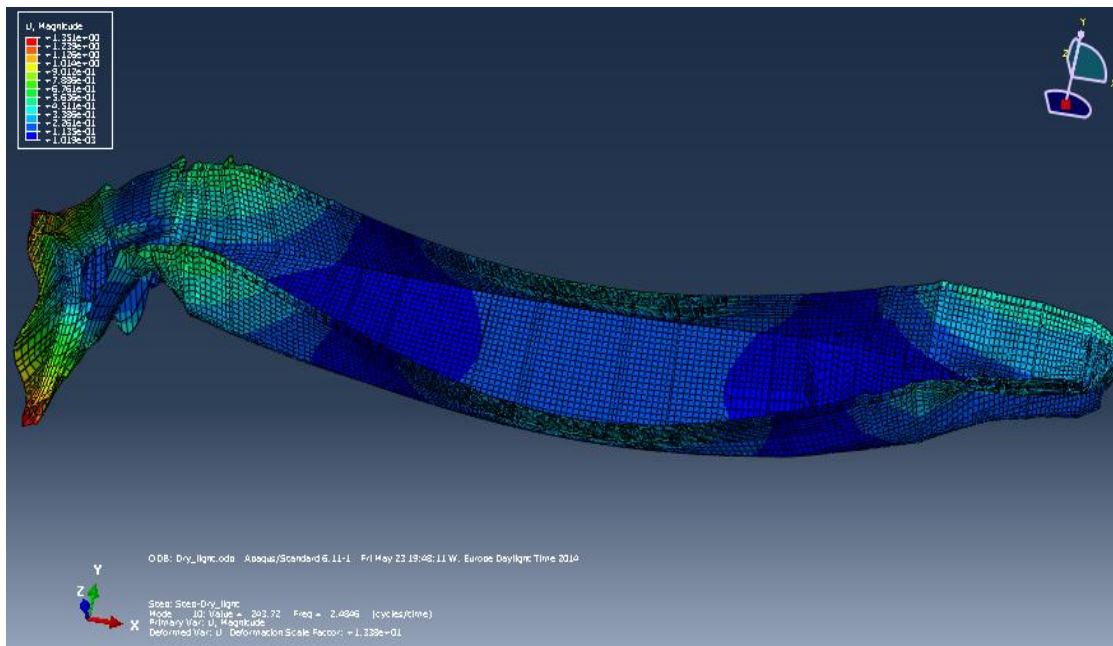


Global Torsional and Horizontal Bending Mode at 1.5123 Hz



3-node vertical bending at 2.1229 Hz





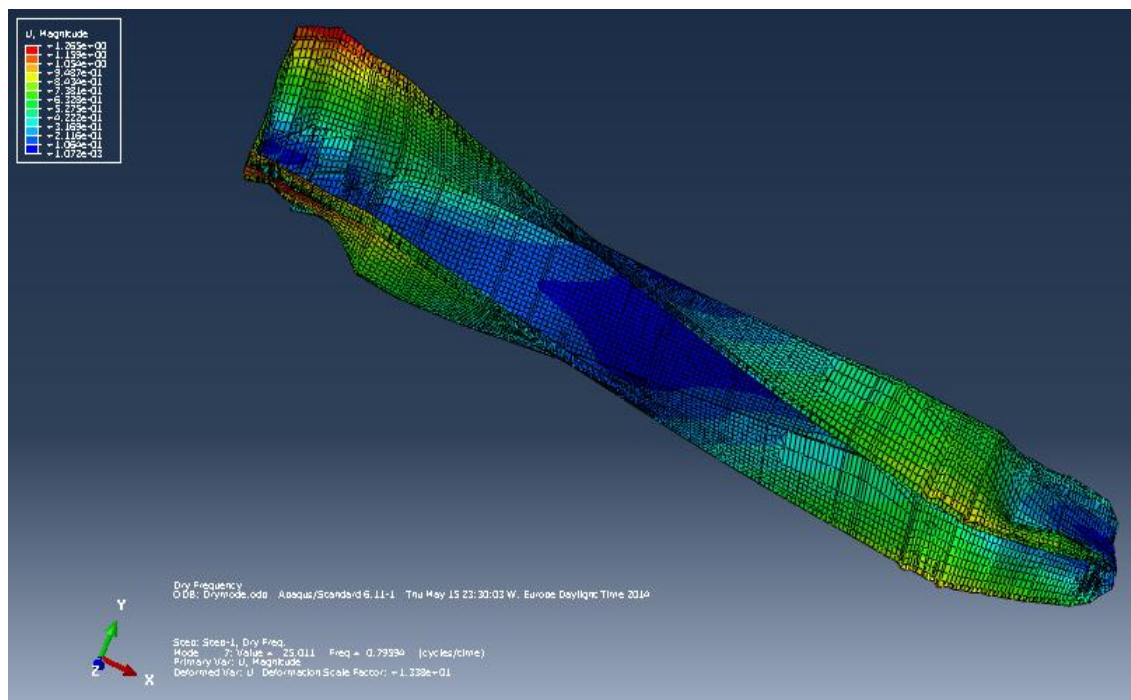
3- node horizontal bending at 2.3763 Hz

## Loaded Condition

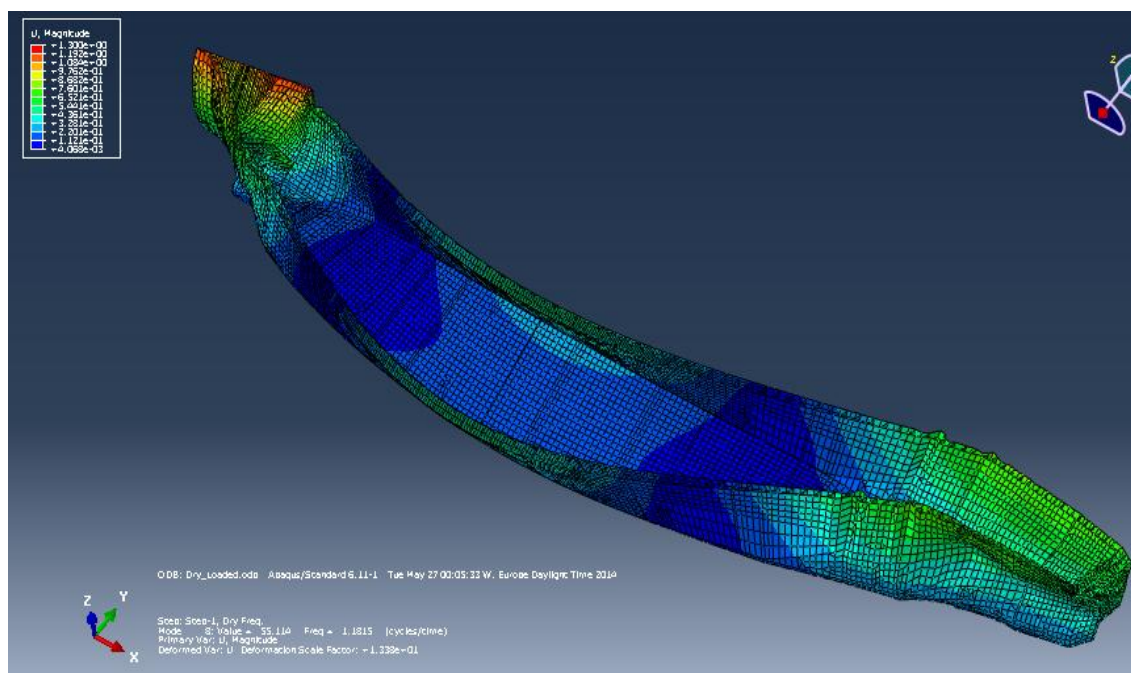
Step Name	Description
Step-1	Dry Freq.

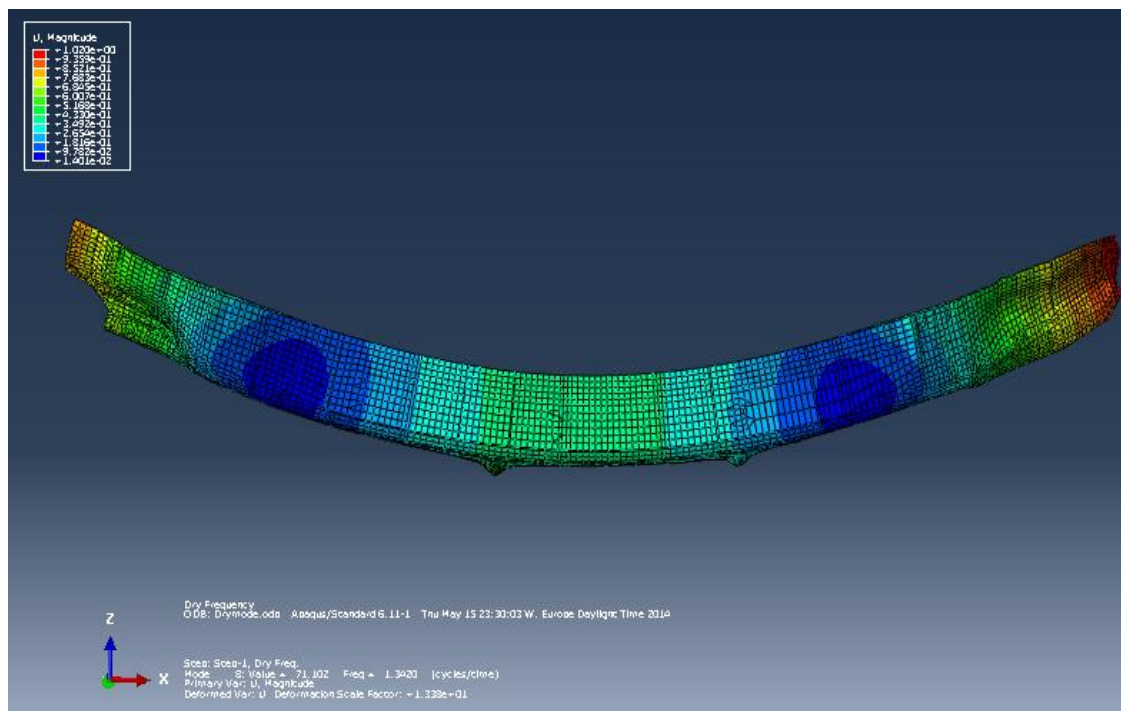
Index	Description
0	Increment 0: Base State
1	Mode 1: Value = -6.16523E-10 Freq = 0.0000 (cycles/time)
2	Mode 2: Value = -7.56861E-11 Freq = 0.0000 (cycles/time)
3	Mode 3: Value = -2.24554E-11 Freq = 0.0000 (cycles/time)
4	Mode 4: Value = 5.78561E-11 Freq = 1.21058E-06 (cycles/time)
5	Mode 5: Value = 3.09565E-10 Freq = 2.80025E-06 (cycles/time)
6	Mode 6: Value = 4.52069E-10 Freq = 3.38394E-06 (cycles/time)
7	Mode 7: Value = 14.882 Freq = 0.61398 (cycles/time)
8	Mode 8: Value = 55.114 Freq = 1.1815 (cycles/time)
9	Mode 9: Value = 59.546 Freq = 1.2281 (cycles/time)
10	Mode 10: Value = 159.61 Freq = 2.0107 (cycles/time)
11	Mode 11: Value = 218.23 Freq = 2.3511 (cycles/time)
12	Mode 12: Value = 247.34 Freq = 2.5031 (cycles/time)
13	Mode 13: Value = 260.86 Freq = 2.5706 (cycles/time)
14	Mode 14: Value = 281.42 Freq = 2.6699 (cycles/time)
15	Mode 15: Value = 283.85 Freq = 2.6814 (cycles/time)



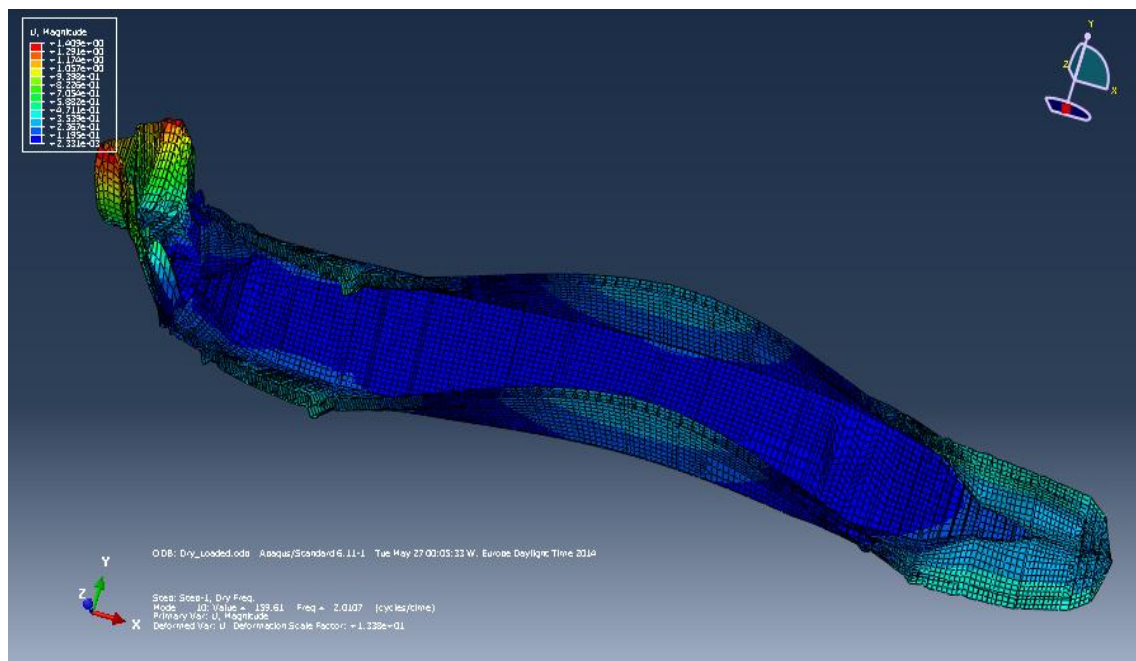
Global Torsion Mode at 0.61398 Hz.



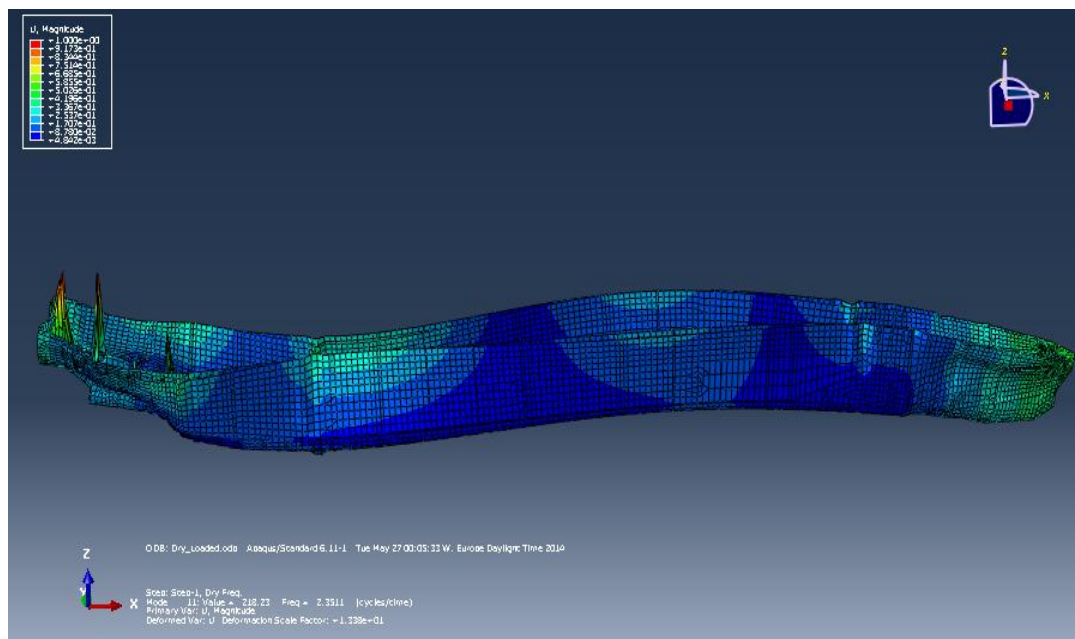
Horizontal bending /torsion mode at 1.1815 Hz



2-node Vertical Bending Mode at 1.2281 Hz



3-node Horizontal bending at 2.0107 Hz



3- node vertical bending at 2.3511 Hz